

PURIFICATION AND CHARACTERIZATION OF RICE GLYCOSIDE
HYDROLASE FAMILY 3 β -XYLOSIDASE OsXYL1



A Thesis Submitted in Partial Fulfillment of the Requirements for the
Degree of Doctor of Philosophy in Biochemistry
Suranaree University of Technology
Academic Year 2021

การทำโปรตีนบริสุทธิ์และศึกษาการทำงานของไกลโคไซด์ไฮโดรเลส กลุ่ม 3
จากข้าว เบต้าไซโลซีเดส OsXYL1



นางสาวเกศญา สาลา

วิทยานิพนธ์นี้เป็นส่วนหนึ่งของการศึกษาตามหลักสูตรปริญญาวิทยาศาสตรดุษฎีบัณฑิต
สาขาวิชาชีวเคมี
มหาวิทยาลัยเทคโนโลยีสุรนารี
ปีการศึกษา 2564

PURIFICATION AND CHARACTERIZATION OF RICE GLYCOSIDE HYDROLASE
FAMILY 3 β -XYLOSIDASE OsXYL1

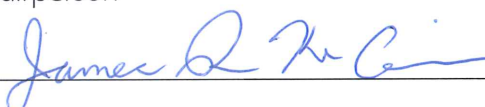
Suranaree University of Technology has approved this thesis submitted in partial fulfillment of the requirements for the Degree of Doctor of Philosophy.

Thesis Examining Committee



(Asst. Prof. Dr. Anyanee Kamkaew)

Chairperson



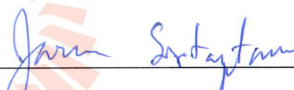
(Prof. Dr. James R. Ketudat-Cairns)

Member (Thesis Advisor)



(Assoc. Prof. Dr. Prachumporn Kongsaree)

Member



(Assoc. Prof. Dr. Jaruwan Siritapetawee)

Member



(Assoc. Prof. Dr. Mariena Ketudat-Cairns)

Member



(Asst. Prof. Dr. Rung-Yi Lai)

Member



(Assoc. Prof. Dr. Chatchai Jothityangkoon) (Prof. Dr. Santi Maensiri)

Vice Rector for Academic Affairs
and Quality Assurance

Dean of Institute of Science

เกษฏา สาขา : การทำโปรตีนบริสุทธิ์และศึกษาการทำงานของไกลโคไซด์ไฮโดรเลส กลุ่ม 3 จากข้าว เบต้าไซโลซิเดส OsXYL1 (PURIFICATION AND CHARACTERIZATION OF RICE GLYCOSIDE HYDROLASE FAMILY 3 β -XYLOSIDASE OsXYL1. อาจารย์ที่ปรึกษา : ศาสตราจารย์ ดร.เจมส์ เกตุทัต-คาร์นส์, 96 หน้า.

คำสำคัญ: เบต้าไซโลซิเดส/ไกลโคไซด์ไฮโดรเลส กลุ่ม 3/ไซโลโอลิโกแซ็กคาไรด์

เอนไซม์ไกลโคไซด์ไฮโดรเลสชนิดต่าง ๆ ที่ผลิตออกนอกเซลล์เกี่ยวข้องกับการย่อยสลาย การปรับโครงสร้าง และการดัดแปลงโพลีแซ็กคาไรด์ของผนังเซลล์พืชในการเจริญเติบโตและการพัฒนาของพืช เอนไซม์เหล่านี้ถูกใช้กันอย่างแพร่หลายในการย่อยสลายสารชีวมวล เอนไซม์ในตระกูลไกลโคไซด์ไฮโดรเลส 3 จากพืช มีส่วนร่วมในการดัดแปลงและการย่อยสลายโครงสร้างของผนังเซลล์ มีเอนไซม์จากพืชชั้นสูงเพียงบางชนิดที่มีการศึกษาคุณสมบัติมาแล้ว เอนไซม์เบต้าไซโลซิเดสจากข้าว (*Oryza sativa*) OsXYL1 ซึ่งอยู่ในตระกูลไกลโคไซด์ไฮโดรเลส 3 ถูกโคลนเข้าสู่เวกเตอร์ pPICZ α BH8 เพื่อการแสดงออกในเชื้อ *Pichia pastoris* สายพันธุ์ SMD1168H ทำให้บริสุทธิ์ และศึกษาคุณสมบัติโปรตีนที่หลั่งออกมาในอาหารเลี้ยงเชื้อหลังจากการเหนี่ยวนำเป็นเวลา 5 วัน ที่อุณหภูมิ 20 °C สามารถทำให้บริสุทธิ์ได้สำเร็จ พิวชั้นเบต้าไซโลซิเดส OsXYL1 โปรตีนที่มีฮิสทีดินแท็ก ที่ตำแหน่งและมี N-glycosylation สามตำแหน่ง ถูกทำให้บริสุทธิ์โดยโครมาโตกราฟีสองขั้นตอน คือ Ni-immobilized metal affinity chromatography (IMAC) ตามด้วยโครมาโตกราฟีแบบแยกขนาดด้วย Superdex S200 โปรตีนที่ถูกตัดหมู่น้ำตาลออกมีน้ำหนักโมเลกุล (MW) ประมาณ 84 kDa จากการวิเคราะห์ด้วย SDS-PAGE ซึ่งตรงกับขนาดที่คาดการณ์ไว้ เอนไซม์ OsXYL1 ที่บริสุทธิ์มีความสามารถในการย่อย 4NP- β -D-xylopyranoside (4NPXyl) ได้ดีที่สุดที่ pH 4.0 และอุณหภูมิ 60 °C และทนต่ออุณหภูมิ 30-50 °C เป็นเวลาอย่างน้อย 4 ชั่วโมง เอนไซม์ OsXYL1 สามารถย่อย 4NPXyl และไซโลโอลิโกแซ็กคาไรด์ที่เชื่อมต่อกันด้วยพันธะ β -1,4 (XOS, ที่มี DP 2 ถึง 6 หน่วย) เอนไซม์นี้สามารถย่อย 4-nitrophenyl glycosides อื่น ๆ ได้แก่ 4NP- α -L-arabinofuranoside (4NPArf), 4NP- α -L-arabinopyranoside (4NPArap), 4-NP-N-acetyl- β -D-glucosaminide และ 4NP- β -D-glucopyranoside ไม่เกิน 10% ของ 4NPXyl ค่าจลนศาสตร์ของ OsXYL1 ต่อ 4NPXyl ซึ่งมีความชอบสูง ได้แก่ ค่าคงที่ Michaelis-Menten (K_m) เท่ากับ 0.65 ± 0.03 mM และค่า

ประสิทธิภาพการเร่งปฏิกิริยา (k_{cat}/K_m) สูงถึง $19.0 \text{ mM}^{-1}\text{s}^{-1}$ กิจกรรมการย่อยถูกยับยั้งด้วยไซโลสที่มีค่าคงที่การยับยั้ง (K_i) แบบแข่งขัน เท่ากับ $1.41 \pm 0.06 \text{ mM}$ นอกจากนี้ OsXYL1 สามารถย่อย β -1,4-xylo-oligosaccharides (XOSs) ที่มีระดับการเกิดพอลิเมอร์ไรเซชัน (DP) 2 ถึง 6 หน่วย ซึ่งมีค่าประสิทธิภาพการเร่งปฏิกิริยา (k_{cat}/K_m) เท่ากับ 2.56, 4.17, 3.11, 2.80 และ $1.47 \text{ mM}^{-1}\text{s}^{-1}$ ตามลำดับ ซึ่งมีสัมพันธ์แบบผกผันกับระดับของพอลิเมอร์ไรเซชันจาก 3 ถึง 6 หน่วย สำหรับกิจกรรมทรานส์ไกลโคซิเลชันได้ผลิตผลิตภัณฑ์อัลคิลไซโลไซด์ที่มีตัวรับแอลกอฮอล์ในปฏิกิริยาใช้เวลาในการสะสมผลิตภัณฑ์นานกว่า 4 วัน



ผลการวิจัยนี้แสดงให้เห็นว่า เอนไซม์เบต้าไซโลซิเดส OsXYL1 จากข้าวอาจทำหน้าที่ในการย่อยสลายไซแลนในการรีไซเคิลผนังเซลล์พืช และกิจกรรมทรานส์ไกลโคซิเลชันของเอนไซม์กับตัวรับแอลกอฮอล์เพื่อผลิตผลิตภัณฑ์อัลคิลไซโลไซด์ได้



สาขาวิชาเคมี
ปีการศึกษา 2564

ลายมือชื่อนักศึกษา

ลายมือชื่ออาจารย์ที่ปรึกษา

KADSADA SALA : PURIFICATION AND CHARACTERIZATION OF RICE GLYCOSIDE HYDROLASE FAMILY 3 β -XYLOSIDASE OsXYL1. THESIS ADVISOR : PROF. JAMES R. KETUDAT-CAIRNS, Ph.D. 96 PP.

Keyword: β -XYLOSIDASE/GLYCOSIDE HYDROLASE FAMILY 3/XYLOOLIGO-SACCHARIDES

Various extracellular glycoside hydrolases are involved in degrading, remodeling, and modifying polysaccharides in plant cell wall in plant growth and development, and these enzymes are widely employed in degradation of biomass. Plant glycoside hydrolases family 3 members have been associated with modification and degradation of cell wall matrix, but few have been characterized in higher plants. A rice (*Oryza sativa*) β -xylosidase designated as OsXYL1, which belongs to glycoside hydrolase family 3, was recombinantly cloned for expression, purification and characterization. OsXYL1 β -xylosidase from the pPICZ α BH8/OsXYL1 vector in heterologous *Pichia pastoris* SMD1168H strain was successfully purified from the secreted protein in culture medium after induction for 5 days at 20 °C. The fusion protein with histidine tags, 3C Precision sites and three N-glycosylation sites in OsXYL1 β -xylosidase was purified by two chromatographic steps, Ni-immobilized metal affinity chromatography (IMAC), followed by Superdex S200 size exclusion chromatography. The molecular weight (MW) of the deglycosylated protein was estimated as 84 kDa by SDS-PAGE, which matched the predicted mass. The purified OsXYL1 showed the optimal hydrolysis activity toward 4NP- β -D-xylopyranoside (4NPXyl) at pH 4.0 and at 60 °C, and it was relatively stable at temperatures ranging from 30-50 °C for at least 4 h. OsXYL1 had hydrolysis activity on 4NPXyl and also on β -1,4-linked xylooligosaccharides (XOS, with DP 2-6). The relative activity was not greater than 10% of that on 4NPXyl with the other 4-nitro-phenyl glycosides, including 4NP- α -L-arabinofuranoside (4NPAr α f), 4NP- α -L-arabinopyranoside (4NPAr α p), 4NP-N-acetyl- β -D-glucosaminide, and 4NP- β -D-glucopyranoside. Kinetic parameters of OsXYL1 with the highly preferred 4NPXyl included an apparent Michaelis-Menten constant (K_m) value of 0.65 ± 0.03 mM, and high catalytic efficiency (k_{cat}/K_m) value of $19.0 \text{ mM}^{-1}\text{s}^{-1}$. The hydrolytic activity was inhibited by xylose with a competitive inhibition constant (K_i) of 1.41 ± 0.06 mM. In addition, OsXYL1 hydrolyzed

β -1,4-xylo-oligosaccharides (XOSs) with degree of polymerization (DP) of 2-6 with apparent catalytic efficiency (k_{cat}/K_m) values 2.56, 4.17, 3.11, 2.80, and 1.47 $\text{mM}^{-1}\text{s}^{-1}$, respectively, which were inversely related to its degree of polymerization from 3 to 6. Transglycosylation activity produced alkyl xyloside products with alcohol acceptors in reactions in which the products accumulated for over 4 days.

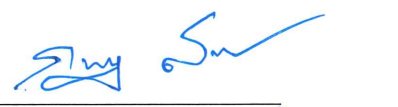

These data indicate that rice β -xylosidase OsXYL1 might function in degradation of xylans in plant cell wall recycling, and its transglycosylation activity with alcohol acceptors to produce alkyl xyloside products may be a useful application of this enzyme.



School of Chemistry
Academic Year 2021

Student's Signature

Advisor's Signature

ACKNOWLEDGEMENTS

I would like to express my deepest appreciation to my advisor Prof. Dr. James R. Ketudat-Cairns for providing me an opportunity to study towards my Ph.D. degree in Biochemistry, for his patience and guidance, unconditional support, inspiration and encouragement throughout my study period.

I sincerely thank Assoc. Prof. Dr. Prachumporn Kongsaree from Kasetsart University, Assoc. Prof. Mariena Ketudat-Cairns from School of Biotechnology, Assoc. Prof. Dr. Jaruwan Siritapetawee, Asst. Dr. Rung-Yi Lai and Asst. Prof. Dr. Anyanee Kamkaew from School of Chemistry, Suranaree University of Technology, for patiently reading this dissertation and providing helpful comments.

I would to thank all Biochemistry lecturers at Suranaree University of Technology for providing me many valuable knowledge, laboratory technique, and opened up a whole biochemistry world for me.

Special thanks are extended to and Assoc. Prof. Dr. Sompong Sansenya for his boosting my energy, cheering and supporting me for this study as long as our friendship from Maejo University till now. I like to thank Dr. Salila Pengthaisong, Biochemistry friends and all members of Centre for Biomolecular Structure, Function and Application (CBSFA) for their help, support, valuable hint of encouragement.

Finally, my deepest gratitude will go to myself and my family for faith in my decision, supporting and encouraging me throughout my studies.

Kadsada Sala

CONTENTS

	Page
ABSTRACT IN THAI.....	I
ABSTRACT IN ENGLISH.....	III
ACKNOWLEDGEMENTS.....	V
CONTENTS.....	VI
LIST OF FIGURES	IX
LIST OF TABLES	XII
LIST OF ABBREVIATIONS	XIII
CHAPTER	
I INTRODUCTION	1
1.1 Glycoside hydrolases	1
1.2 Glycoside hydrolases family 3	3
1.3 Plant cell wall	6
1.4 Hemicelluloses and heteroxylans	10
1.5 β -Xylosidase	15
1.6 Research objectives	19
II MATERIALS AND METHODS	20
2.1 Sequence analysis	20
2.2 General methods	20
2.2.1 Competent bacterial cell preparation	20
2.2.2 Bacterial transformation	21
2.2.3 Bacterial glycerol stocks	21
2.2.4 Plasmid extraction by alkaline lysis	22
2.2.5 Colony PCR	24
2.2.6 Agarose gel electrophoresis	24
2.2.7 Gel extraction and DNA clean up	25
2.2.8 DNA determination by Nanodrop spectrophotometer	25
2.2.9 Protein concentration determination	25

CONTENTS (Continued)

	Page
2.2.3 SDS-PAGE electrophoresis	26
2.3 DNA and microbes for cloning and expression	28
2.3.1 Oligosaccharides	28
2.3.2 Microorganisms	29
2.3.2 Plasmid for <i>E. coli</i> expression	29
2.3.4 Plasmid for <i>P. pastoris</i> expression	30
2.3.5 PCR amplification of insert from pUC57/OsXYL1	31
2.4 Yeast transformation	32
2.4.1 SMD1168H competent cell preparation	32
2.4.2 Plasmid preparation for <i>Pichia</i> transformation	34
2.4.3 <i>Pichia</i> Transformation	34
2.5 Protein expression	35
2.5.1 Expression screening in <i>E. coli</i> optimization of conditions	35
2.5.2 Protein expression and extraction of OsXYL1 in <i>E. coli</i>	35
2.5.3 Screening <i>Pichia</i> transformants and optimization for expression	36
2.5.4 Protein expression of OsXYL1 in <i>P. pastoris</i>	37
2.6 Purification of β -xylosidase OsXYL1	37
2.7 Characterization of β -xylosidase OsXYL1	38
2.7.1 Enzyme assays	38
2.7.2 pH and temperature optima	38
2.7.3 Effect of metal ions and sugars	39
2.7.4 Deglycosylation OsXYL1	39
2.7.5 Transglycosylation activity	40
2.7.6 Substrate specificity	40
2.7.7 Hydrolysis of xylooligosaccharides	42

CONTENTS (Continued)

	Page
2.8 Kinetic parameters	42
2.8.1 Hydrolysis of nitrophenyl glycosides	42
2.8.2 Hydrolysis of xylooligosaccharides	43
2.8.3 Xylose inhibition	44
III RESULTS AND DISCUSSION	45
3.1 Expression pattern of OsXYL1 (Accession No. AK119887, Locus ID. Os02g0752200) in rice	45
3.2 Sequence analysis of rice β -xylosidase OsXYL1	46
3.3 Expression and purification of OsXYL1 in <i>E. coli</i>	52
3.4 Expression and purification of OsXYL1 in <i>P. pastoris</i>	56
3.5 Effect of pH and temperature on β -xylosidase OsXYL1	61
3.6 Effects of carbohydrates on β -xylosidase OsXYL1	64
3.7 Effect of metal ions and EDTA on β -xylosidase OsXYL1.....	65
3.8 Transglycosylation of β -xylosidase OsXYL1.....	67
3.9 Substrate specificity β -xylosidase OsXYL1	69
3.10 Kinetic study of the β -xylosidase OsXYL1	72
3.11 Xylose inhibition of β -xylosidase OsXYL1	76
IV CONCLUSION	78
REFERENCES	81
CURRICULUM VITAE	96

LIST OF FIGURES

Figure	Page
1.1 General catalytic mechanism of glycoside hydrolase	1
1.2 Endo-/Exo-acting glycoside hydrolase	1
1.3 Schematic representation of glycoside hydrolase mechanisms	3
1.4 Plant cell wall structure and compositions	7
1.5 Plant cell wall structure	9
1.6 Chemical structure of (glucurono)arabinoxylan	12
1.7 Representations of chemical structures of xylans	13
1.8 Plant cell wall polysaccharides and substrate specificity of degradation enzymes.....	14
1.9 The glycoside hydrolase retaining mechanism	16
1.10 Schematic representation of hydrolysis and transglycosylation activity of GH3 β -xylosidases	17
1.11 Schematic representation of degradation of xylooligosaccharides by β -xylosidases into released D-xylose	18
2.1 Schematic representation of the expression cassettes in the recombinant plasmids (A), pET32a/OsXYL1 for expression in <i>E. coli</i> and (B), pPICZ α BNH8/ OsXYL1 for expression in <i>P. pastoris</i>	30
3.1 Expression profile of OsXYL1 in different organs and tissue	46
3.2 Phylogenetic relationships of OsXYL1 and other plant GH3 members	47
3.3 Alignment analysis of plant GH3 amino acid sequences	49
3.4 Homology model of OsXYL1 based on the X-ray crystal structure of the <i>Hypocrea jecorina</i> β -xylosidases Xyl3A (Bxl1) in complex with 4-thioxylobiose (PDB code 5AE6)	50
3.5 Amino acid alignment of the rice β -xylosidases OsXYL1 and the fungal <i>Hypocrea jecorina</i> β -xylosidases Xyl3A (Bxl1)	52

LIST OF FIGURES (Continued)

Figure	Page
3.6 SDS-PAGE analysis of insoluble (A) and soluble (B) fractions of crude extracts of pET32a/OsXYL1 in Origami(DE3) after IPTG induction	53
3.7 SDS-PAGE analysis of insoluble (A) and soluble (B) fractions of crude extracts of pET32a/OsXYL1 in OrigamiB(DE3) after IPTG induction	54
3.8 SDS-PAGE analysis of expression of recombinant OsXYL1 in OrigamiB(DE3)	55
3.9 Expression of <i>P. pastoris</i> transformants of OsXYL1 in BMMY broth induced with 0.5% (v/v) methanol for 6 days and β -xylosidase activity assay	56
3.10 10% SDS-PAGE of pooled fractions of secreted OsXYL1 protein	58
3.11 S200 Gel filtration protein elution profile of OsXYL1	59
3.12 12% SDS-PAGE analysis of sample taken during the purification of secreted OsXYL1	60
3.13 Activity versus pH profile of purified OsXYL1 over the range of 2.5-11.0 (in 0.5 increment)	62
3.14 Activity versus temperature profile of purified OsXYL1 over the temperatures range of 30-80 °C (in 5 °C increment)	63
3.15 Thermostability of purified OsXYL1	64
3.16 Effect of carbohydrates on β -xylosidase OsXYL1	65
3.17 Effect of metal ions and EDTA on β -xylosidase OsXYL1	66
3.18 TLC patterns of transglycosylation products of OsXYL1 with alcohol acceptors	67
3.19 TLC patterns of transglycosylation products of OsXYL1 with 1-octanol in co-solvent mixture	68
3.20 Hydrolysis of β -xylosidase OsXYL1 toward xylooligosaccharides	71
3.21 Michaelis-Menten (A) and Hanes-Woolf (B, C) plot of β -xylosidase OsXYL1 toward nitrophenyl glycoside substrates	72
3.22 Michaelis-Menten plot of β -xylosidase OsXYL1 hydrolysis toward xylooligosaccharide substrates (DP 2-6)	74

LIST OF FIGURES (Continued)

Figure	Page
3.23 Lineweaver-Burk plot of β -xylosidase OsXYL1 toward 4NPXyl with different concentration of xylose inhibitor.....	76
3.24 Derivative plot to determine the k_{ic} value.....	77



LIST OF TABLES

Table	Page
1.1 Occurrence of hemicelluloses in primary and secondary cell wall of plants.....	11
2.1 Stock solutions and buffer for plasmid DNA production	23
2.2 Cycling parameter for amplification of colony PCR	24
2.3 Solutions and buffer for SDS-PAGE	27
2.4 Oligo primers for amplification, colony PCR, and DNA sequencing	28
2.5 Selective antibiotic used for cloning, transformation and expression	29
2.6 Cycling parameter for OsXYL1 amplification	31
2.7 Materials used in transformation and expression <i>P. pastoris</i>	33
2.8 Reagents used in protein purification	38
2.9 Substrates for studies β -xylosidase OsXYL1 activity	41
3.1 Enzyme yields during purification of OsXYL1	61
3.2 Relative activity of β -xylosidase OsXYL1 toward nitrophenyl glycoside substrates	70
3.3 Apparent kinetic parameters of β -xylosidase OsXYL1 toward nitrophenyl glycoside substrates	73
3.4 Apparent kinetic parameters of β -xylosidase OsXYL1 toward xylooligosaccharide substrates (DP 2-6)	75

LIST OF ABBREVIATIONS

(n, μ , m)g	(nano, micro, milli) Gram
(n, μ , m)L	(nano, micro, milli) Liter
(μ , m)M	(micro, milli) Molar
°C	Degree Celsius
Abs	Absorbance
bis-acrylamide	N,N-methylene-bis-acrylamide
(k)bp	(kilo) Base pair DNA
BSA	Bovine serum albumin
CAZymes	Carbohydrate active enzymes
CV	Column volume
DMSO	Dimethyl sulfoxide
dNTPs	Deoxynucleoside triphosphates
DNaseI	Deoxyribonuclease I
EC	Enzyme commission
EDTA	Ethylenediaminetetraacetate
EtOAc	Ethyl acetate
GH3	Glycoside hydrolase family 3
h	Hour
HPLC	High performance liquid chromatography
IMAC	Immobilized metal affinity chromatography
IPTG	Isopropyl thio- β -D-galactoside
kDa	Kilo Daltons
LB	Luria-Bertani lysogeny broth
MeOH	Methanol
min	Minute
MW	Molecular weight
MWCO	Molecular weight cut off
NaCO ₃	Sodium carbonate

LIST OF ABBREVIATIONS (Continued)

NaOAc	Sodium acetate
(NH ₄) ₂ SO ₄	Ammonium sulfate
nm	Nanometer
OD	Optical density
PCR	Polymerase chain reaction
PMSF	Phenylmethylsulfonyl fluoride
4NP	4-Nitrophenyl
4NPA ^f	4NP- α -L-arabinofuranoside
4NPA ^p	4NP- α -L-arabinopyranoside
4NPGlc	4NP- β -D-glucopyranoside
4NPXyl	4NP- β -D-xylanopyranoside
rpm	Rotations per minute
S200	Superdex 200
SDS	Sodium dodecyl sulfate
SDS-PAGE	Polyacrylamide gel electrophoresis with SDS
SEC	Size exclusion chromatography
TEMED	Tetramethylenediamin
TLC	Thin-layer chromatography
T _m	Melting temperature
Tris	Tris-hydroxymethyl-aminoethane
UV	Ultraviolet radiation
v/v	Volume by volume
w/v	Weight by volume
X2	1,4- β -D-Xylobiose
X3	1,4- β -D-Xylotriose
X4	1,4- β -D-Xylotetraose
X5	1,4- β -D-Xylopentaose
X6	1,4- β -D-Xylohexaose

CHAPTER I

INTRODUCTION

1.1 Glycoside hydrolases

Glycoside hydrolases (GH; EC 3.2.1-3.2.3) are found widely in living organisms, in which they hydrolyze the glycosidic bonds between two carbohydrates or between carbohydrate (glycon) and non-carbohydrate (aglycon) moieties. Glycoside hydrolases are also referred to as glycosyl hydrolases, glycosidases, and carbohydrases. Glycoside hydrolases can catalyze the hydrolysis of O-, N- and S-linked glycosidic bonds and can be endo- or exo-acting glycosidases (Figures 1.1 and 1.2). Different glycosidases produce different products and display different ranges of bond specificity (Burmeister *et al.*, 1997; Lombard *et al.*, 2014).

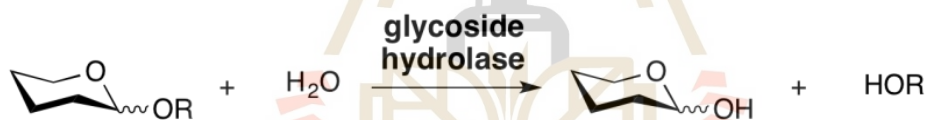


Figure 1.1 General catalytic mechanism of glycoside hydrolase. (<https://www.cazy-pedia.org>)

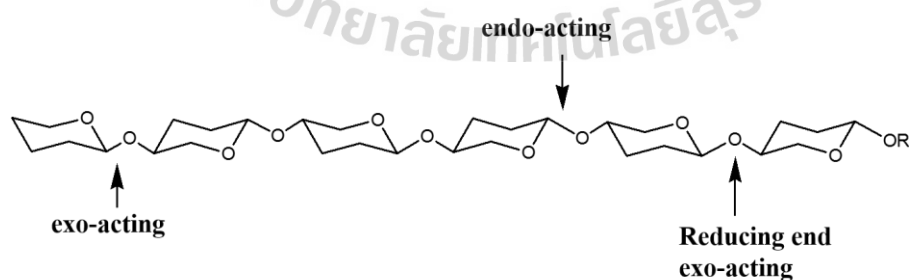


Figure 1.2 Endo-/exo-acting glycoside hydrolase. (www.cazypedia.org)

Glycoside hydrolases have been classified based on two independent criteria. The first criterion is substrate specificity, as designated by their EC (Enzyme Commission) numbers, while the second criterion is sequence homology (Henrissat, 1991; Rojan *et al.*, 2004). On the basis of sequence similarity, GH have been grouped into 173 families by the Carbohydrate-Active Enzymes (CAZy) classification system (<http://www.cazy.org> accessed 13 May, 2022; Cantarel *et al.*, 2009; Lombard *et al.*, 2014). In the case of poly-domain proteins, each catalytic module is considered separately.

A family was initially defined as a group of at least two amino acid sequences displaying significant similarity and with no significant similarity with other families (Henrissat, 1991). Later, some related families of glycosidases have been combined into clans (Henrissat and Bairoch, 1996; Henrissat and Davies, 1997). According to its definition, a clan is a group of families that are thought to have a common ancestry, which is recognized by significant similarities in tertiary structure, together with conservation of the catalytic residues and catalytic mechanism. Since three-dimensional structures are more strongly conserved than the sequence, clans (or superfamilies) are groups of GH families of enzymes with related structures (Henrissat and Bairoch, 1993; Henrissat and Davies, 1997). For example, glycosidases catalyze hydrolysis of glycosidic bonds of their substrates via two general mechanisms (Figure 1.3), leading to either overall inversion or retention of the anomeric configuration at the cleavage point, and members of one clan will generally all be either inverting or retaining (McCarter and Withers 1994; Davies and Henrissat 1995; Henrissat and Davies, 1997). To date, 18 GH clans (GH-A to GH-R) have been assigned in the database (<http://www.cazy.org> accessed 13 May, 2022).

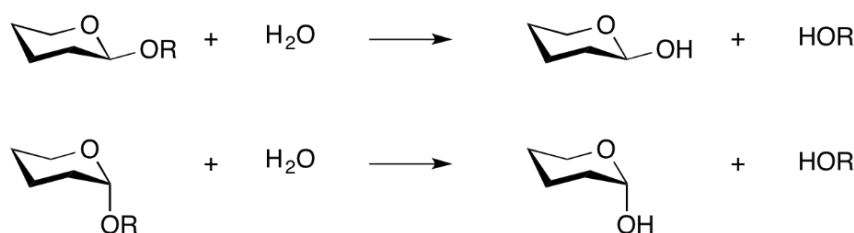
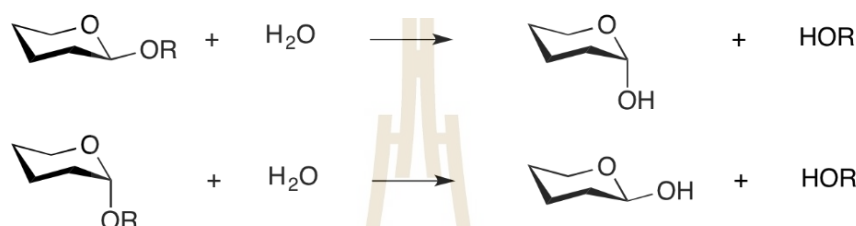
Retaining glycoside hydrolases:**Inverting glycoside hydrolases:**

Figure 1.3 Schematic representation of glycoside hydrolase mechanisms. (<https://www.cazypedia.org>)

1.2 Glycoside hydrolase family 3

Glycoside hydrolase family 3 (GH3) currently comprises enzymes with a number of known activities, such as β -glucosidase (EC 3.2.1.21), β -D-xylosidase (EC 3.2.1.37), α -L-arabinofuranosidases (EC 3.2.1.55), N-acetyl β -glucosaminidase (EC 3.2.1.52), exo- β -1,3-1,4-glucanase (EC 3.2.1), glucan β -1,3-glucosidase (EC 3.2.1.58), and cello-dextrinase (EC 3.2.1.74). GH3 is one of the largest and most diverse GH families in the CAZY database (Largaert, S. *et al.*, 2014; Suzuki, K. *et al.*, 2013). The GH3 is the main GH family of exo-acting as β -glucosidases, β -xylosidases, and α -L-arabinofuranosidases which are enzymes that are remove single glycosyl residues from the nonreducing ends of their substrates. Members of GH3 have a broad range of substrate specificities, and are widely distributed in fungi, bacteria, and higher plants, which suggests their distribution to play a significant role in such fundamental biological processes as the plant growth, development, and modification in response to environment stress and degradation of carbohydrate structures (Hrmova and Fincher, 2001; Suen *et al.*, 2003; Suzuki *et al.*, 2013). The microbial GH3 enzymes catalyze their

own cell wall glycans and have been applied for degrading of plant cell wall polysaccharides in biomass conversions (Reen *et al.*, 2003; Zhou *et al.*, 2011; Pozzo *et al.*, 2010, 2016; Dilokpimol *et al.*, 2011; Thongpoo *et al.*, 2013; 2014; Gruninger *et al.*, 2014; Takahashi *et al.*, 2018; de Carvalho *et al.*, 2018; Tong *et al.*, 2021). A number of GH3 enzymes are reported to be bi/multifunctional activity against particularly artificial substrates, such as 4-nitrophenyl- β -D-xyloside (4NPXyl), 4NP- α -L-arabinoside (4NPAr) and 4NP- β -D-glucoside (4NPGlc) and/or natural substrates (Lee, R. *et al.*, 2003; Zhou, *et al.*, 2011; Ditokpimol *et al.*, 2011; Yan *et al.*, 2012; Shi, *et al.*, 2013; Gruninger *et al.*, 2014; Nieto-Dominguez *et al.*, 2015; Tong, *et al.*, 2021).

GH3 enzymes vary considerably in the lengths of their polypeptide chains, and consequently, in the number of tertiary structure domains. Despite the high number of GH3 sequences in databases, relatively few three-dimensional (3D) structures are available from this GH family in the Protein Data Bank (PDB, <https://www.rcsb.org/>). A GH3 3D structure was the first determined in 1999, the HvExoI exo-glucan hydrolase from barley (*Hordeum vulgare* L., Varghese *et al.*, 1999), and it was used to explore structural understanding of the other enzymes in GH3 members. Interestingly, the known structures in GH3 members generally have multidomain architectures and display a varieties of domain organizations and contribution of different domains in supplying crucial catalytic residues. Nonetheless, the most common features of the domain organization is an N-terminal $(\alpha/\beta)_8$ TIM-barrel domain 1, which is more conserved and contains the active site pocket and catalytic nucleophile, followed by a (α/β) -sandwich domain, which is more variable and contains the catalytic acid/base residue. Examples of this structural variation in (α/β) sandwich domains are the $(\alpha/\beta)_6$ domain in β -glucan exoglucosidase HvExoI from barley (Harvey *et al.*, 2000), KmBglI from *K. marxianus* (Yoshida *et al.*, 2010) and HjCel3A from *Hypocrea jecorina* (Karkehabadi *et al.*, 2014), and the $(\alpha/\beta)_5$ domain found in the third domains of β -glucosidase HjCel3A from *H. jecorina* (Karkehabadi *et al.*, 2014) and TnBgl3B from *T. neapolitana* (Pozzo *et al.*, 2010; 2016). The GH3 third domain with unspecified fold was refined in β -xylosidase from *Trichoderma reesei* (Rojas *et al.*, 2005) and β -glucosidase TnBgl3B from *T. neapolitana*. A PA14 domain is inserted in the domain 2

and was shown to bind glucose and to play a critical role in the substrate specificity of the *KmBgl* (Yoshida *et al.*, 2010).

The catalytic nucleophile in all GH3 members is a conserved aspartate (Asp or D) residue in domain 1 of the plant enzymes and it is located in a highly conserved GFVSDW motif and surrounded by a landscape of amino acid residues with similar characteristics in other family 3 enzymes. However, the catalytic acid/base residue occurs in a highly variable region and is difficult if not impossible to predict from simple alignments. The catalytic acids in studied β -glucosidases, exoglucanase and glucosylceramidase is a glutamate (Glu or E) residue is positioned in the (α/β) sandwich domain 2 and the active site is located at the interface of the two domains (Chir *et al.*, 2002; Pozzo *et al.*, 2010; Varghese *et al.*, 1999; Yoshida *et al.*, 2010). In studied glucosidases from *K. marxianus* and *T. neopolitana*, a pocket with a -1 and +1 subsite occurs in this region with most of the interactions taking place at the -1 subsite (Pozzo *et al.*, 2010; Yoshida *et al.*, 2010).

Although plant GH3 members are still largely incompletely understood, in terms of their physiological functions and biological roles, the predicted functions of the GH3 enzymes (Luang S., Hrmova, M., and Ketudast Cairns, J.R., 2010) involve: (i) the biodegradation and assimilation of oligo- and polysaccharides, (ii) modification of bacterial macrolide antibiotics and other toxic plant compounds, and (iii) turnover of cell wall components. The plant GH3 enzymes can be broken into two major phylogenetic groups containing β -glucosidases/exoglucanases in one and β -D-xylosidases/ α -L-arabinosidases in the other (Prawisut *et al.*, 2020).

Biochemical and genetic characterization implicated GH3 enzymes action in cell wall in different tissues of various plants. This includes their distribution and activity for autolysis function that can lead to modification and reorganization of wall polysaccharides, such as the barley *HvExoI* and *HvExoII* β -glucan exohydrolase found in the cell wall of the starchy endosperm (Hrmova *et al.*, 1996), and exo- β -D-glucanase from the cell wall of developing maize seedling (Kim *et al.*, 2000), and exoglucanase in coat and cell wall of maize pollen grain (Suen *et al.*, 2003). Similarly, an endo-1,3-1,4- β -D-glucanase and α -L-arabinofuranosidase were isolated from maize primary root during elongation (Zhu *et al.*, 2006). A bifunctional of β -xylosidase/ α -L-arabino-

furanosidase for arabinoxylan cell wall turnover of XLY and ARA-I was isolated from germinated barley grain (Lee *et al.*, 2003), MsXyl1 from alfalfa roots (Xiong *et al.*, 2007) and RsAraf from immature seeds of radish for seed development and young seedling (Kotake *et al.*, 2006). GH3 enzymes were also implicated in cell wall modification in developing and ripening in fruits (Itali *et al.*, 2003; Martinez *et al.*, 2004; Tateishi *et al.*, 2005; Bustamante *et al.*, 2006; Figueroa *et al.*, 2010; Sun *et al.*, 2013). Other authors identified genes and enzymes exhibiting activity in stem tissues of Arabidopsis (Goujon *et al.*, 2003; Minic *et al.*, 2004) and in microspore and pollen during development of tobacco (Hrubá *et al.*, 2005). GtGen3A β -glucosidase of *Gentiana* is involved in the gentio-oligosaccharide metabolism (Takahashi *et al.*, 2018). The PtaBXL1 wood-associated xylosidase gene was reported as a putative xylan remodeling enzymes in poplar tension wood (Decou *et al.*, 2009).

1.3 Plant Cell Wall

The cell wall is the protective layer in many cells including plants, fungi, algae, and bacteria. It is a dramatically feature of plant physiology not seen in animal cells. Plant cell walls are constructed outside the cellular membrane to give plants a strong barrier and connection to the environment and neighbor cells. The cell wall has many functions in plants, such as providing structural support for the plant body, keeping the shape and allow the plant to grow to great heights, providing limited plasticity, preventing loss of water and overexpansion caused by water, filtering, and also protecting the plant against biotic and abiotic stresses, such as from insects and pathogens (Somerville *et al.*, 2004; Malinovsky *et al.*, 2014; Carpita, N. and McCann, 2015). Plant cell walls contribute to the value of many plant-derived commercial products, including wood, fibers and fabrics, thickening agents, drug delivery systems, and fruits. As robust cell wall architectures are integrated during plant growth and development, a biosynthesis and deposition of polysaccharides begins with the aggregation of secretory vesicles to form a cell plate (Drakakaki *et al.*, 2015; Rennie and Scheller, 2014). The cell wall composition is cell-specific and linked to its function that depends on their cell type and in response to environment stimuli (Carpita and

McCann, 2015; Houston *et al.*, 2016; Voiniciuc, Pauly, and Usadel, 2018; Barnes and Anderson, 2018; Camacho-Fernandez *et al.*, 2021).

Plant cell wall structure is complex, as presented in Figure 1.4, and contains polysaccharides (cellulose and hemicellulose), and phenolic polymers (lignin), together with other less abundant compounds, such as pectins and soluble protein. These constituents vary in different cell types and plant species (Heredia, *et al.*, 1995; Crosgrave, 2016; Hernandez-Beltran *et al.*, 2019; Camacho-Fernandez *et al.*, 2021).

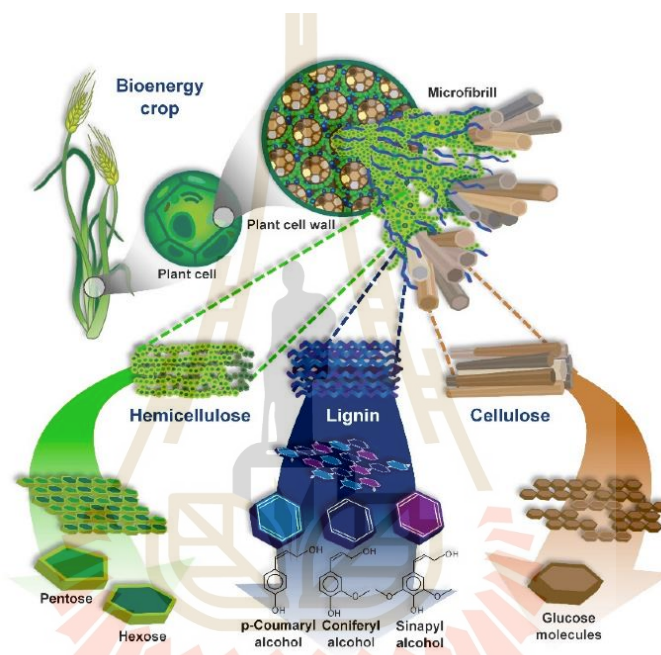


Figure 1.4 Plant cell wall structure and compositions. The plant biomass is mainly composed of cellulose, hemicelluloses, and lignins. (Derived from Hernandez-Beltran *et al.*, 2019).

Multilayer structures of plant cell wall consist of up to three sections: the middle lamella, primary cell wall, and secondary cell wall (Cosgrove, 2016). As shown in Figure 1.5A, the middle lamella is the top in the space connected to the adjacent cells and is pectin polysaccharide rich. The primary cell wall is a middle layer held together by the sticky layer of middle lamella to form the conducting tissue system arranged in numerous vascular bundles which is established in young cells during division in the first stages of cell development and act to provide flexibility and basic structure support, protecting cells, and mediating cell-cell interactions. The secondary

wall is gradually deposited between the primary cell wall and the plasma membrane at a later stage when the cell has fully expanded in specialized cells (xylem and fibers). Alternatively, primary cell walls can be divided into type I or type II based on their compositions, as shown in Figure 1.5B. Type I primary cell walls are found in noncommelinoid monocots, eudicots, and gymnosperms while type II walls are typical for commelinoid monocots, including grasses (Carpita, 1996; Vogel, 2008). Type I and type II cell walls have a similar amount of cellulose, but are different in non-cellulosic polymers, which in the type I walls are largely xyloglucan with small amounts of glucuronoxylan and glucomannans, and about 35% of the wall mass is pectin, while the type II walls have a low xyloglucan and pectin content, but are high in arabinoxylan (Carpita, 1996; Vogel, 2008). Type II walls also contain hydroxycinnamic acid bound to arabinoxylan, which has not as yet been found in type I walls (Vogel, 2008; Mimic and Jouanin, 2006). The secondary cell wall compositions contain more cellulose with a higher degree of polymerization and crystallinity for better mechanical strength, and the structure is reinforced in woody tissues. Thickening of secondary cell walls is mostly due to the deposition of cellulose (cotton fibers), xylans (wood), and lignins (lignins in xylem vessels or sclerenchyma fibers). Lignin is a polyphenolic polymer that crosslinks with polysaccharides and hydroxycinnamic residues found on xylans (Vogel, 2008). The secondary wall composition increases the strength of the walls and reduces their flexibility, allowing the resulting tube-like structure to serve as water conduits and as the mechanical or structural support for the plant. Additional hydrophobic lignins can result in dehydration of the wall compartment (Marriott *et al.*, 2016; Lampugnani *et al.*, 2018).

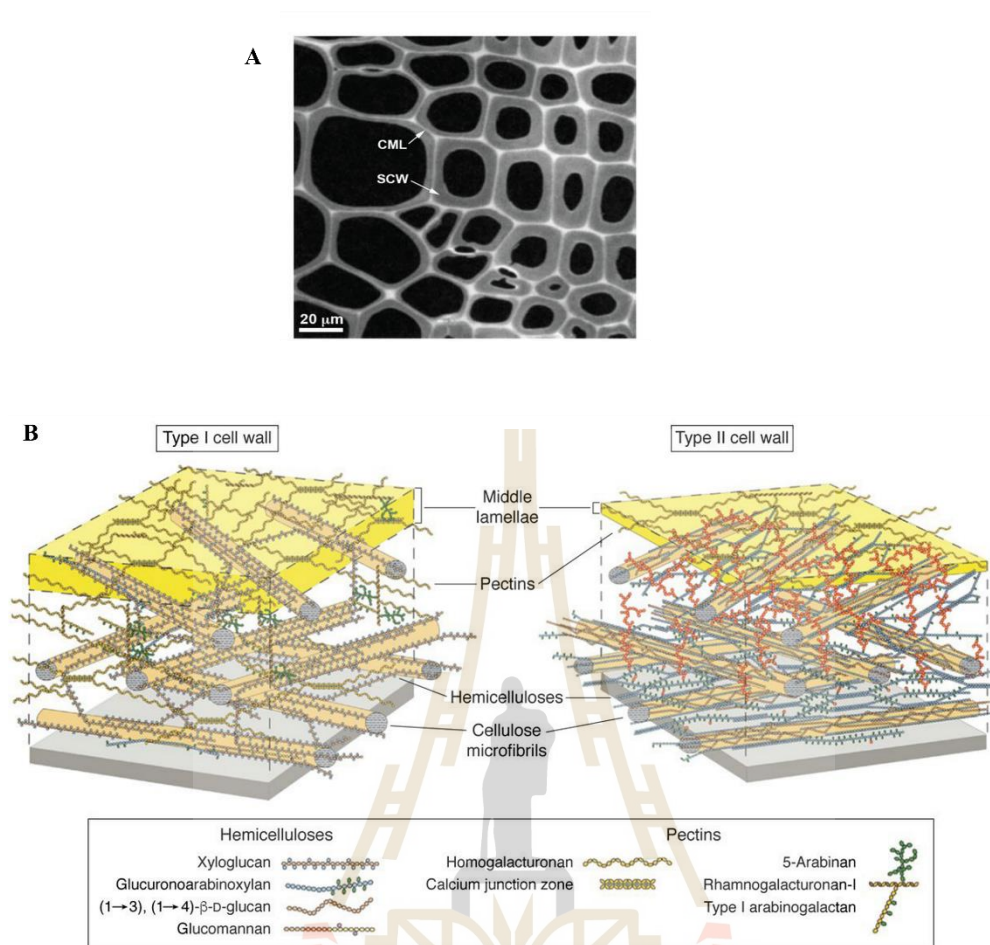


Figure 1.5 Plant cell wall structure. (A) Microscopic view of plant cell wall by fluorescence image of a cross-section of developing wood in the stem of *Pinus radiata*. The compounds of middle lamella (CML) fuses with the primary wall. A secondary cell wall (SCW) is elaborated with the CML. (B) Models of primary cell wall type I and II assembled and arranged in layers that contains cell wall compositions (Derived from Carpita and McCann, 2020).

Cell wall composition is tightly controlled in different cell types and in relation to growth and development, the differences between various cell types in cell wall composition and structure could reflect differences in its function (Somerville *et al.*, 2004; Barnes and Anderson, 2018; Lampugnani *et al.*, 2018; Carpita and McCann, 2020). The wall itself is synthesized in dynamic manner: mobile cellulose synthesis complexes produce cellulose microfibrils at the cell surface, glucans present in the

cell wall, including cellulose (multiple chains of β -(1,4)-glucan), callose (β -(1,3)-glucan), xyloglucan (β -(1,4)-glucan backbone with sidechains) and mixed linkage β -(1,3)-(1,4)-glucan, are synthesized mainly in the form of crystalline microfibrils as well as in an amorphous form (Carpita and McCann, 2000). In contrast, matrix polysaccharides of hemicelluloses and pectins, and glycoproteins are produced in the Golgi by the membrane-bound enzymes and deposited to the cell surface via the secretory apparatus (Kim and Brandizzi, 2016), the structures of matrix polysaccharides are modified by various apoplast enzymes (Amos and Mohnen, 2019). The lignification occurs in the final step of secondary cell wall biosynthesis with monolignols embedded in the polysaccharide wall matrix polymerized by oxidative enzymes such as laccases and peroxidases. Plant cell wall related enzymes are located in the wall itself or in the plasma membrane after biosynthesis and deposition, and participate in the degradation of different cell wall polysaccharides except for cytoplasmic xylanase from barley (Casper *et al.*, 2001).

The study of cell wall biosynthesis requires strategies of genetic and genomic application to identify genes and proteins which function to synthesize polysaccharides found in the complexity in wall. However, overall knowledge regarding the biochemistry, cell biology, and regulation of polysaccharide biosynthesis are still largely incomplete. Many research efforts focus on the enzymes involved in wall polysaccharides processing.

1.4 Hemicelluloses and Heteroxylans

Hemicelluloses are the second most abundant polysaccharides in the plant cell wall, after cellulosic polymer. Hemicelluloses are heteromeric polysaccharides that associate with cellulose microfibrils via hydrogen bonds to provide a cross-link network, and in some walls also link with lignin (Mussatto *et al.*, 2008). The most important biological role of hemicelluloses is their contribution to strengthening the cell wall, their abundance varies depending on their source. Hemicelluloses include xyloglucans, heteroxylans, heteromannans, and mixed linkage glucans. The structures of xyloglucans, heteroxylans and heteromannans are based on an essentially linear backbone of β -1,4-linked monosaccharides (Scheller and Ulvskov, 2010).

Hemicelluloses have varied monosaccharide contents, comprising pentoses: D-xylose (Xyl) and L-arabinose (Ara); hexoses: D-glucose (Glc), D-galactose (Gal), L-fucose (Fuc), D-mannose (Man), and L-rhamnose (Rha); and uronic acids: D-glucuronic acid (GlcA) and 4-O-methyl-D-glucuronic acids (MeGlcA), some of which are represented in the monosaccharides of glucuronylarabinoxylan in Figure 1.6. Occurrence of hemicelluloses in primary and secondary walls of plants is summarized in Table 1.1.

Table 1.1 Occurrence of hemicelluloses in primary and secondary cell walls of plants. Amounts of polysaccharides in wall are given in % (w/w).

Polysaccharide	Grass walls		Dicots walls	
	Primary	Secondary	Primary	Secondary
Xyloglucan	2-5	Minor	20-25	Minor
(Glucurono)arabinoxylan	20-40	40-50	5	-
Glucuronoxylan	-	-	-	20-30
(Gluco)mannan	2	0-5	3-5	2-5
Galactoglucomannan	-	-	-	0-3

Xyloglucans, as there are presented in Figure 1.5B, are the most common polysaccharides in the type I primary walls found in dicots and consist of β -1,4-linked glucose backbone which is substituted with α -xylopyranose (α -D-Xylp) residues at C-6. Some of the α -D-Xyl residues are substituted at C-2 with β -D-Gal or an α -L-Fuc-1,2- β -D-Gal substituted with an *O*-acetyl (Ac) group. A whole series of oligosaccharides that was generated enzymatically have been characterized and reveal rarer structures. There are, therefore, at least eight linkages that have to be accounted for in the enzymology of xyloglucan synthesis.

(Glucurono)arabinoxylans make up the major component of hemicelluloses in primary wall (mainly in type II) of monocots, especially in grasses, which are also a minor constituent of dicot primary walls (Vogel, 2008). Their deposition in the primary walls is a function of the extent of development of growing cells, and they also function as carbohydrate reserves in seeds and bulbs of certain plant species. The (glucurono)arabinoxylans consist of β -1,4-linked D-Xylp backbone, are mostly

substituted with single α -L-Ara, Gal, and GlcA-rich side chains. Less commonly, oligosaccharides, such as β -D-Xylp-(1,2)- α -L-Araf- and β -D-Galp(1,4)- β -D-Xylp-(1,2)- α -L-Araf- are added to the xylan backbone. The Araf residues are mostly linked to the C-3 position of the main chain Xyl residues, but in some cases are found on C-2 or on both C-2 and C-3. The GlcpA residues are usually linked to the C-2 of the Xyl residues (Fincher and Stone, 2004; Izydorczyk, M.S. and Dexter, J.E., 2008). Other hemicelluloses of monocot walls are the mixed linked glucans. Their general structure was also deduced enzymatically using a sequence-dependent endoglycanase, a β -D-glucanohydrolase from *Bacillus subtilis* that catalyzes the hydrolysis of a β -1,4-glucosyl linkage only if preceded by a β -1,3-linked glucosyl unit on the nonreducing side. Some galactans have also been considered hemicellulosic polysaccharides on the basis of extractability.

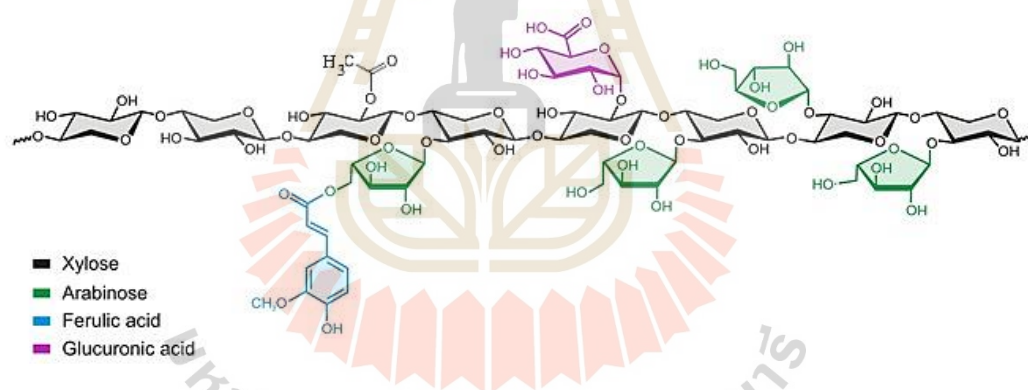


Figure 1.6 Chemical structure of (glucurono)arabinoxylan. The backbone of β -(1,4) xylose residues (long chain) and side chains: arabinose (green), acetyl groups (black), glucuronic acid (magenta) and ferulic acid (blue). (Derived from Dyoni, M. O. *et al.*, 2019)

Glucuronoxylans are the major hemicelluloses in secondary cell walls in higher plants, and thus in wood tissue that is required for normal plant growth and development that increases cell wall recalcitrance and defend against herbivores and pathogens. They broadly consist of β -1,4-linked Xylp backbone are substituted by units of α -(1,2)-GlcA, MeGlcA, Ara, and ester bond with acetyl groups (Ac). There are at least six types of linkages involved in their biosynthesis. In dicots, the side chains

are linked via an α -(1,2) with D-glucuronic acid (GlcA) or 4-O-methyl-D-glucuronic acid (MGA) at the O-2, resulting in glucuronoxylans (GX; Vries, D. R. and Visser, J., 2001) and wood xylans are acetylated. The acetyl groups play a major role in the organization of lignified cell walls, since they can cross-link with lignin and interact with cellulose (Hatfield et al., 1999). The α -L-arabinose residues (Ara) may be α -(1,2) or α -(1,3) linked in xylans. Other minor components are D-galactose (Gal) and ferulic acid (FeA) or *p*-coumaric acid residues linked to the O-5 of some α -L-arabinofuranosyl residues can also be found. (Vries, D. R. and Visser, J., 2001).

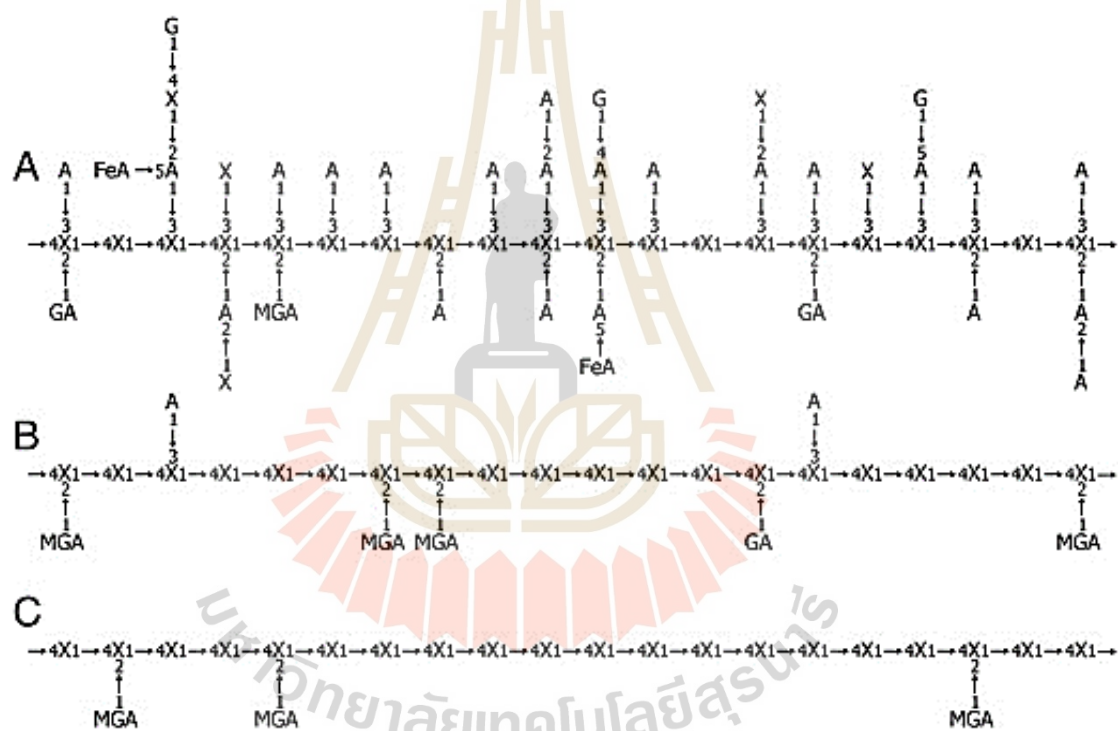


Figure 1.7 Representations of chemical structures of xylans. The xylans typical of (A) grasses and cereals; (B) softwood; (C) hardwood are shown. (X, D-xylose; A, L-arabinose; G, D-galactose; GA, D-glucuronic acid; MGA, 4-O-methyl-D-glucuronic acid; FeA, ferulic acid) (Derived from Rudolf, D. and Robert F.H.D., 2012).

In order to break down the many structures of cell wall polymers, plant cell wall degrading enzymes are a heterogeneous group of enzymes and divided in many categories and sub-categories depending on their action on the wall polysaccharides. However, hemicellulose is mainly hydrolyzed by glycoside hydrolases and the most used in industrial applications are endo-acting GH, such as xylanase, galactonases and mannanases, and exo-acting enzymes, such as β -xylosidase, α -L-arabinofuranosidase, β -galactosidase, and β -mannosidase (Giovanna *et al.*, 2020). These enzymes are mainly produced from hyperthermophilic microorganisms, such as fungi and bacteria, including those in the rumen biota of animals (Sunna, A. & Antranikian, G., 1997; Prade, R.A., 1996, Beg, Q.K., et al, 2001, Pozzo et al., 2010; 2016), which serve as the source of enzymes for industrial applications.

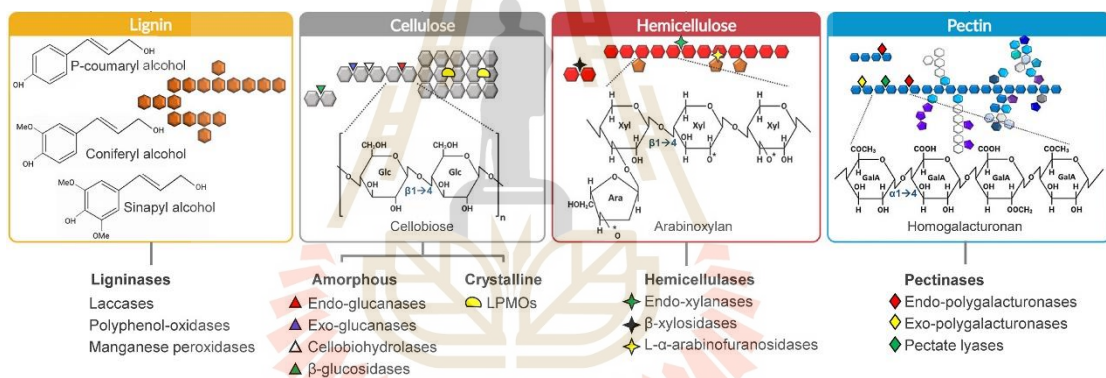


Figure 1.8 Plant cell wall polysaccharides and substrate specificity of degrading enzymes. (Derived from Giovanna *et al.*, 2020)

Glycoside hydrolase involved in degrading the arabinoxylan component of the hemicellulose (as shown in Figure 1.8) include endo-xylanase (EC 3.2.1.8) that act to cleave the xylan backbone at the β -(1,4)-linkages to break it into xylooligosaccharides (XOS), β -xylosidase (EC 3.2.1.37) that cut the glycosidic bonds at the nonreducing termini to cleave XOS to xylose units. In addition, debranching enzymes, such as α -L-arabinofuranosidases (EC 3.2.1.55) that are exo-acting at the α -(1,2)- or α -(1,3)-linkage of α -L-arabinofuranose residues, and α -glucuronidases (EC 3.2.1.139) that hydrolyzes α -(1,2)-linkage of glucuronic acid. Complete breakdown also requires feruloyl esterases

(EC 3.1.1.73) that detach the ferulic acid from α -L-arabinofuranose residue, and acetyl xylan esterases (EC 3.1.1.72) that deacetylate xylan.

The cell walls of grasses are classified as type II primary cell walls, because their hemicellulose characteristically contains a larger amount of heteroxylan polysaccharides, i.e. (glucurono)arabinoxylan, than xyloglucan and pectic polysaccharides (Vogel, 2008). Importantly, the heteroxylans in grasses have advantage in practical applications of cereal bread making and brewing, and provide soluble dietary fiber for nutrition and human health (Collins, *et al.*, 2010). In addition, cell walls from straw and bran have received considerable attention for use in biofuel production (Burton and Fincher, 2014; Loque *et al.*, 2015; Fry, 2017) and production of other biomaterials with valuable commercial applications (Bar-Cohen, Y., 2012). As mentioned before, (glucurono)arabinoxylans also synthesized by enzymes in the Golgi apparatus. (Glucurono)arabinoxylans synthesis thus requires the coordinated action and regulation of these synthetic enzymes as well as others that synthesize and transport substrates into the Golgi.

1.5 β -Xylosidase

β -Xylosidase (3.2.1.37) from various sources are currently divided into 11 families (GH1, GH3, GH5, GH30, GH39, GH43, GH51, GH52, GH54, GH116 and GH120) based on amino acid sequence similarities. Members of each family exhibit characteristic substrate specificities, reaction mechanisms, and three-dimensional structures (Herissat, 1998). Except for GH43, these families use the retaining mechanism that remove single residues from the nonreducing end of their substrate by a two-step mechanism through a covalent enzyme-glycon intermediate, which is subsequently hydrolyzed via an oxocarbenium ion-like transition state (David, G., and Henrissat, B., 1995). Most β -xylosidases are found in bacteria, fungi and higher plants. However, enzymes that exhibit β -xylosidase activity in plants belong only to the GH3 and GH51 families.

The retaining β -xylosidases operate via a two-step mechanism (Koshland, 1953), the configuration of the substrate is regenerated by inversion in each of the

glycosylation and deglycosylation steps (Zechel, D.L. and Withers, S. 2001). In the glycosylation step, one carboxylic acid group acts as catalytic nucleophile, forming a glycosyl-enzyme intermediate complex at the anomeric carbon with inverted (α -) configuration. The transition state has a mainly dissociative character, breaking of the glycosidic linkage occurs before the attack by the nucleophilic group. The other carboxylic acid group acts as a protonated acid/base to transfer a proton to the glycosidic oxygen. Departure of the aglycon creates space, allowing a nucleophilic water molecule to come closer to the anomeric center. In the deglycosylation step, wherein the enzyme complex is hydrolyzed by water, the water molecule that serves as the nucleophile is activated by proton extraction by the now negatively charged acid/base carboxylic group and attacks the anomeric carbon to release the glycon product from the intermediate. The attack re-inverts the inverted configuration at the anomeric carbon and the released glycon is in the same stereochemistry as the substrate. The hydrolysis of the β -glycosidic linkage can lead to β -configuration, as shown in Figure 1.9, as can the transglycosylation activity on a β -glycosidic linkage (Figure 1.10) with other acceptors, such as monosaccharides, disaccharides, sugar alcohols, aliphatic or aromatic alcohols and hydroquinones of GH3 β -xylosidases were reported (Dilokpimol *et al.*, 2011; Kurakake *et al.*, 2005; Eneyskaya *et al.*, 2003; Park *et al.*, 2017).

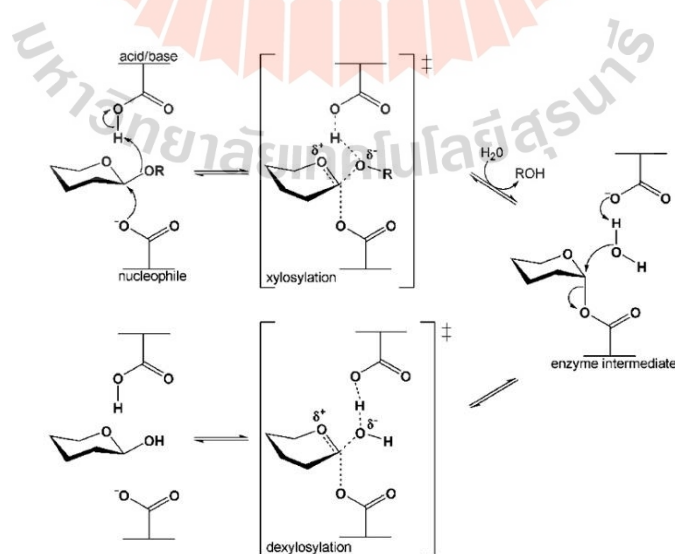


Figure 1.9 The glycoside hydrolases retaining mechanism. (Derived from (Figure 1b.) Jordan, D.B. and Wagschal, K., 2010).

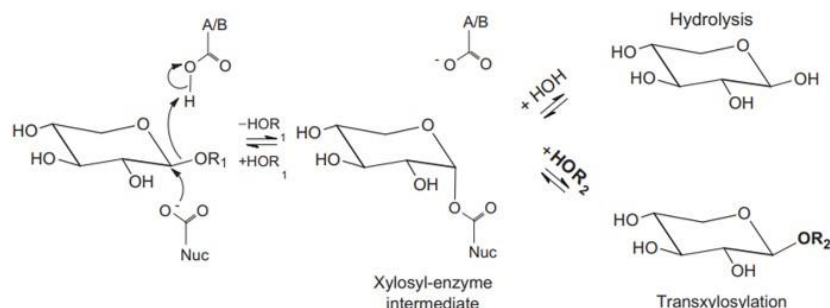


Figure 1.10 Schematic representation of hydrolysis and transglycosylation activity of GH3 β -xylosidases. A/B, catalytic acid/base; Nuc, catalytic nucleophile; R1, R2, carbohydrate residues. (Derived from Dilokpimol *et al.*, 2011)

Exo-acting β -xylosidases have a unique ability to hydrolyze the bonds to nonreducing β -D-xylosyl residues of xylooligosaccharides (XOS) to release single xylose units (Figure 1.11). β -Xylosidases can cleave the xylobiose and XOS and thereby improve the efficiency of endoxylanases by removing a cause of inhibition, resulting in more efficient xylan hydrolysis (Zanoelo *et al.*, 2004). The purified β -xylosidases usually do not hydrolyze xylan and their best substrate is xylobiose and their affinity for XOS is inversely proportionate to its degree of polymerization, with most efficient and generally highly specific hydrolysis of small unsubstituted XOS (DP 3-7) (Polizeli *et al.*, 2005). However, most of the characterized β -xylosidases are also inhibited by xylose, arabinose, glucose, and/or other monosaccharides (Jordan, D.B. and Wagschal, K., 2010).

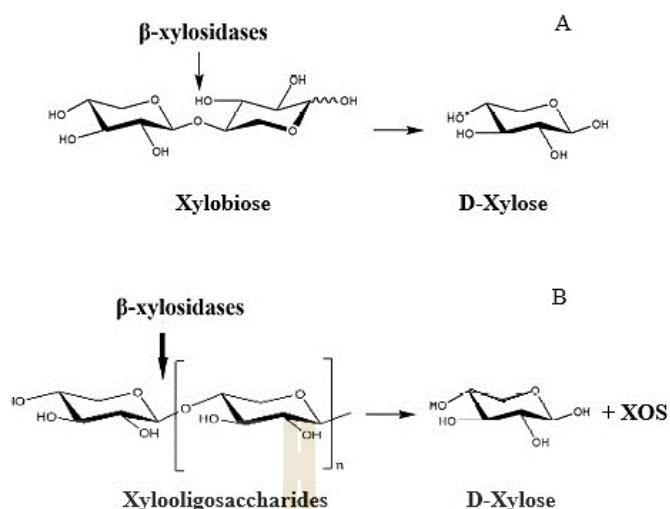


Figure 1.11 Schematic representation of degradation of xylooligosaccharides by β -xylosidase to released D-xylose. Hydrolysis of xylobiose (A) and xylooligosaccharides (B). (Derived from Kousar *et al.*, 2013),

In plants, β -xylosidases have been purified and partially characterized from wheat flour (Cleemput *et al.*, 1997), sycamore cell culture (Tezuka *et al.*, 1993), pea seedlings (O'Neill *et al.*, 1989), and sugarcane (Chinen *et al.*, 1982). The ARA-I and XYL enzymes and their genes from young barley seedlings were purified, sequenced, and biochemically characterized (Lee *et al.*, 2003). XYL1 (encoded by the *AtBXL1* gene), XYL3, and XYL4 from *Arabidopsis thaliana* encoding putative β -xylosidases were identified, and a role in secondary cell wall metabolism and plant development proposed (Goujon *et al.*, 2003; Mimic *et al.*, 2004; 2006; 2007). Other plant β -xylosidases have been reported and characterized so far include cell wall proteins from maize (*Zea mays*) involved in primary root elongation (Zhu *et al.*, 2006) and during senescence stage (Han and Chen, 2010), and those in potato tubers (Peyer *et al.*, 2004). Other genetically characterized GH3 genes include At3g62710 and At5g10560 in *Arabidopsis* and similar genes in tobacco microspores and pollen development (Hruba *et al.*, 2005), *LeXYL1* and *LeXYL2* from tomato expressed during fruit development and ripening (Itali *et al.*, 1999; 2003), PpARF2 from Japanese Pear (*Pyrus pyrifolia*) fruit (Tateishi *et al.*, 2005), *FaXyl1* β -xylosidase in strawberry (*Fragaria xananassa*) fruit (Martinez *et al.*, 2004; Bustamante *et al.*, 2006), RsAraf1 in

the immature seeds from radish (*Raphanus sativa*) (Kotake *et al.*, 2006), *MsXyl1* expressed in roots, root nodules, and flowers of alfalfa (*Medicago sativa* L., Xiong, J.-S., *et al.*, 2007), the *PtaBXL1* of wood-associated xylosidase gene for xylan remodeling enzymes in poplar tension wood (Decou *et al.*, 2009). Another example from fruit is *PpAz152* β -xylosidase gene regulated during abscission, organ senescence and wounding in peach (Ruperti *et al.*, 2002). However, there are many more genetic studies than enzymatic characterizations of GH3 enzymes.

To gain more insight into plant β -xylosidase enzymes, the recombinant expression, purification and characterization of a putative rice GH3 β -xylosidase was conducted in this thesis. Its substrate specificity, kinetic study and molecular properties were studied with specific artificial 4NPXyl and XOSs, as well as its potential for application to make glycosides by transglycosylation.

1.6 Research objectives

1.6.1 To clone and express a putative OsXYL1 β -xylosidase from a putative rice GH3, optimize for suitable expression conditions and purify the protein.

1.6.2 To characterize the physicochemical properties and enzyme activity of the purified OsXYL1 β -xylosidase.

1.6.3 To identify substrates for OsXYL1, as a means of assessing its biochemical and biological function and potential application.

CHAPTER II

MATERIALS AND METHODS

2.1 Sequence analysis

The sequences of putative GH3 β -xylosidase from rice and characterized plant GH3 proteins were downloaded from NCBI database (<https://www.ncbi.nlm.nih.gov>), along with the structural domain analysis from Pfam done by NCBI. Protein sequence alignments were performed by the Clustal Omega (1.2.4) algorithm in the EMBL-EBI website (<https://www.ebi.ac.uk/Tools/msa/clustalo>), and a sequence-based phylogenetic tree was computed by the Neighbor-Joining algorithm in Clustal Omega without distance correction. A phylogenetic tree was also calculated by the maximum likelihood method using the software MEGA11. Translations of a nucleotide to a protein sequence was done with the ExPASy-Translate tool (<https://web.expasy.org>). Homology modeling was used to build the predicted structure model from the protein sequence based on the X-ray crystal structures by SWISS-MODEL (<https://swiss-model.expasy.org/interactive>). The DNA sequencing results were analyzed for the sequence profile and plasmid maps generated by SnapGene viewer (<https://www.snapgene.com>). N-Glycosylation was predicted by the NetN-Glyc 1.0 Server (<http://www.cbs.dtu.dk/services/NetNGlyc>) at the Technical University of Denmark. Melting temperature (T_m) was calculated from Basic T_m Calculations (<http://insilico.ehu.es/tm.php>).

2.2 General methods

2.2.1 Competent bacterial cell preparation

The glycerol stock of competent cell was streaked on an LB agar plate without antibiotic and incubated at 37 °C for 16-18 h until colonies were visible. A single colony was inoculated into 5 mL of LB broth without antibiotic and grown at 37 °C with 200 rpm shaking for 14-16 h as starter, then, 500 μ L starter culture was inoculated to 50 mL of LB broth in a 250 mL Erlenmeyer flask, and cultured at 37 °C, 200 rpm until the optical density at 600 nm (OD_{600}) reached 0.4-0.6 (shaking 3-5 h). The culture medium

was poured into pre-chilled 50 mL centrifuge tubes and chilled on ice for 10 min for cooling the cells just prior to centrifugation to collect the cells at 3,500 rpm at 4 °C for 10 min. The cell pellet was kept on ice and resuspended in 10 mL of ice-cold, sterile 0.1 M CaCl_2 , gently and slowly mixed by pipetting while keeping the tube on ice until it looked homogeneous and further kept on ice for 20 min. This step was washing out the residual LB medium that may interfere with the transformation. The cell resuspension was centrifuged at 3,500 rpm, 4 °C for 10 min to collect the pellets. Finally, the pellets were resuspended with 2 mL of 0.1 M CaCl_2 , incubated on ice 1 h and glycerol was added to 15% final concentration. The suspension was then aliquoted into 1.5 mL microcentrifuge tubes with 50 μL per tube. The competent cells were used immediately or kept at -80 °C until use.

2.2.2 Bacterial transformation

After thawing 50 μL of competent cells on ice, ligation mixtures, mutagenesis reactions or plasmid controls (1 or 2 μL) were added and gently mixed by pipetting up and down. The mixture was immediately placed on ice for 30 min then heat shocked at 42 °C for exactly 45 s and quickly chilled on ice for 2 min. Then, 200-400 μL LB broth was added to the cell mixture, which was then incubated at 37 °C for 1 h. Two hundred microliters of the transformed cells were spread on the selective LB agar plate containing the selective antibiotic(s). Once dry, the plates were incubated inverted at 37 °C for 12-16 h.

2.2.3 Bacterial glycerol stocks

Bacterial cell stocks were prepared by adding 250 μL of 60% (v/v) sterile glycerol (15% final concentration) to 750 μL of freshly grown 5 mL overnight culture. The glycerol mixture was placed on ice and then stored at -80 °C.

2.2.4 Plasmid extraction by alkaline lysis

The composition of solutions and buffer used in this method are listed in Table 2.1. A single colony was picked and inoculated into 5-10 mL of LB broth in a 50 mL centrifuge tube, followed by incubation at 37 °C, 200 rpm for 16-18 h. The cultures were pelleted in sterile microcentrifuge tubes by centrifugation at 12,000 rpm, for 1 min. Cell pellets were resuspended in 150 µL of ice-cold resuspension buffer by pipetting, followed by adding 300 µL freshly prepared lysis solution and the tubes were inverted gently by hand 5-10 times, until they were completely mixed, and incubated on ice for 5 min. After that, 300 µL of ice-cold 3 M potassium acetate, pH 4.8, was added and the tubes briefly inverted 5-10 times. The reaction was incubated on ice for 5 min, then centrifuged at 12,000 rpm at 4 °C for 10 min. The clear solution containing the plasmid was separated and transferred to a new tube. One equal volume of 1:1 (v/v) phenol:chloroform:isoamyl alcohol solution was added to the tube, then inverted 10 times. The mixture was centrifuged at 12,000 rpm for 10 min at room temperature, then the upper layer was carefully transferred into a new tube without disturbing the lower layer. Two volumes of absolute ethanol were added to precipitate DNA, and the tube was briefly inverted 5-10 times, then incubated on ice for 30 min. The precipitated DNA was collected by centrifugation at 12,000 rpm for 10 min. Then, the DNA pellet was resuspended in 100 µL of TE buffer (pH 8.0) containing 2 µg RNase A, followed by incubation 37 °C for 10 min. After that, 70 µL of cold 20% PEG 6000/2.5 M NaCl was added and the tube was subsequently incubated on ice for 1 hour, then centrifuged. The pellet was washed with 500 µL 70% ethanol and centrifuged to remove the remaining PEG and NaCl. The left-over ethanol was removed by speed vacuum at 50 °C, 2,000 rpm. Finally, the DNA was re-dissolved in 20 µL of HPLC water or TE buffer, the DNA solution was measured the concentration and purity by measuring the absorbance at 260 nm and 280 nm on a NanoDrop spectrophotometer, then immediately used or kept in -30 °C until use.

Table 2.1 Stock solutions and buffer for plasmid DNA production.

Stock solution	Composition
100 mg/mL Ampicillin	5 g Ampicillin in 50 mL of distilled H ₂ O
30 mg/mL Kanamycin	1.5 g Kanamycin in 50 mL of distilled H ₂ O
12.5 mg/mL Tetracycline	0.625 g Tetracycline in 50 mL of 70% EtOH
25 mg/mL Chloramphenicol	1.25 g Chloramphenicol in 50 mL of 70% EtOH
LB media	2% Peptone, 1% yeast extract, 1% NaCl, autoclaved
LB plates	LB media, 1.5% (w/v) agar, autoclaved
Resuspension buffer	50 mM Glucose, 10 mM EDTA, 50 mM Tris-HCl, pH 8.0
Lysis buffer	1% Sodium dodecyl sulfate (SDS), 0.2 N NaOH
Phenol: chloroform: isoamyl alcohol (25:24:1, v/v)	25 mL Phenol, 24 mL chloroform, 1 mL isoamyl alcohol
1 mg/mL RNase A	10 mg RNase A in 10 mL TE buffer
TE buffer	50 mM Tris HCl, pH 8.0, 10 mM EDTA
20% (w/v) PEG6000/ 2.5 M NaCl	8 g of PEG6000, 40 mL of 2.5 M NaCl
10% (w/v) SDS	10 g of SDS in 100 mL of autoclaved H ₂ O
DNA gel loading dye	0.025% (w/v) bromophenol blue, 0.025% (w/v) xylene cyanol, 30% (v/v) sterilized glycerol
50X TAE buffer	40 mM Tris HCl, pH 8.0, 20 mM acetic acid, 1 mM EDTA, pH 8.0
5X TBE buffer, pH 8.3	445 mM Tris-borate, 445 mM boric acid, 0.01 mM EDTA
TE buffer	10 mM Tris HCl, pH 8.0, 1 mM EDTA
10 mM dNTP mix	10 mM dATP, 10 mM dCTP, 10 mM dGTP, 10 mM dTTP in 0.6 mM Tris-HCl

2.2.5 Colony PCR

Colony PCR was used for determination of the presence of the OsXYL1 insert in plasmid constructs in *E. coli* colonies transformed with ligation products. Colony PCR was carried out by *Taq* DNA polymerase using the primers of T7 promoter and T7 terminator for pET32a clones and 5' α -Factor and 3' AOX1 for pPICZ α BNH8 clones, and the temperature cycling parameters shown in Table 2.2. Colonies were selected, streaked onto a replica grid plate and incubated at 37 °C for 16-18 h. A single colony was picked and lysed in 20 μ L autoclaved HPLC water and boiled 5 min. The lysed DNA solution was centrifugated at 12,000 rpm for 10 min and the supernatant was used as a template for the PCR reaction. A 1 μ L aliquot of supernatant was added as a DNA template for PCR amplification in a 20 μ L the total volume of the reaction mixture composed of 2 μ L of 50 mM MgCl₂, 2 μ L of 10X buffer S, 0.5 μ L of 10 mM dNTP mixture, 0.5 μ L of 10 μ M forward primer, and 0.5 μ L of 10 μ M reverse primer (listed in Table 2.4). The PCR amplification product was subsequently checked by agarose gel electrophoresis.

Table 2.2 Cycling parameter for amplification of colony PCR.

Segment	Cycles	Temperature	Time
1	1	95 °C	30 s
2	30	95 °C	30 s
		55 °C	30 s
		72 °C	3 min
3	1	72 °C	5 min

2.2.6 Agarose gel electrophoresis

DNA were checked for apparent size by agarose gel electrophoresis through 1-2% agarose gels (depending on the DNA size, below 500 bp in 2% agarose, and more than 500 bp in 1% agarose) prepared in 1X TAE or TBE buffer. The DNA samples was mixed 5:1 with 6X NEB DNA loading dye (New England Biolabs, Beverly, MA, USA). Agarose gel electrophoresis was performed in a gel electrophoresis apparatus (Bio-Rad Corp., Hercules, CA, USA) at a constant voltage of 100-120 V for 25-35 min. The DNA

bands were detected by staining with ethidium bromide (0.1 µg/mL) for 1 min, then de-staining in distilled water. The DNA bands were visualized by UV irradiation on a transilluminator (Bio-Rad Corp., Hercules, CA, USA). The size of DNA bands was estimated by comparing their migration with those of the GeneRuler™ 1 kb DNA ladder (Thermo Scientific, Waltham, MA, USA).

2.2.7 Gel extraction and DNA cleanup

The correct-size DNA fragment separated by 1% agarose gel electrophoresis was extracted or cleaned up with a QIAquick® Gel extraction kit (QIAGEN, Hilden, Germany). The agarose gel containing target DNA was sliced with a blade cutter and transferred to a microcentrifuge tube. The DNA was purified according to the QIAquick® Gel extraction kit manufacturer's instructions.

2.2.8 DNA evaluation by spectrophotometry

The concentration and purity of the DNA solution were assessed by measurement of absorbance on a NanoDrop 2000c spectrophotometer (Thermo Scientific, Waltham, MA, USA). The DNA solution (1-2 µL) was placed on the sample window and the absorbance at 260 nm and 280 nm determined. The DNA concentration was estimated from A_{260} , multiplying by the dilution factor, and using the conversion factor (1 A_{260} = 50 µg/mL DNA), and calculated the amount of total DNA by multiplying the DNA concentration with the final total volume of the DNA solution, as in the following equations:

$$[\text{DNA concentration}] (\mu\text{g/mL}) = A_{260} \times \text{dilution factor} \times 50 \mu\text{g/mL}$$

$$\text{DNA yield } (\mu\text{g}) = \text{DNA concentration} \times \text{total sample volume (mL)}$$

The purity was checked at the ratio of absorbance at 260 nm divided by that at 280 nm, with good purity indicated by a ratio in the range from 1.80-2.00.

2.2.9 Protein concentration determination

The protein concentrations in the crude extracts and fractions and pools from the purification steps were determined by measuring the absorbance at 280 nm in the NanoDrop spectrophotometer. The protein concentration was calculated from the A_{280} with an extinction coefficient, which was calculated with the PROTEIN PARAMETERS program on the ExPASy website (<https://web.expasy.org>). The protein concentration calculation used the following equation:

[Protein concentration] (mg/mL) = (A_{280} / extinction coefficient) x dilution fold x 1/path length

Protein yield (mg) = Protein concentration (mg/mL) x total sample volume (mL)

The rice β -xylosidases OsXYL1 (Genbank accession number AK119887) were predicted by the ExPASy bioinformatic analysis the resulted in theoretical molecular mass of 83.952 kDa and an extinction coefficient of 100,700 M⁻¹cm⁻¹ for determined protein concentration (1 Abs = 1 mg/mL).

2.2.10 SDS-PAGE electrophoresis

The protein profile and the apparent molecular weights were determined by sodium dodecyl sulfate – polyacrylamide gel electrophoresis, SDS-PAGE. SDS-PAGE was performed as described by Laemmli (1970). Polyacrylamide gels were prepared with 10% or 12% separating gel and 5% stacking gel (Table 2.3). SDS-PAGE solution and buffers are also shown in Table 2.3. Protein samples were mixed with loading buffer and boiled at 100 °C for 5 min. The sample was centrifuged to collect the solution and loaded onto the sample wells under running buffer and placed in an electric field of 160 volts for 1 h or until the dye front reached the bottom of the gel. The gels were subsequently stained by Coomassie brilliant blue staining solution for 30 min and destained with destaining solution for 1-2 h. The molecular masses of protein bands were compared to the standard molecular weight protein markers (GE Healthcare, Uppsala, Sweden), which consist of phosphorylase b (97 kDa), bovine serum albumin (66 kDa), ovalbumin (45 kDa), bovine carbonic anhydrase (31 kDa), soybean trypsin inhibitor (21 kDa), and bovine milk α -lactalbumin (14 kDa).

Table 2.3 Solutions and buffer for SDS-PAGE.

Solution	Composition
10% separating gel (10 mL per 2 gels)	3.8 ml of deionized H ₂ O (DI-H ₂ O), 2.6 ml of 1.5 M Tris-HCl, pH 8.8, 3.4 ml of 30% acrylamide/bisacrylamide solution, 100 μ L of 10% (w/v) SDS, 100 μ L of 10% (w/v) ammonium persulfate (APS), 10 μ L N, N', N', N'-Tetramethyl ethylenediamine (TEMED)
12% separating gel (10 mL per 2 gels)	3.345 ml of DI-H ₂ O, 2.5 ml of 1.5 M Tris-HCl, pH 8.8, 4 ml of 30% acrylamide/bisacrylamide solution, 100 μ L of 10% SDS, 100 μ L of 10% (w/v) APS, 10 μ L TEMED
30% acrylamide/ bisacrylamide solution	29.22 g of acrylamide and 0.78 g of bis-acrylamide in 100 mL of DI-H ₂ O
5% stacking gel (5 mL per 2 gels)	2.77 ml of DI-H ₂ O, 1.26 ml of 0.5 M Tris-HCl, pH 6.8, 0.83 ml of 30% acrylamide/bisacrylamide solution, 50 μ L of 10% SDS, 50 μ L of 10% (w/v) APS, 5 μ L TEMED
5X Loading dye buffer	0.05 M Tris-HCl pH 6.8, 10% (w/v) SDS, 50% (v/v) glycerol, 0.5 mg/ml bromophenol blue, 20% (v/v) 2-mercaptoethanol
Running buffer	25 mM Tris, 192 mM glycine, 0.1% (w/v) SDS
Staining solution	0.1% (w/v) Coomassie brilliant blue R-250, 40% (v/v) ethanol (EtOH), 10% (v/v) acetic acid
Destaining solution	40% (v/v) EtOH, 10% (v/v) acetic acid, 50% (v/v) DI-H ₂ O
DNA gel loading dye	0.025% (w/v) bromophenol blue, 0.025% (w/v) xylene cyanol, 30% (v/v) sterilized glycerol

2.3 DNA and microbes for cloning and expression

2.3.1 Oligonucleotides

The oligonucleotide primers were synthesized from Bio Basic Inc. (Toronto, Canada). These oligonucleotides are listed in Table 2.4.

Table 2.4 Oligo primers for amplification, colony PCR, and DNA sequencing.

Primer	Sequence (5' → 3')	T _m (°C)	Function
OsXYL1optFwd	CCATGGCTGCAGCA CATCACCATC	61	Forward primer for pPICZαBNH8/OsXYL1
OsXYL1_no_stopXbaIR	TTGTTCTAGACCTG GACCTTGGAAACAAA ACTTCAAG	63	Reverse primer for pPICZαBNH8/OsXYL1
T7 promoter	TAATACGACTCACT ATAGGG	48	T7 promoter, forward primer for DNA sequencing of pET32a
T7 terminator	GCTAGTTATTGCTCA GCGG	51	T7 terminator, reverse primer for DNA sequencing of pET32a
STag 18mer	GAACGCCAGCACAT GGAC	53	Forward primer for DNA sequencing of pET32a
5' AOX (Invitrogen)	GACTGGTTCCAATTG ACAAGC	52	For <i>Pichia</i> vectors with AOX1 promoter, forward primer for DNA sequencing of pPICZαBNH8
3' AOX	GCAAATGGCATTCT GACATCC	52	For <i>Pichia</i> vectors with AOX1 terminator, reverse primer for DNA sequencing for pPICZαBNH8

2.3.2 Microorganisms

The *E. coli* strains used included DH5 α for cloning and plasmid propagation, and BL21(DE3), Origami(DE3) and Origami B(DE3) for expression in *E. coli*. The *Pichia pastoris* strain used the SMD1168H. The antibiotics used for selectively growing plasmid-containing clones are listed in Table 2.5.

Table 2.5 Selective antibiotic used for cloning, transformation, and expression.

Strain	Antibiotics resistance	Function
DH5 α	None	Bacteria strain for plasmid propagation and cloning
BL21(DE3)	None	Bacteria strains for expression of proteins
Origami(DE3) and OrigamiB(DE3)	kanamycin, and tetracycline	Bacteria strains for expression of proteins
SMD1168H	None	<i>Pichia</i> strain for protein expression (protease deficient)
Plasmid vector (Size)		
pUC57 (~2.7 kb)	Ampicillin	Cloning
pET32a(+) (~5.9 kb)	Ampicillin	Cloning and expression in bacteria
pPICZ α BNH8 (~3.6 kb)	Zeocin	Cloning and expression in <i>Pichia</i>

2.3.3 Plasmid for *E. coli* expression

The pUC57/OsXYL1 plasmid was transformed into the *E. coli* DH5 α competent cells (Section 2.2.2) and extracted by alkaline lysis plasmid preparation (Section 2.2.4). The plasmid was digested with endonucleases restriction enzymes under the conditions recommended by the supplier (New England Biolabs, Beverly, MA, USA).

OsXYL1 fragments (2.4 kb) with restriction sites were separated and purified from the agarose gel with a QIAquick® Gel extraction kit (QIAGEN, Hilden, Germany), and subsequently ligated into the pET32a vector by *T4* DNA ligase from Promega (Madison, WI, USA). Colony PCR (Section 2.2.5) was used for screening the ligation products with forward 5'T7 and reverse 3'T7 primer. The recombinant plasmid pET32a/OsXYL1 is presented in a schematic diagram in Figure 2.1A. It was used to produce an N-terminal thioredoxin fusion with an enterokinase cleavage site for removal of this tag after expression in *E. coli*. The DNA insertion was checked by restriction digestion followed by size (8.3 kb) estimation by agarose gel electrophoresis, and confirmed by automated DNA sequencing by Macrogen Corp. (Seoul, Korea). The pET32a/OsXYL1 construct was used for expression in *E. coli*.

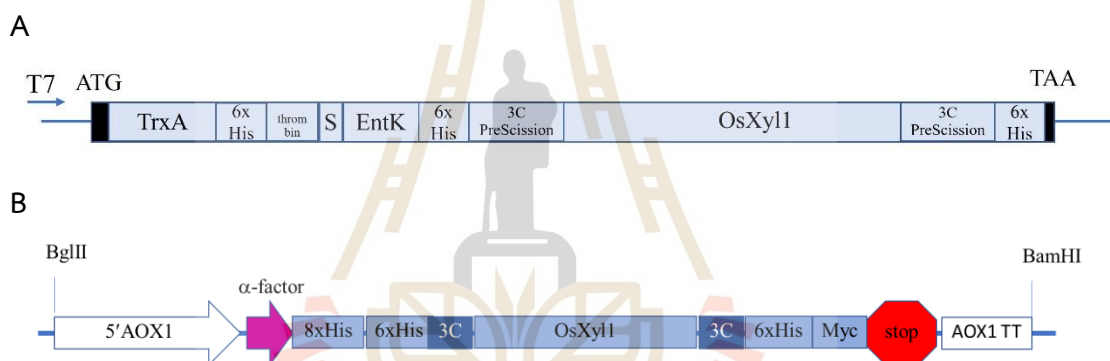


Figure 2.1 Schematic representation of the expression cassettes in the recombinant plasmids (A), pET32a/OsXYL1 for expression in *E. coli* and (B), pPZαBNH8/OsXYL1 for expression in *P. pastoris*.

2.3.4 Plasmid for *Pichia pastoris* expression

The pUC57/OsXYL1 plasmid was transformed into the *E. coli* DH5α competent cells (section 2.2.2) and extracted by alkaline lysis plasmid preparation (section 2.2.4). The plasmid was digested with endonucleases restriction enzymes under the conditions recommended by the supplier (New England Biolabs, Beverly, MA, USA). OsXYL1 fragments (2.4 kb) with restriction sites were separated and purified from the agarose gel with a QIAquick® Gel extraction kit (QIAGEN, Hilden, Germany), and subsequently ligated into the pPZαBNH8 vector (Toonkool, *et al.*, 2006), *Pst*I and *Xba*I

sites by *T4* DNA ligase from Promega (Madison, WI, USA). Colony PCR method (section 2.2.5) was used for screening the ligation products with forward OsXYL1optFwd and reverse OsXYL1_no_stopXbaIR primers. The recombinant pPZC α BNH8/OsXYL1 are presented in schematic in Figure 2.1B. The DNA insertion was checked by restriction digestion followed by size (6 kb) estimation by agarose gel electrophoresis and confirmed with DNA sequencing result by automated DNA sequencing by Macrogen Corp. (Seoul, Korea). The recombinant pPZC α BNH8/OsXYL1 were used for transformation to *Pichia pastoris* SMD1168H strains. The recombinant of pPZC α BNH8/OsXYL1 construct is represented fusion protein that contains an N-terminal alpha-factor as a secretion signal for expression in *P. pastoris*.

2.3.5 PCR amplification of insert from pUC57/OsXYL1

The β -xylosidase encoding gene (GenBank Accession No. AK119887) was optimized and synthesized by GenScript Corp. (NJ, USA) and provided in the pUC57 vector. The optimized OsXYL1 gene was amplified from the synthesized pUC57/OsXYL1 plasmid template with *Pfu* polymerase with primers including *Pst*I and *Xba*I sites. A 200- μ L reaction, which included 20 μ L DNA template (\sim 10 ng/ μ L), 20 μ L 10X *Pfu* buffer, 4 μ L dNTP mix, 4 μ L 10 μ M OsXYL1optFwd primer, 4 μ L 10 μ M OsXYL1_no_stopXbaIR primer (Table 2.4), and 4 μ L of 2.5 U *Pfu* DNA polymerase, was aliquoted into four 50 μ L fractions in PCR tubes. An annealing temperature gradient was calculated from T_m calculator from the primer sequences. The amplification reactions were achieved by the temperature cycling parameters shown in Table 2.6. The PCR product was analyzed on a 1% agarose gel.

Table 2.6 Cycling parameter for OsXYL1 amplification.

Segment	Cycles	Temperature	Time
1	1	95 °C	30 s
2	30	95 °C	30 s
		62 °C - 67 °C	30 s
		72 °C	5 min
3	1	72 °C	10 min

2.4 Yeast transformation

2.4.1 SMD1168H competent cell preparation

The *P. pastoris* SMD1168H strain glycerol stock was streaked onto Yeast extract Peptone Dextrose (YPD) agar without antibiotic and incubated at 30 °C for 2-3 days until colonies were visible. A single colony was picked and inoculated into 50 mL of sterile YPD broth without antibiotic in a sterile 250 mL Erlenmeyer flask, and grown with shaking at 28 °C, 200 rpm for 24 h. The cell culture was poured into pre-chilled 50 ml centrifuge tubes and chilled on ice for 10 min for cooling the cells prior to centrifuging at 3,500 rpm for 5 min at 4 °C. Then, the cell pellet was kept on ice (the cells must be on ice and kept cold all the time for high competency). The cell pellet was resuspended in 25 mL of ice-cold, sterile HPLC water, kept on ice for 5 min, and centrifuged at 3,500 rpm, 4 °C for 5 min. The cell pellets were resuspended with 20 mL of ice-cold sterile 1 M sorbitol and incubated on ice for 5 min, then centrifuged at 3,500 rpm, 4 °C for 5 min. The pellets were collected, and the wash repeated one time with 10 mL of ice-cold sterile 1 M sorbitol. Finally, the pellets were resuspended with 0.5 mL sterile 1 M sorbitol, incubated on ice and 80 µL aliquots were pipetted to microcentrifuge tubes. The cells were kept on ice and used that day for transformation by electroporation. The compositions of buffers and reagents used in *Pichia* transformation and expression are listed in Table 2.7.

Table 2.7 Materials used in transformation and expression of *P. pastoris*.

Material	Composition
10X (20%) Glucose	20 g Glucose in 100 mL DI-H ₂ O, filter sterilized
1 M Sorbitol	18.2 g Sorbitol in 100 mL H ₂ O, autoclaved
3 M Sodium acetate	24.61 g Sodium acetate in 100 mL of distilled H ₂ O, pH adjusted to 5.2 with glacial acetic acid, then autoclaved
1 M Potassium phosphate, pH 6.0	132 mL of 1 M K ₂ HPO ₄ , 868 mL of 1 M KH ₂ PO ₄ , the pH was confirmed at 6.0 ± 0.1 (adjusted pH by phosphoric acid or KOH), autoclaved
10% (v/v) Glycerol	10 mL of glycerol, 90 mL of H ₂ O, autoclaved
10% (v/v) MeOH	10 mL of methanol, 90 mL of sterilized H ₂ O, filter sterilized
10X YNB	13.4% YNB (34 g of YNB (w/o NH ₄ SO ₄ and amino acid, 100 g of NH ₄ SO ₄) in 1000 mL of sterilized H ₂ O, filter sterilized
500X (0.02%) Biotin	20 mg biotin in 100 mL of sterilized H ₂ O, filter sterilized
YPD broth	1% Yeast extract, 2% peptone, 2% glucose, autoclaved
YPD agar	YPD broth, 1.5% agar, autoclaved
YPDS agar	YPD broth, 1 M sorbitol, 2% agar, autoclaved
BMGY Medium containing 25 µg/mL zeocin	(1000 mL) 700 mL of autoclaved YPD broth, 100 mL of autoclaved 10% glycerol, 100 mL of sterilized 10X YNB, 100 mL of autoclaved 1 M potassium phosphate, pH 6.0, 2 mL of filter sterilized 0.02% (w/v) 500X biotin, 250 µL of 100 mg/mL zeocin
BMMY broth	(1000 mL) 700 mL of autoclaved YPD broth, 100 mL of autoclaved 10% MeOH, 100 mL of sterilized 10X YNB, 100 mL of autoclaved 1M potassium phosphate, pH 6.0, 2 mL of filter sterilized 500X biotin

2.4.2 Plasmid preparation for *Pichia* transformation

The *Pichia* expression vector DNA pPICZ α BNH8/OsXYL1 and pPICZ α BNH8 were transformed to *E. coli* DH5 α and the plasmid DNA extracted by alkaline lysis. The plasmids were linearized with *SacI*. The restriction enzyme was deactivated by heating at 65 °C for 10 min. Linearized *Pichia* expression vector DNA was checked by 1% agarose gel electrophoresis. The linearized DNA in the reaction was precipitated by mixing with 1/10 volumes of 3 M sodium acetate buffer pH 5.2 and 2-3 volumes of absolute ethanol, and incubated on ice for 30 min to 1 hour. The DNA pellet was collected by centrifugation at 12,000 rpm for 10 min. The pellet was washed with 500 μ L of 70% ethanol, then centrifuged at 12,000 rpm for 10 min, the supernatant was carefully removed by pipetting, and the pellet was dried by speed vacuum at 2,000 rpm, 50 °C for 10 min. The dried samples were dissolved with 20 μ L of HPLC water. The DNA concentration was measured by NanoDrop spectrophotometer. The linearized DNA samples were kept on ice and used that day for transformation.

2.4.3 *Pichia* transformation

The electrocompetent cells (in 2 mm electroporation cuvettes and 1.5 mL tubes) were placed on ice for 5 min while cleaned the electroporation machine. The 5-10 μ L (10-30 μ g) linearized *Pichia* expression vector DNA was carefully transferred to 80 μ L of competent SMD1168H cells and mixed by flicking the tube gently. The cell/DNA mixture was transferred into a chilled cuvette without introducing bubbles and adjusted to make sure that the cells were deposited across the bottom of the cuvette, then the cuvette was incubated on ice for 5 min. Electroporation was done with the conditions: 1.5 kV, 25 μ F and 400 Ω , and the typical time constant was 10 milliseconds. One milliliter of cold 1 M sorbitol was immediately added to the cuvette and gently mixed up and down twice. The transforming reaction was transferred to the new 1.5 mL microcentrifuge tube and incubated at 30 °C without shaking for 1 h. The transforming cells were spread at 200 μ L, 300 μ L, and 500 μ L volumes on selective YPDS plates containing 100 μ g/mL zeocin. The dried YPDS plates were incubated inverted at 30 °C for 3-5 days until colonies were visible. Each transformant should yield approximately 50 colonies. The empty *Pichia* pPICZ α BNH8 vector were similarly transformed to SMD1168H and analyzed as negative controls.

2.5 Protein expression

2.5.1 Expression screening in *E. coli* and optimization of conditions

Protein expression condition of the construct pET32a/OsXYL1 was optimized after transforming this plasmid into *E. coli* BL21(DE3), Origami (DE3) and Origami B(DE3) strains. Transformation of pET32a/OsXYL1 and control pET32a plasmid to the *E. coli* strains was performed as described in Session 2.2.3 and spread onto selectable LB agar plate containing 50 µg/mL ampicillin, 12.5 µg/mL tetracycline and 15 µg/mL kanamycin and incubated inverted at 37 °C for 16-18 h. The selected clones of transformant were picked and inoculated into 5 mL of LB broth with antibiotics resistance in 50 mL centrifuge tube, grown at 37 °C, shaking 200 rpm for 16-18 h, to produce a starter culture. To express OsXYL1, 100 µL of starter culture (1%) was added into the 10 mL the same type of media and cultured at 37 °C, shaking 200 rpm until OD₆₀₀ reached 0.6-0.8. The optimal expression conditions were determined by IPTG induction with varying final concentrations of 0, 0.1, 0.2, 0.3, 0.4 and 0.5 mM, varying the expression time from 3-16 h and varying the temperature at 20, 25 and 37 °C. The cell pellets were collected by centrifugation at 3,500 rpm, 4 °C for 10 min to remove the supernatant and the pellets kept at -80 °C before extraction. The pellet cells were thawed and 1 mL of DI-H₂O was added and incubated on ice for 10 min, to wash out the LB residue in water, followed by centrifugation at 3,500 rpm, 4 °C for 5 min. The cells were lysed by adding 5 mL of extraction buffer (100 mM Tris-HCl, pH 8.0, 150 mM NaCl, 200 µg/mL lysozyme, 1% (v/v) Triton-X 100, 1 mM PMSF, 4 µg/mL DNase I) per 1 g of cell weight, mixing well by pipetting, and incubating at room temperature for 1 h. The crude solution containing soluble protein was harvested by centrifugation and the supernatant and pellet kept on ice. The soluble and insoluble proteins were checked on SDS-PAGE and enzyme activity to hydrolyze 4-nitrophenyl β-D-xylopyranoside (4NPXyl) substrate assayed as section 2.7.2.

2.5.2 Protein expression and extraction of OsXYL1 in *E. coli*

The optimized pET32a/OsXYL1 was transformed to Origami B (DE3) and spread onto LB agar containing antibiotic resistances, and the plate was inverted and incubated overnight at 37 °C. The transformant was picked and inoculated into 50 mL of LB broth with ATK antibiotics in a 250 mL flask, grown at 37 °C, shaking 200 rpm for

16-18 h to produce a starter culture. Eight milliliters of starter culture (1% of the final volume) were added into the 800 mL of the same type of media in a 2 L flask and cultured at 37 °C, shaking 200 rpm until the OD₆₀₀ reached 0.6-0.8. The protein gene expression was induced with a final concentration of 0.1 mM IPTG, shaking at 200 rpm at 20 °C for 16 h. The cells were collected by centrifugation at 3,500 rpm, 4 °C for 20 min and the pellet kept at -80 °C before use. The pelleted cells were thawed and 5 mL of DI-H₂O per 1 g of pellet was added and incubated on ice for 10 min, followed by centrifugation at 4,500 rpm, 4 °C for 5 min. Proteins were lysed by adding 5 mL of extraction buffer per 1 g of cell weight, mixing well by pipetting, and incubating at room temperature for 1 h. The mixture was chilled on ice for 10 min. The crude solution containing soluble protein was harvested by centrifugation at 3,500 rpm, 4 °C for 15 min and the supernatant kept on ice for protein purification. The protein concentration was estimated by spectrophotometrically measuring 280 nm absorbance (A₂₈₀). The protein mixture complexity and molecular weight were estimated by SDS-PAGE and the enzyme activity to hydrolyze 4NPXyl assayed as section 2.7.2.

2.5.3 Screening *Pichia* transformants and optimization of expression

The colonies of *P. pastoris* harboring pPICZBNH8/OsXYL1 and pPICZ α BNH8 were selected for screening on YPD plates containing varied the appropriate zeocin (over 100 to 500 μ g/mL) and incubated overnight at 30 °C. Small scale expression of positive yeast clones was performed for expression optimization. The selected colonies were picked and inoculated into 5 mL of BMGY Medium containing 25 μ g/mL zeocin. The cultures in BMGY medium were grown at 28 °C with shaking at 200 rpm for 24 h, and a 15% glycerol stock in 1.5 mL microcentrifuge tube of the cells that grew was stored at -80 °C. Cells were pelleted by centrifugation and resuspended in 10 mL of BMMY Medium. The BMMY medium was cultured at 20 °C, shaking at 200 rpm for 5-7 days. Methanol was added every 24 h to the final concentration of 0.5 % (v/v) to induce protein production. A 200 μ L sample of the cultivation media was collected every 24 h for assaying activity. The activity profile of each clone was plotted against the number of days of incubation.

2.5.4 Protein expression of OsXYL1 in *P. pastoris*

For OsXYL1 protein production, the highest expression clone was expressed in large scale. The clone from the optimization condition was re-streaked from its glycerol stock onto YPD-agar containing 100 µg/mL zeocin and grown for 2-3 days at 28 °C. A single colony was inoculated into 400 mL BMGY medium and grown at 28 °C with shaking 200 rpm for 24 h. Cells were harvested by centrifugation (5,000 rpm, 8 °C, 20 min) and resuspended in 800 mL BMMY. Expression of OsXYL1 was induced with 0.5% (v/v) methanol added each day for 5 days to a culture grown at 20 °C with shaking at 200 rpm. The 5-days culture medium were centrifuged at 5,000 rpm at 8 °C for 20 min to remove yeast cells and debris. The crude supernatant pH was adjusted to 7.5 with 2 M K₂HPO₄, filtered through 0.45 µm membrane filters and kept on ice for protein purification.

2.6 Purification of β -xylosidase OsXYL1

Two chromatographic steps were used to purify OsXYL1 protein. First, crude supernatant, pH 7.5, was mixed with Ni²⁺-bound IMAC (GE Healthcare, Sweden) resin which was pre-equilibrated with IMAC equilibration buffer. The bounded protein was loaded into the column and washed with 2 CV of IMAC equilibration buffer (Table 2.8) without imidazole, then subsequently 2 CV of each 25, 50, 75, 150, and 250 mM imidazole in equilibration buffer. The fractions that were enzyme activity toward 4NPXyl were concentrated, and imidazole was removed by centrifugal ultrafiltration in 30 kDa MWCO Amicon Ultra-15 centrifugal filters and dialyzed against 50 mM Tris-HCl buffer, pH 8.0.

The second purification step was done by size-exclusion chromatography. The concentrated enzyme solution was injected into an FPLC ÄKTA Purifier system (GE Healthcare) to apply it to a Superdex™ 200 increase 10/300 GL column (GE Healthcare) equilibrated with 20 mM Tris-HCl, pH 8.0, containing 150 mM NaCl. After sample injection, the column was washed with 2 CV of equilibrated buffer at a flow rate of 0.3 mL min⁻¹, while collecting 0.5 mL fractions. Then, the fractions were assayed for β -xylosidase activity and those with activity were collected and pooled together. A 30,000 MWCO Amicon Ultra-4 centrifugal filter was used for concentration of OsXYL1.

The protein concentration and specific activity of the purified OsXYL1 was determined and it was aliquoted to 10-50 µg protein portions that were kept at -80 °C for further analysis. The reagents used for OsXYL1 protein purification are listed in Table 2.8.

Table 2.8 Reagents used in protein purification.

Reagents	Composition
1 M Tris-HCl pH 8.0	121 g Tris base in 1000 mL of DI-H ₂ O, adjusted pH 8.0 by HCl, filtered and autoclaved
0.5 M EDTA pH 8.0	186.1 g EDTA in 1000 mL DI-H ₂ O, adjusted pH 8.0 by NaOH, filtered and autoclaved
IMAC equilibration buffer	20 mM Tris-HCl buffer, pH 8.0, 150 mM NaCl
5 M NaCl	292 g NaCl in 1000 mL, filtered and autoclaved
0.5 M imidazole pH 8.0	34.0 g Imidazole in 1000 mL sterilized DI-H ₂ O, adjusted pH 8.0 by HCl

2.7 Characterization of β -xylosidase OsXYL1

2.7.1 Enzyme assay

The β -xylosidase activity was assayed in 96-well plate, a 140 µL reaction mixture containing 10-40 µL of sample protein depending on the purified step, 1 mM of 4NPXyl in 50 mM sodium acetate, pH 4.0. The reaction mixtures were incubated at 60 °C for 30 min, then terminated by adding 70 µL of 2 M Na₂CO₃. The 4NP released was immediately measured as absorbance at A₄₀₅ by microplate reader (Multiskan™ GO Microplate Spectrophotometer, Thermo Scientific, Waltham, MA, USA). The absorbance of the substrate blank (reaction without enzyme) was subtracted from that of the reaction.

2.7.2 pH and temperature optima

The optimum pH was determined by incubating 3.5 nmol of purified OsXYL1 with 1 mM 4NPXyl in Mcllvaine citrate-phosphate buffers, with pH ranging from 2.5 to 11.0 (in 0.5 increments) at 37 °C for 30 min. The optimum temperature was determined over the range of 30-80 °C (in 5 °C increments), by pre-incubating the reactions of 1

mM 4NPXyl in 50 mM sodium acetate buffer, pH 4.0, at temperatures between 30 to 80 °C for 10 min, after which 3.5 nmol OsXYL1 was added and incubated at the same temperature for a further 30 min, as described in section 2.7.1. Each experiment was performed in triplicate. The results of both reactions were expressed as the percentage of activity relative to the maximum value at the optimum.

To determine the temperature stability, 3.5 nmol of purified OsXYL1 was preincubated at temperature 30-70 °C (in 10 °C increments) for 4 h, samples were collected at different times and then the residual activity was measured at the optimum pH and temperature (section 2.7.1). Each experiment was performed in triplicate. The β -xylosidase activity without preincubation was defined as 100%, and thus corresponds to the initial activity.

2.7.3 Effect of metal ions and sugars

The effects of the metal ion salts LiCl, NaCl, KCl, MgCl₂, MgSO₄, CaCl₂, MnCl₂, FeSO₄, CoCl₂, Co(NO₃)₂, NiSO₄, CuSO₄, and ZnSO₄, and the metal chelator EDTA at the final concentrations of 5 mM and 10 mM on the OsXYL1 reaction were tested. The effects of sugars (xylose, arabinose, glucose, galactose, mannose, maltose, lactose, fructose, and sucrose) at the final concentration of 10 mM and 50 mM were also tested in the standard reaction mixture with these compounds added. The reactions were preincubated 3.5 nmol OsXYL1, containing the reagent being tested in 50 mM NaOAc buffer, pH 4.0, at 60 °C, in reaction volume 140 μ L for 10 min before adding 1 mM 4NPXyl substrate. The reaction mixture was incubated further in standard assay (section 2.7.1). The relative activity of each reaction with a reagent was calculated compared to control reaction without additives, which was considered as 100%. Each experiment was performed in triplicate. A substrate blank reaction was set up in the same condition with buffer instead of the enzyme and its absorbance subtracted from the corresponding reactions.

2.7.4 Deglycosylation OsXYL1

The *N*-glycosylation linked OsXYL1 glycoprotein was deglycosylated by Endoglycosidase H (Endo H) enzyme according to the New England Biolabs manual. The reaction contained approximately of 5-10 μ g protein with 0.5 units Endo H, and was incubated at 37 °C for 1 h in a total volume 10 μ L. The molecular weight of purified

OsXYL1 and deglycosylated OsXYL1 were visualized by 12% gel SDS-PAGE. Separation of reaction products was determined by comparison with protein markers and the known size of Endo H (29 kDa).

2.7.5 Transglycosylation activity

Transglycosylation reactions of OsXYL1 were carried out in 70 μ L reaction mixtures by incubating 7 nmol OsXYL1 with 5 mM final concentration of 4NPXyl substrate, containing 15% (v/v) alcohols in 50 mM NaOAc buffer, pH 4.0, at 40 °C for 1 h. The reaction was stopped by boiling for 10 min, and dried. The reaction products were redissolved in water and spotted onto a silica gel 60 F₂₅₄ thin layer chromatography (TLC) plate (Merck Millipore, Massachusetts, USA). The TLC plate was developed in a solvent of 3:2:1 ethyl acetate–acetic acid–water (v/v/v), visualized under ultraviolet (UV) light and stained with 10% sulfuric acid in ethanol and heated at 110 °C until the product spots were observed. Transglycosylation products were analyzed and qualified by comparing with control reaction and xylose and 4NPXyl standards.

Transglycosylation reactions of 1-octanol were performed in co-solvent mixtures of acetone and 1-octanol in buffer. The reaction mixture of 1 mM 4NPXyl with various of proportion 0-50% (v/v) of acetone included 5 nmol OsXYL1 in standard 140 μ L reaction conditions. Octanol was added 0-25% (v/v) 1-octanol as the acceptor substrate and co-solvent with 10-30% (v/v) acetone in the reaction mixture. The reaction of 30% (v/v) acetone and 20% (v/v) 1-octanol was carried out in a 200 μ L reaction volume, containing 5 mM 4NPXyl in 50 mM sodium acetate, pH 4.0, and was catalyzed by OsXYL1 for 6 h. Aliquots of reaction mixtures were removed at different incubation times: 30 min, 1 h, 2h, 3h, 4h, 5h, and 6h, and were boiled and analyzed by TLC plate.

2.7.6 Substrate specificity

The substrate specificity of OsXYL1 toward nitrophenyl glycosides was assessed in 140 μ L reactions in a 96-well plate. The nitrophenyl glycosides tested are listed in Table 2.9, for OsXYL1 substrates studied. The reactions were preincubated with final concentration 5 mM substrates in 50 mM sodium acetate buffer, pH 4.0, at 40 °C for 10 min. The reaction was catalyzed by 3.57 nmol OsXYL1 (in the case of 1mM 4NPXyl,

0.89 nmol OsXYL1) and incubated at 40 °C for 30 min and stopped by adding 70 μ l of 2 M Na₂CO₃. The 4NP released was immediately quantified by measuring A₄₀₅. Each experiment was performed in triplicate. A substrate blank reaction was set up in the same condition by adding buffer instead of the enzyme. The relative enzyme activity was calculated by comparing the absorbance to that of the reaction with 4NPXyl (1 mM substrate hydrolyzed with dilution 4-fold of OsXYL1), which considered as 100%.

Table 2.9 Substrates for studies of β -xylosidase OsXYL1 activity.

Substrate	Abbreviated	Molecular weight (g/mol)
4NP- β -D-xylopyranoside	4NPXyl	271.22
4NP- α -L-arabinopyranoside	4NPArap	271.22
4NP- α -L-arabinofuranoside	4NPAraf	271.22
4NP- α -L-fucopyranoside	4NP α Fuc	285.30
4NP- β -D-fucopyranoside	4NP β Fuc	285.30
4NP- β -D-glucopyranoside	4NPGlc	301.25
4NP- α -D-glucopyranoside	4NP α Glc	301.25
2NP- β -D-glucopyranoside	2NPGlc	301.25
4NP- β -D-galactopyranoside	4NP β Gal	301.25
4NP- α -D-galactopyranoside	4NP α Gal	301.25
2NP- β -D-galactopyranoside	2NPGal	301.25
4NP- β -D-glucoropyranoside	4NPGluA	315.23
4NP-N-acetylglucosaminide	4NPGlcNac	342.30
4NP β -D-maltoside	4NPMal	463.39
1,4- β -D-Xylobiose	X2	282.24
1,4- β -D-Xylotriose	X3	414.4
1,4- β -D-Xylotetraose	X4	546.5
1,4- β -D-Xylopentaose	X5	678.6
1,4- β -D-Xylohexaose	X6	810.7

2.7.7 Hydrolysis of xylooligosaccharides

Enzyme activity of OsXYL1 toward 1,4- β -D-xylopyranooligosaccharides (DP 2-6, as listed in Table 2.9) was determined in 50 μ L reaction mixture, containing 5 mM XOSs (X2-X6) in 50 mM NaOAc buffer, pH 4.0, at 40 °C overnight. The reaction was stopped by boiling at 100 °C for 10 min. The hydrolyzed products were dried, redissolved in 5 μ L DI-H₂O and spotted onto TLC plate. The TLC was developed in ethyl acetate–acetic acid–water (2:1:1), visualized under ultraviolet (UV) light and stained with 10% sulfuric acid in ethanol and heated at 110 °C until the product spots were observed and then identified by comparing with marker of standard D-xylose (X1) mixed with 1,4- β -D-xylobiose (X2) to 1,4- β -D-xylohexaose (X6).

The quantification of the liberated xylose of hydrolysis of XOSs were determined by the D-xylose assay kit (Megazyme, MI, USA). The xylose released was determined using an enzyme coupled of xylose dehydrogenase (XDH) and xylose mutarotase (XMR) spectrophotometric assay to measure absorbance of NADH produced at 340 nm. Following the company procedure, the assay was carried out in 96-well plate, a 297 μ L reaction mixture containing 10 μ L reaction xylose released, 200 μ L of DI-H₂O, 40 μ L buffer pH 7.5, 40 μ L of NAD⁺ plus ATP, 2 μ L hexokinase were mixed and measured A_{340} after 4 min (A1), then 5 μ L XDH/XMR was added and mixed, measured A_{340} after 15 min (A2). The amount of xylose released was multiplied by a 5-fold dilution factor and compared to the standard curve of xylose concentration.

2.8 Kinetic analysis

2.8.1 Hydrolysis of nitrophenyl glycosides

All kinetic parameters of OsXYL1 toward 4NPXyl, 4NPAr_f, and 4NPAr_p were determined from triplicate assay containing 3.5-5 nmol enzyme, containing 1 μ g/mL BSA in 50 mM sodium acetate buffer, pH 4.0, in a total volume of 140 μ L, at 40 °C for time intervals that had linear activity versus time curves to show that they were initial velocities (pseudo-first order rate of v_0). Time course of each substrate was first determined to find the first order rate constant of OsXYL1 with 3-5 substrate concentrations, and the reaction was stopped at three different time points (10-30

min). Time course assays were done for the highest and lowest substrate concentrations for each substrate to ensure that the velocities measured were in the linear range, and all absorbance readings were measured in the range of 0.1-1.5 absorbance units. The amount of 4NP released was compared to the standard curve of 4NP concentration (0.0025-0.03 μmol). The kinetic reactions were incubated OsXYL1 with substrate concentrations covering at least the range of $0.3K_m$ - $3K_m$ whenever possible.

The Grafit 5.0 computer program (Erithacus Software, Horley, UK) was employed to calculate kinetic parameters K_m and V_{max} . The kinetic parameter was calculated by fitting the rate of product formation and substrate concentration in nonlinear regressions analysis of the Michaelis-Menten equation. The apparent k_{cat} values were calculated by dividing the V_{max} by the total amount of enzyme in the reaction.

2.8.2 Hydrolysis of xylooligosaccharides

Kinetic parameters of OsXYL1 with XOSs (X2-X6) was determined from triplicate assays containing 0.02 μmol purified OsXYL1, containing 1 $\mu\text{g/mL}$ BSA in 50 mM sodium acetate buffer, pH 4.0, in a total volume of 50 μL at 40 °C for time intervals that had linear activity versus time curves. Time course of each substrate was first determined to find the first order rate constant with 3-5 substrate concentrations, and the reaction was stopped at three different time points (10-30 min). Time course assays were done for the highest and lowest substrate concentrations for each substrate, and all absorbance readings were measured in the range of 0.1-1.5 absorbance units. The enzyme was inactivated by boiling the reaction mixture for 10 min, and the reaction was cleared by centrifugation (12,000 rpm, 5 min). The xylose released was measured by xylose assay, following the section 2.7.7. The amount of xylose released was compared to the standard curve of xylose concentration (0.007-0.13 μmol), according to the company protocol. The kinetic reactions were incubated OsXYL1 with XOSs concentrations covering at least the range of $0.3K_m$ - $3K_m$ whenever possible. Data was fitted by nonlinear regression to the Michaelis-Menten plot and the figure was generated by GraFit 5 (Erithacus Software).

2.8.3 Xylose inhibition

The β -xylosidase OsXYL1 inhibited by xylose was determined. The reaction was carried out at 40 °C by pre-incubating 7 nmol OsXYL1 enzyme in 50 mM sodium acetate buffer, pH 4.0, containing 1 μ g/mL BSA, with varied xylose concentration, in reaction volume 140 μ L for 10 min. The residual activity was assayed with varied of saturated concentration of 4NPXy1 substrate, as described in section 2.8.1. Inhibition constants (K_i) were calculated by linear regression of a plot of the apparent K_m/V_{max} values (slope of Lineweaver-Burk plot) *versus* xylose concentrations.



CHAPTER III

RESULTS AND DISCUSSION

3.1 Expression pattern of OsXYL1 (Accession No. AK119887, Locus ID. Os02g0752200) in rice

The Rice Expression Profile Database (RiceXPro, URL: <https://ricexpro.dna.affrc.go.jp/>) provides the expression profile of nearly all rice genes, based on microarray RNA expression analysis. It was queried to uncover the expression patterns of OsXYL1, as shown in Figure 3.1. From the analysis, the gene is fairly broadly expressed, but it is most highly expressed in the ovary in the 1-5 days after flowering (DAF) growth stage and in the embryo at 7 to 10 days after flowering. In different plant tissues, transcripts of β -xylosidase related genes have been found in flower and siliques of *Arabidopsis* (Goujon *et al.*, 2003; Minic *et al.*, 2006; Xiong *et al.*, 2007), in pollen of tobacco and *Arabidopsis* (Hruba *et al.*, 2005), in alfalfa roots (Xiong *et al.*, 2007), in seedling of barley (Lee *et al.*, 2003) and pea (O'Neill *et al.*, 1989), in immature seeds of radish (Kotake *et al.*, 2006), and in ripening fruits of tomato (Itai *et al.*, 2003), Japanese pear (Itai *et al.*, 1999; Itai *et al.*, 2003; Tateishi *et al.*, 2005), and strawberry (Figueroa, *et al.*, 2010; Bustamante *et al.*, 2006). The genes of flower and siliques play a role in loosening and remodeling of cell walls in sporophytic tissues, while genes in pollen plays a role in wall development of mitotic microspores (Hruba *et al.*, 2005). The genes in roots play a function in cell wall turnover of roots at rapidly growing stages. The genes induced in ripening fruits are likely to play a role alternating the cell wall texture during softening. On the other hand, genes AtXYL from *Arabidopsis* (Goujon *et al.*, 2003), XYL from barley (Lee *et al.*, 2003) show a broad expression pattern, and their transcripts were detected in various tissues.

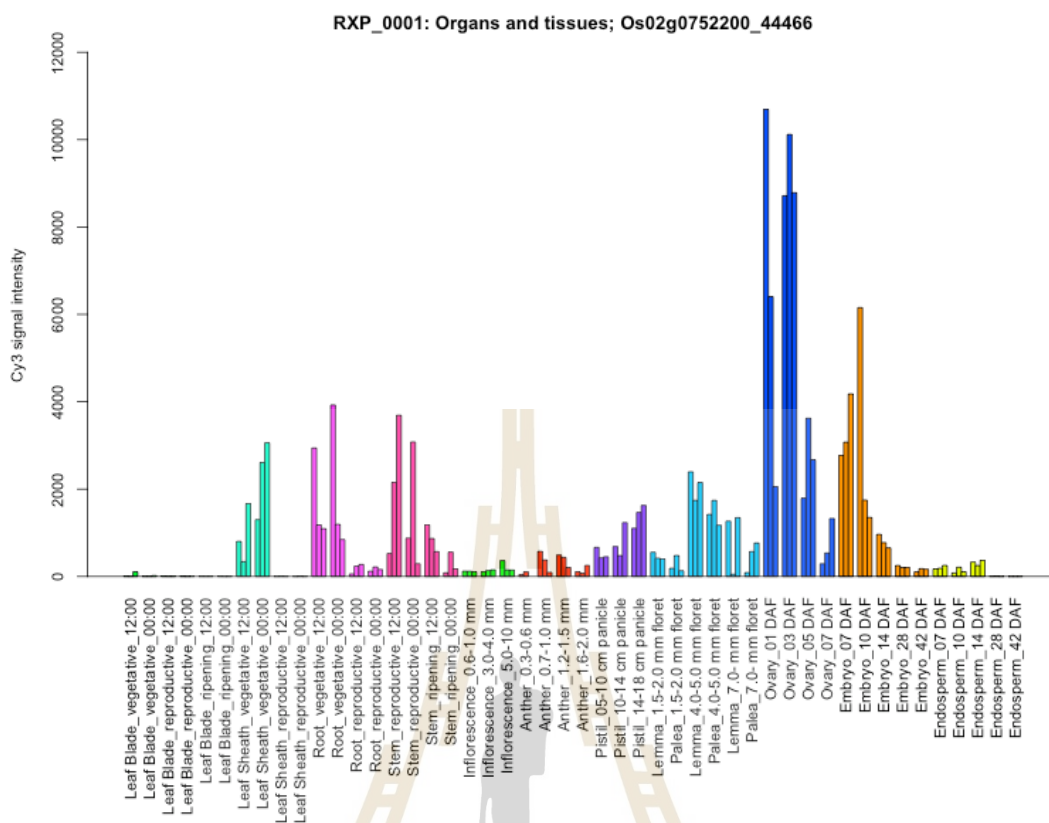


Figure 3.1 Expression profile of OsXYL1 in different organs and tissues. The data were collected from the Rice Expression Profile Database, which is based on microarray RNA expression analysis (Os02g0752200, Kikuchi, S., *et al.*, 2003).

3.2 Sequence analysis of rice β -xylosidase OsXYL1

The rice putative β -xylosidase OsXYL1 protein sequence obtained using genetic analysis. The relationship with other characterized plant GH3 sequences in the GenBank was evaluated using protein-protein BLAST (BLASTp, <http://www.ncbi.nlm.nih.gov/BLAST/>). A phylogenetic tree constructed of 24 protein sequences of characterized plant GH3 proteins retrieved from NCBI is shown in Figure 3.2.

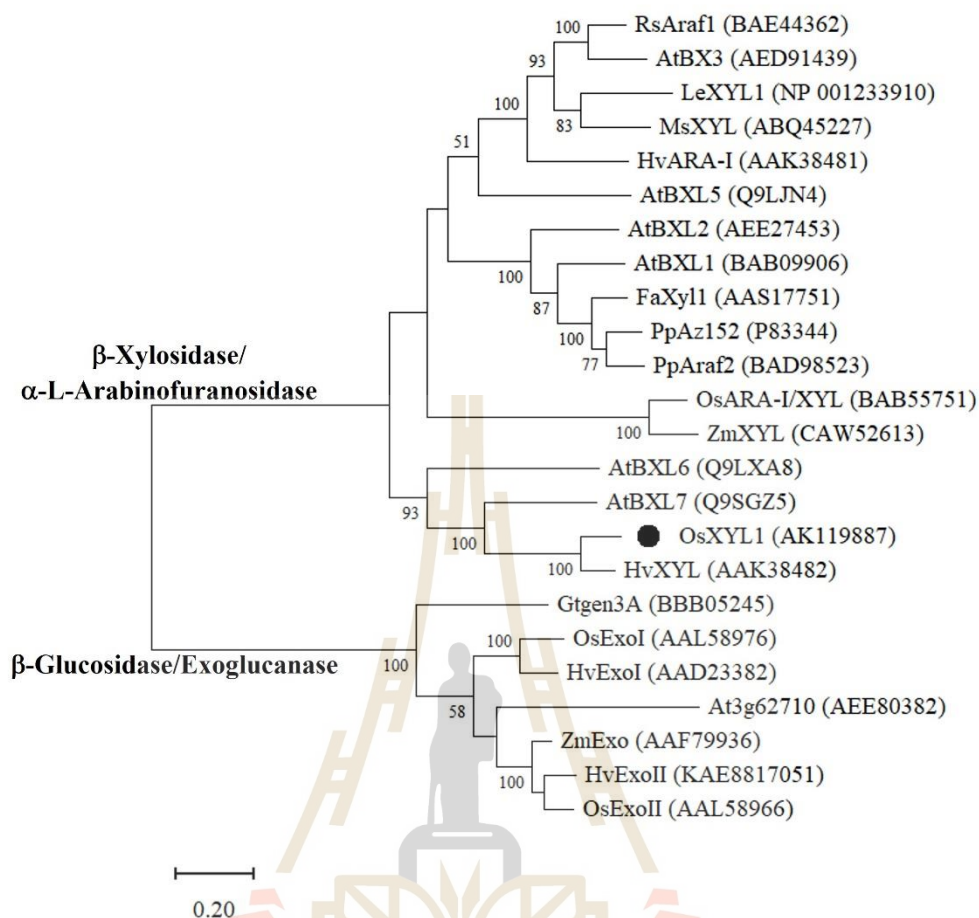


Figure 3.2 Phylogenetic relationship of OsXYL1 and other plant GH3 members. Amino acid sequences were aligned with the MUSCLE method in MEGA11. The phylogenetic tree was constructed by the Neighbor-Joining algorithm. Branch length are drawn in proportion to calculated distances between sequences. Bootstrap values for percent reproducibility are shown at the base of each branch. The plants GH3 protein sequences retrieved from NCBI and their accession numbers are given in parentheses: rice (Os), barley (Hv), Maize (Zm), radish (Rs), *Arabidopsis* (At), alfalfa (Ms), Japanese pear (Pp), strawberry (Fa) and *Gentiana* (Gt). Rice OsXYL1 β -xylosidase is marked with a filled circle.

The sequence of OsXYL1 is most similar to barley β -xylosidase, *HvXYL* (Lee, *et al.*, 2003) with 83% amino acid sequence identity, and it shared 47-50% with the putative β -xylosidases from *Arabidopsis* (Goujon *et al.*, 2003, Minic *et al.*, 2006), and 42-48% with other β -xylosidase of *LeXYL1* from tomato (Itali *et al.*, 2006), *FaXYL1* from

strawberry (Bustamante *et al.*, 2006), and ZmXYL putative β -xylosidase from maize (Puzio *et al.*, 2009). Among arabinofuranosidases, it shared only 42-50% identity with RsAraf1 from radish (Kotake *et al.*, 2006), HvARA-I from barley (Lee *et al.*, 2003), and with the bifunctional OsARA-I/XYL from rice (Sasaki *et al.*, 2004), MsXYL from alfalfa (Xiong *et al.*, 2007) and PpAraf2 from Japanese pear (Tateishi *et al.*, 2005) and shared only 26-29% amino acid sequence identity with the other enzymes in this phylogenetic cluster.

The positions of conserved amino acids in plant GH3 enzymes from rice, barley, maize, alfalfa, and tobacco are shown in the Clustal Omega protein sequence alignment in Figure 3.3. The catalytic nucleophile residue is strictly conserved in family GH3 (Henrissat *et al.*, 1998). Identical amino acid residues were found at 78 positions, which included the WGR and KH motifs and the catalytic nucleophile, aspartate (D) residue in the GFVISDW motif of β -glucosidase/exoglucanase enzymes, and GYITSDC motif of β -xylosidase/ α -L-arabinosidase enzyme, found in the N-terminal domain 1 (Harvey *et al.*, 2000). Based on the multiple sequence alignment (Figure 3.3), the conserved catalytic nucleophile of rice β -xylosidase OsXYL1 is similar with barley HvXYL and tobacco AtBXL6, which is situated in the conserved GYITSDC motif. On the other hand, the catalytic acid is conserved as glutamate (E) residue in a variety of motifs, the position of the catalytic acid/base and surrounding amino acids vary in GH3 members making it complicated to predict (Hrmova *et al.*, 2002).

HvExoII_ (KAE8817051)	PHWGRCYESYSEDPKVVQSMT-TLISGLQGDVPAG-S-----EGRPYVGGSKKV	222
ZmExo_ (AAF79936)	PHWGRCYESYSEDPKVVQSMT-SLISGLQGDAPAD-S-----AGRPHYVGGSKKV	222
OsExoII_ (AAL58966)	PHWGRCYESYSEDPKVVQSMT-TLISGLQGDVPSN-D-----VGRPHYVGGSKKV	222
OsExoI_ (AAL58976)	PHWGRCYESYSEDHRIVQAMT-ELIPGLQGDVPANFT-----SGMPYVAGKNNV	275
HvExoI_ (AAD23382)	PHWGRCYESYSEDHRIVQAMT-ELIPGLQGDVPANFT-----SGMPYVAGKNNV	226
OsARA-I/YXL_ (BAB55751)	PHWGRASETPGEDPFVVGRYAVNFVRGMQDIDGATTAASAAAAT-----DAFSRPIKV	238
ZmXYL_ (CAW52613)	PHWGRASETPGEDPFVVGRYAVNFVRGMQDIDDRPYA----AAA-----DPFSRPIKV	250
HvARA-I_ (AAK38481)	PHWGRGQETPGEDPLLASKYAVGYVTGLQDAGAG-----GVTDGALKV	216
LeXYL1_ (NP_001233910)	PHWGRGQETPGEDPTLTSTKYGVAYVEGLQQTDDG-----S--TNKLKV	211
MsXYL_ (ABQ45227)	PHWGRGQETPGEDPLLSSKYAAGYVKGQLQQTDDG-----D--SDKLKV	215
AtBXL6_ (Q9LXA8)	PHWGRGQETPGEDPKVVSEYGVFVRGFGQEKKKRVLKRRFSDDVDDDRHDDADGKML	222
OsXYL1_ (AK119887)	PHWGRGQETPGEDPTVTGKYAAVFRGVQGYALAG-----AINSTDLEA	211
HvXYL_ (AAK38482)	PHWGRGQETPGEDPTMTGKYAAVFRGVQGYGMSG-----AINSDLEA	209
	***** * ** * *	
HvExoII_ (KAE8817051)	AACAKHIVG-DGGTFMGINEN--DTIIDAHGLMTIHMPAYYNSIIRG-VSTVMTSYSSWN	278
ZmExo_ (AAF79936)	AACAKHIVG-DGGTHNGINEN--NTIIDTHGLLSIHMPYYSIIRG-VSTVMYSYSSWN	278
OsExoII_ (AAL58966)	AACAKHIVG-DGGTVKGINEN--NTIIDTHGLLSIHMPYYSIIRG-VSTVMYSYSSWN	278
OsExoI_ (AAL58976)	AACAKHIVG-DGGTQNGVNE--NTIIDRGLMTIHMPAYLNALQKG-VSTVMYSYSSWN	331
HvExoI_ (AAD23382)	AACAKHIVG-DGGTVKGINEN--NTIIDRGLMTIHMPAYLNALQKG-VSTVMYSYSSWN	282
OsARA-I/YXL_ (BAB55751)	SSCCKHYAAYDVAWNGTDRLTDFARVQERDMVETFERPFEMCIRDGDASCVMCSYNRIN	298
ZmXYL_ (CAW52613)	SSCCKHYAAYDVAWFKADRLTFDAQVEERDMVETFERPFEMCIRDGDASCVMCSYNRIN	310
HvARA-I_ (AAK38481)	AACCKHYTAYDVAWNGVRYTDFDAKVSQDLDLDTFQPPFKSCVLDGNAVASVMCSYNKVN	276
LeXYL1_ (NP_001233910)	AACCKHYTAYDVAWNGVRYTDFDAKVSQDLDLDTFQPPFKSCVLDGNAVASVMCSYNKVN	271
MsXYL_ (ABQ45227)	AACCKHYTAYDVAWNGVRYTDFDAVVSQDLDLDTFQPPFKSCVLDGNAVASVMCSYNKVN	275
AtBXL6_ (Q9LXA8)	SACCKHYTAYDLEKWNFTRYDFNAVVTEDQMEDTYQPPFETCIRDGKASCLMCSYNVAVN	282
OsXYL1_ (AK119887)	SACCKHYTAYDLENWKGVTTRYAFDAKVTADQLADTYNPPFRSCVEDGGASGIMCSYNRNV	271
HvXYL_ (AAK38482)	SACCKHYTAYDLENWKGVTTRYAFDAKVTEDQLADTYNPPFRSCVEDGGASGIMCSYNRNV	269
	* ** * * * *	
HvExoII_ (KAE8817051)	GKKMHANHFLVTDFLKNKLKFRGFVISDWDGIDRITSPPGV-N--YSYSVEAGVGAGIDM	335
ZmExo_ (AAF79936)	GKKMHANHFLVTDFLKNKLKFRGFVISDWDGIDRITTPPHA-N--YSYSIEAGVGAGIDM	335
OsExoII_ (AAL58966)	GKKMHANHFLVTDFLKNKLKFRGFVISDWDGIDRITSPPHK-N--YSYSIEAGVGAGIDM	335
OsExoI_ (AAL58976)	GKKMHANHFLVTDFLKNKLKFRGFVISDWDGIDRITTPAGS-N--YSYSVQAGVLAGIDM	388
HvExoI_ (AAD23382)	GKKMHANHFLVTDFLKNKLKFRGFVISDWDGIDRITTPAGS-D--YSYSVQAGVLAGIDM	339
OsARA-I/YXL_ (BAB55751)	GVPACADARLLTETVRRDWQLHGYIVSDCDSDVRVMVRDAKWLGYTGVEATAAMKAGLDL	358
ZmXYL_ (CAW52613)	GVPACADARLLTETVRRDWQLHGYIVSDCDSDVRVMVRDAKWLGYTGVEATAAMKAGLDL	370
HvARA-I_ (AAK38481)	GKPTCADKDLLEGVIRGDWKLNGYIVSDCDSDVLDVLTQQHY-TKTPEEAAATIKSGVDL	335
LeXYL1_ (NP_001233910)	GKPTCADKDLLEGVIRGDWKLNGYIVSDCDSDVLDVLTQQHY-TKTPEEAAALGNSGVDL	330
MsXYL_ (ABQ45227)	GKPTCADPDLKGVIRGKWLNGYIVSDCDSDVEVLKQDQHY-TKTPEEAAATILSGLDL	334
AtBXL6_ (Q9LXA8)	GVPACAQGDLLQK-ARVEWGFEGYITSDCAVATIFAYQGY-TKSPPEAAVADAIKAGVDI	340
OsXYL1_ (AK119887)	GVPTCADYNLLSKTARGDWRFYGYITSDCAVSIHHDVQGY-AKTAEDAVADVILKAGMDV	330
HvXYL_ (AAK38482)	GVPTCADHNLKSKTARGDWRFYGYITSDCAVAIIHHDVQGY-AKAPEDAADVILKAGMDV	328
	* * * * *	
	Catalytic nucleophile	
HvExoII_ (KAE8817051)	VVVGEPFYAETFG-DNLNLTIPAPGPSVIQTVCKSVR--CVVVLISGRPLVLEPYISAMD	559
ZmExo_ (AAF79936)	VVVGEPFYAETFG-DNLNLTIPAPGPSVIQSVCGAAK--CVVVLISGRPLVLEPYLGDM	557
OsExoII_ (AAL58966)	VVVGEPFYAETFG-DNLNLTIPAPGPSVIQTVCKSVR--CVVVLISGRPLVLEPYIGGID	559
OsExoI_ (AAL58976)	VVVGEPHYTETKG-DNLNLTIPDPGSTVATVCGAAQ--CATVLISGRPVVQPLGAMD	611
HvExoI_ (AAD23382)	VVVGEPHYTETKG-DNLNLTIPDPGSTVATVCGAAQ--CATVLISGRPVVQPLGAMD	563
OsARA-I/YXL_ (BAB55751)	VVAGLNMVSVERESNDREDLLLPWSQASWINAVAEASPSPIVLVIMSAGGVVDSFAQDNPK	581
ZmXYL_ (CAW52613)	VVAGLNMVSVERESNDREDLLLPWNQSSWINAVAMASPTPIVLVIMSAGGVVDSFAHNTPK	599
HvARA-I_ (AAK38481)	LVMGADQSIKESLDRTSLLLPGQQTQLVSAVANASSGPVILVVMSSGGFFDISFAKASDK	558
LeXYL1_ (NP_001233910)	LVMGADQSIKESLDRTSLITLPGQQTQLVSAVANASSGPVILVVMSSGGGMVDVQFVADNPK	552
MsXYL_ (ABQ45227)	IVVGANLAI EAESLDRTSLITLPGQQTQLVNEVANVSKGPVILVIMSGGGMVDVSAKTNDK	556
AtBXL6_ (Q9LXA8)	VVAGLNLQETEDKDRVSLSLPGQKQDLVSHVAASVSKPVILVITCGGPFVDVTFKNNPK	564
OsXYL1_ (AK119887)	LFMGLDQDQEREVDRLLELSPGQMLNTNTVANAAPKPVILVITCGGPFVDVTFKNNPK	553
HvXYL_ (AAK38482)	LFMGLDQDQEREVDRLLELSPGQMLNTNTVANAAPKPVILVITCGGPFVDVTFKNNPK	551
	* * * * *	
	Catalytic acid	

Figure 3.3 Alignment analysis of plant GH3 amino acid sequences. The partial multiple alignment demonstrates the conserved motifs in plant GH3 rice, barley, maize, alfalfa, and tobacco. Identical residues are shown in asterisks (*), and the conserved motifs are shown in the boxes, with the catalytic nucleophile and acid/base indicated (down-arrow).

The structure of the rice OsXYL1 β -xylosidase fby homology modeling that used the X-ray crystal structure of fungal *Hypocrea jecorina* β -xylosidase Xyl3A (Bxl1) in complex with 4-thioxylobiose (PDB code 5AE6, Mikkelsen *et al.*, 2015), since the

sequence identity is 35%. The distribution in monomer of the secondary structures in the two GH3 enzyme are quite similar. The structure model shows the three distinct domains (Figure 3.4). Domain 1 encompasses residues 42-404, an N-terminal $(\alpha/\beta)_8$ Tim-barrel in which the conserved catalytic nucleophile is aspartate residue (Asp-299) located in a GFVISDW motif. Domain 2 is a six-stranded α/β sandwich that comprises residues 406-636 with the conserved catalytic glutamate residue (Glu-505) at the linker region that is directed toward Asp-299. The extended third domain at the C-terminus consists of a fibronectin type III (FnIII) fold, which is composed of residues 637-774. The measured distance between oxygen of Asp-299 directed to oxygen of Glu-505 residue was about 7.0 Å, consistent with the active site of a glycoside hydrolase with a retaining mechanism.

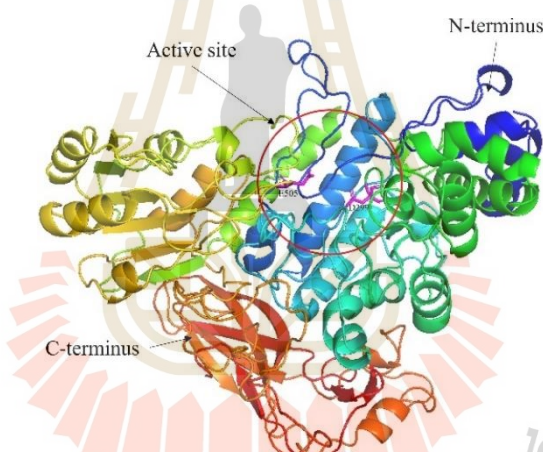
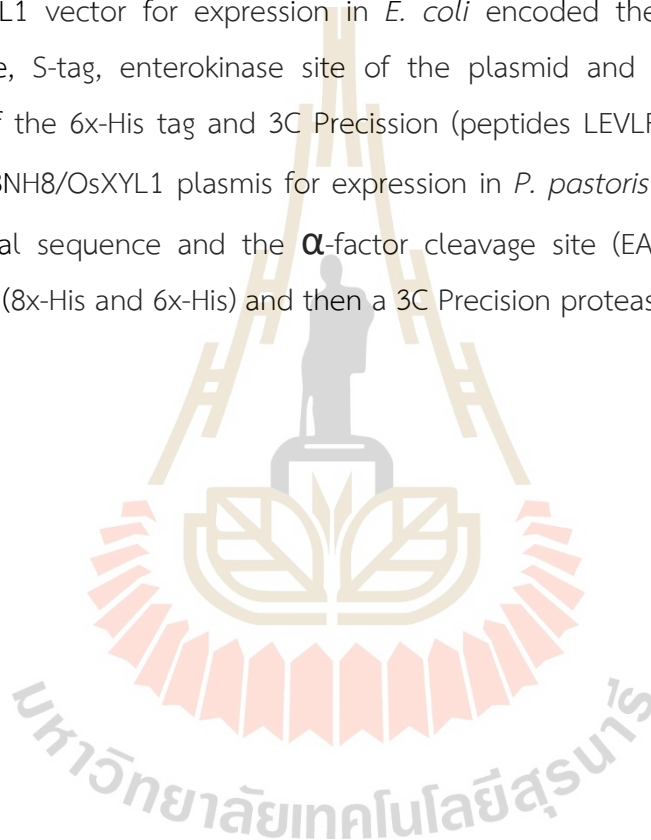


Figure 3.4 Homology model of OsXYL1 based on the X-ray crystal structure of the *Hypocrea jecorina* β -xylosidase Xyl3A (Bxl1) in complex with 4-thioxylobiose (PDB code 5AE6). The catalytic nucleophile (Asp-299) and acid/base residues (Glu-505) are shown in sticks (magenta color) representation and highlighted with a red circle.

The other common conserved GH3 sequences, the WGR and KH motifs, begin at residues Trp-170 and Lys-216, respectively. Finally, in the amino acid sequence alignment in Figure 3.5, the OsXYL1 possesses three potential *N*-glycosylation sites in its protein sequence. The asparagine residues at positions N-205, N475, and N644 may be glycosylated in the ER, based on its predicted subcellular localization in the secretory pathway or outside the cell.

Without considering glycosylation, the synthesized β -xylosidase OsXYL1 contains 772 amino acid residues and was predicted by the ProtParam facility of the ExPASy bioinformatic analysis to have a theoretical molecular mass of 83.952 kDa, pI of 6.12 and an extinction coefficient of $100,700 \text{ M}^{-1}\text{cm}^{-1}$ for determined protein concentration in spectrophotometrically by absorbance at 280 nm. In addition, for the recombinant fusion protein with the N-terminal peptide sequences of the plasmids, there were other tag sequences encoded in the constructs to produce fusion proteins. The pET32a/OsXYL1 vector for expression in *E. coli* encoded the thioredoxin, His-tag, thrombin site, S-tag, enterokinase site of the plasmid and additional N-terminal sequences of the 6x-His tag and 3C Precision (peptides LEVLFQ/GP) cleavage sites. The pPICZ α BNH8/OsXYL1 plasmid for expression in *P. pastoris* also encoded the N-terminal signal sequence and the α -factor cleavage site (EAEA) followed by two histidine tags (8x-His and 6x-His) and then a 3C Precision protease site.



OsXyl1	MGRRARALLHAPAPLLLLLALAAAAAVALASGPPFSCGAPSSAAFCNPRLPPIEQRADDL	60
Bxl1 (5ae6.1.A)	-----KNNLVCDSSAGYVERAQAAL	19
OsXyl1	VSRLTLEEKISQLGDQSPAVDRLGVPAYKWWSEALHGVSNAGRGIHLDGPLRAATSFPQV	120
Bxl1 (5ae6.1.A)	ISLFTLEELILNTQNSGPGVPRLGLPNYQVWNEALHGLDRANFATK-GGQFEWATSFPM	78
OsXyl1	ILTAASFNPHLWYRIGQVIGTEARAVYNNQAEGLTFWAPNINVFRDPRWGRGQETPGED	180
Bxl1 (5ae6.1.A)	ILTTAALNRTLHIQIADIISTQARAFSNSGR-YGLDVYAPNVNGFRSPLWGRGQETPGED	137
	CHO Δ	
OsXyl1	PT-VTGKYAAVFVRGVQGYALAGAINSTDLEASACCKHFTAYDLENWKGVTTRYAFDAKVT	239
Bxl1 (5ae6.1.A)	AFFLSSAYTYEYITGIQGGV-----DPEHLKVAATVKHFTAGYDLENWNNQSRLLGFDIIT	192
OsXyl1	AQDLADTYNPPFRSCVEDGGASGIMCSYNRVNGVPTCADYNLLSKTARGDWRFY--GYIT	297
Bxl1 (5ae6.1.A)	QQDLSEYITPQFLAAARYAKSRSLMCAYNSVNGVPSCANSFFLQTLRESWGFPWGYVS	252
	Catalytic nucleophile ▽	
OsXyl1	SDCDAVSIIHDVQGYAKTAEDAVDLKAGMDVNCGSYVQEHGLSAIQQKITEQDINRA	357
Bxl1 (5ae6.1.A)	SDCDAVYNVFNPHDYASNQSSAAASSLRAGTDIDCGQTYPWHLNESEVAGEVSRGEIERS	312
OsXyl1	LHNLFAVRMLGLFNGNPKYRNYGNIGPDQVCTQEHQNLALEAAQHGVVLLKNDANALPL	417
Bxl1 (5ae6.1.A)	VTRLNANLVRLGYFDKKNQ---YRSLGWKDVVKTDawnisYEAAVEGIVLLKND-GTLPL	368
	CHO Δ	
OsXyl1	SKSQVSSIAVIGHNANDATRLGNFYGPCCISVTPLQVLQGYVKDTRFLAGCNSAACNV	477
Bxl1 (5ae6.1.A)	SK-KVRSIALIGPWANATTQMGGNYGPPAPYLIISPLEAAKAGYHVNFEELGTEIAGNSTT	427
	Catalytic acid ▽	
OsXyl1	SIGEAQQLASSVDYVFLMGLDQDQEREEDVDRLELSPGMQENLNTVANAACKPVILVL	537
Bxl1 (5ae6.1.A)	GFAKIAIAAKKSDAIITLGGIDNTIEQEGADRTDIAWPGNQDLIKQLSE-VGKPLVVLQ	486
OsXyl1	LCGGPVDVTFAYNPKIGAILWAGYPGEAGGIAIAQVLFGEHNPGGRLPVWTYPKEF-TS	596
Bxl1 (5ae6.1.A)	MGGGQVDSSSLKSNKKVNSLVWGGYPGQSGGVALFDILSGKRAPAGRLVTTQYPAYEVHQ	546
	CHO Δ	
OsXyl1	VPMTDMRMADPSTGYPGRTYRFYRGNTVYKFGYGLSYSHHFVANGTKLPSLSSIDG	656
Bxl1 (5ae6.1.A)	FPQNDMNLRPD-GKSNPGQTYIWTYTKPVYEFSGSLFYTTFKETLASHPKSL-KENTSSI	604
OsXyl1	LKAMATAAAGTVSYDVEEIGPETCDKLKFPALVRVQNHGPMGRHPVLLFLRWPNGAAG	716
Bxl1 (5ae6.1.A)	LSA-----PHPGYTYSEQIPVTFEANIKNKSGKTESPYTAMLFVRTSNAG-PA	651
OsXyl1	GRPASQLIGFQSL-HLKSMQTVHMEFEVSPCKHFSRATEDGKKVIDHGSHFMMVGDDFE	775
Bxl1 (5ae6.1.A)	PYPNKWLVGFDRLADIKPGHSSKLSIPIV-SALARVDSHGRIVYPGKYELALNTDES-	709
OsXyl1	MSFTP 780	
Bxl1 (5ae6.1.A)	----- 709	

Figure 3.5 Amino acid alignment of the rice β -xylosidase OsXYL1 with the fungal *Hypocrea jecorina* β -xylosidase Xyl3A (Bxl1). The up-arrow indicates *N*-glycosylation sites in rice OsXYL1. Identical residues in the three sequences are indicated with asterisks (*), the conserved motifs are indicated in the boxes and the putative catalytic nucleophile and acid/base by down-arrows.

3.3 Expression and purification of OsXYL1 in *E. coli*

A recombinant pET32a/OsXYL1 clone was confirmed by DNA sequencing results before it was transformed into *E. coli* strains for protein expression with induction with IPTG (final concentration 0 – 0.5 mM). Screening concentration of IPTG for protein expression was done in *E. coli* Origami (DE3) and Origami B(DE3) strains which grown

on LB broth with induction at 20 °C for 16 h. The harvested cell pellets were thawed and lysed to determined proteins expression patterns by SDS-PAGE (as shown in Figure 3.6-3.7) of both insoluble (Figure 3.6A and 3.7A) and soluble (Figure 3.6B and 3.7B) fractions.

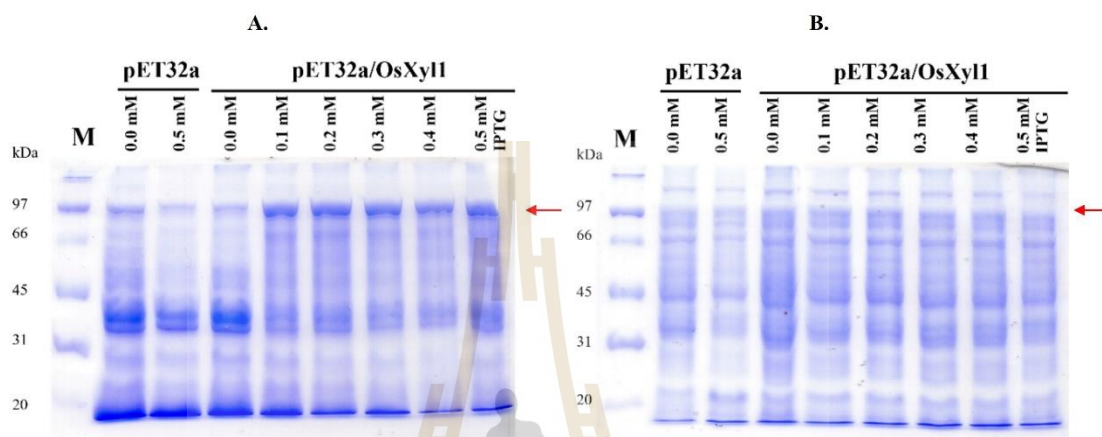


Figure 3.6 SDS-PAGE analysis of insoluble (A) and soluble (B) fractions of crude extracts of pET32a/OsXYL1 in Origami(DE3) after IPTG induction. The pET32a containing cells were induced with 0 and 0.5 mM IPTG induction and analyzed in the same manner for comparison. Lane M is proteins marker.

As seen in Figure 3.6 of SDS-PAGE for the recombinant OsXYL1 protein that was expressed in Origami(DE3) that found the overexpression in induction with all IPTG concentrations (0.1 – 0.5 mM) gave similar levels (Figure 3.6A). A protein band of around 95 kDa was found that was significantly different with the controls of without IPTG induction (0 mM) and empty pET32 plasmid without OsXYL1 insertion (0 and 0.5 mM IPTG). This band was in the insoluble fraction (Figure 3.6B), likely in inclusion bodies, and was not extracted to the cell lysate. The enzyme assay with 4NPXyl substrate also showed low activity (data not shown).

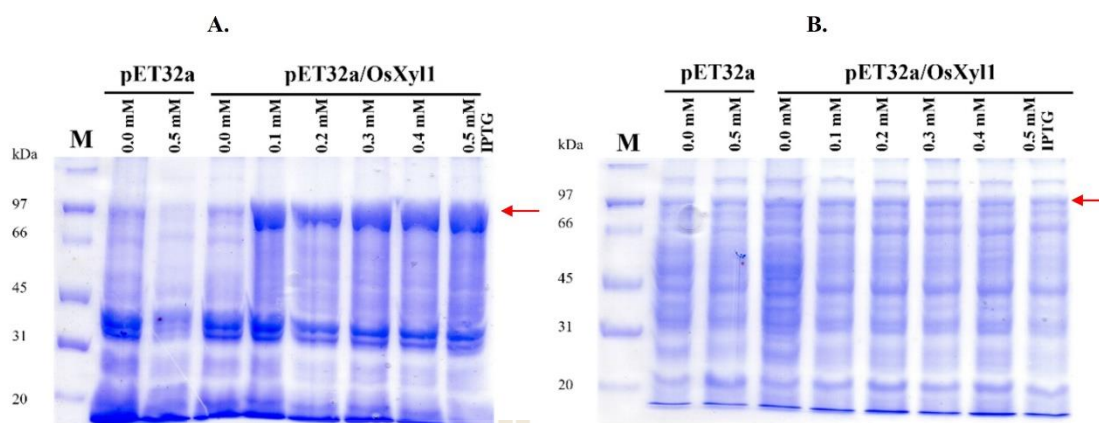


Figure 3.7 SDS-PAGE analysis of insoluble (A) and soluble (B) fractions of crude extracts of pET32a/OsXYL1 in OrigamiB(DE3) after IPTG induction. Cells containing empty pET32a were induced with 0 and 0.5 mM IPTG induction and analyzed in the same manner for comparison. Lane M is proteins marker.

Figure 3.7 shows the SDS-PAGE for the recombinant OsXYL1 expressed in OrigamiB(DE3) that gave a similar trend with Origami(DE3), the overexpression was relatively low in soluble fractions (Figure 3.7B). The OrigamiB(DE3) strain gave higher overexpression than Origami(DE3), as a strong band was seen around 95 kDa (Figure 3.7). However, the overexpression of OsXYL1 in *E. coli* only yielded large amounts of insoluble protein aggregates, likely in the form of inclusion bodies. However, a portion of the recombinant enzyme remained in the soluble fraction and β -xylosidase activity against 4NPXyl substrate was detected in this fraction.

Since the expression partially worked in the *E. coli* system, expression of recombinant OsXYL1 protein in the OrigamiB(DE3) strain in larger scale with 0.1 mM IPTG induction for 16 h was performed to try to purify the protein. The construct of pET32/OsXYL1 containing the thioredoxin and polyhistidine tags linked to N-terminal of OsXYL1 that was provided protein bound with a Ni^{2+} charged IMAC column. The recombinant protein was purified by the eluted in 250 mM imidazole then dialyzed and concentrated before cutting with 3C PreScission protease enzyme to remove the tag proteins, followed by SDS-PAGE analysis.

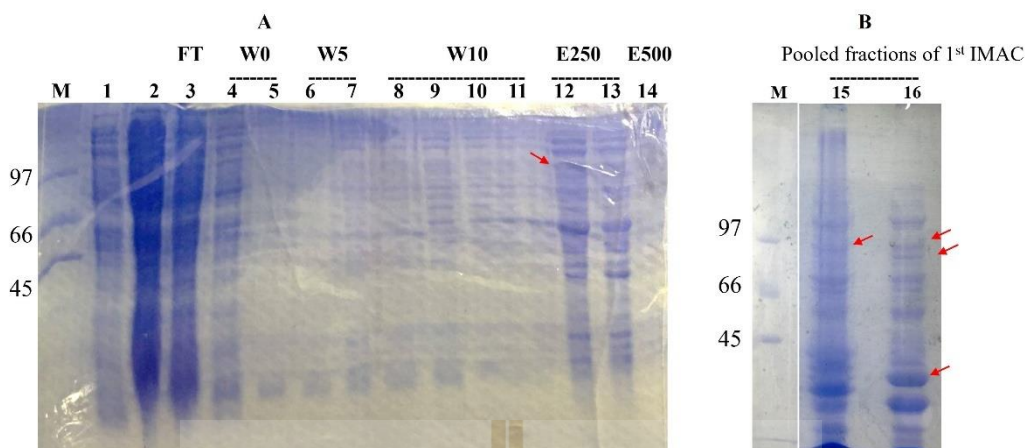


Figure 3.8 SDS-PAGE analysis of expression of recombinant OsXYL1 in OrigamiB(DE3). A, purification by Ni-IMAC. B, Pooled IMAC fractions and reaction with 3C Precision protease. Lanes: 1, insoluble proteins in pellet; 2, supernatant; 3, flow-through; 4-14, washed (W) and eluted (E) fractions with IMAC buffer, 50 mM Tris-HCl, pH 8.0, 300 mM NaCl, 5 mM-500 mM imidazole; 15, pooled fractions of IMAC column; and 16, digested fractions with 3C protease. M, standard markers.

The SDS-PAGE analysis of purified OsXYL1 presented an expected-size band (~95 kDa) and a large number of background protein bands, as seen in Figure 3.8 (A) and (B). Because of the N-terminal tag containing thioredoxin (Mw 12 kDa), plus polyhistidine (6x, 8x-His) tags and other tag, the molecular mass was ~95 kDa, but the first IMAC also showed a great deal of impurity. SDS-PAGE analysis (Figure 3.8B) of the pooled IMAC fraction (lane No. 15) and the result of 3C PreScission protease (lane No. 16) was a lower band under the recombinant OsXYL1 that obtained band after cleavage protein and in the bottom found the extra one band of peptide (Mw ~ 28 kDa) after cleavage at the 3C site from the N-terminal of OsXYL1. However, when this digested protein was subsequently passed through the second IMAC column, the flowthrough included OsXyl, as indicated by weak β -xylosidase activity (data not shown). The process yielded a very low amount of OsXYL1 protein and proteolytic degradation was also observed during the purification, which may contribute to the decreased enzyme activity.

The expression of OsXYL1 protein was problematic to produce in recombinant *E. coli*, so an alternative system was desired. The heterogenous expression systems in

which many plant GH3 proteins have been expressed include the *Pichia* system, in which barley HvExoI was expressed (Luang et al., 2010), and native or heterologous plant system, such as Gtgen3A from Gentian leaves (Takahashi *et al.*, 2018), RsAraf1 from transgenic *Arabidopsis* (Kotake *et al.*, 2006), MsXyl1 purified from transgenic *M. truncatula* plant (Xiong *et al.*, 2007) and *Arabidopsis* AtBXL1 in wild-type plants (Goujon *et al.*, 2003).

3.4 Expression and purification of OsXYL1 in *P. pastoris*

Initially, *Pichia* clones were screened for β -xylosidase activity and those expressing significant β -xylosidase activity were further characterized. The six-exhibiting high β -xylosidase activity in medium from the α -factor fusion protein encoded in pPICZ α BNH8/OsXYL1/SMD116H and two controls of pPICZ α BNH8/SMD1168H colonies were screened in small scale to optimize expression condition, as shown in Figure 3.9. The supernatant of OsXYL1 clones contained β -xylosidase activity hydrolyzing 4NPXyl substrate that increased over time and no increasing significant activity occurred in controls.

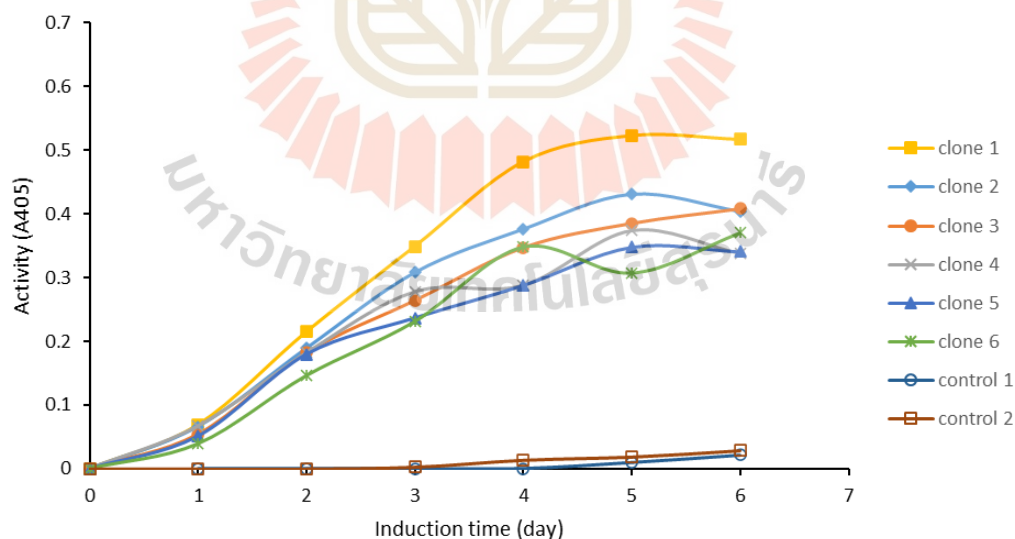


Figure 3.9 Expression of *P. pastoris* transformants of OsXYL1 in BMMY broth induced with 0.5% (v/v) methanol for 6 days and the β -xylosidase activity assay. The activity was assayed with 1 mM 4NPXyl, in 50 mM NaOAc buffer, pH 4.0, at 60 °C for 30 min.

The activity is plotted as A_{405} versus induction times. Clones 1-6, pPICZ α BNH8/OsXYL1; controls 1-2, pPICZ α BNH8.

The β -xylosidase activity resulted in the secreted OsXYL1 *P. pastoris* media was slowly increased until 4 days when induction with 0.5% (v/v) methanol at 20 °C, and reached maximum at day 5. No increase in β -xylosidase activity was observed in *Pichia* transformant of control pPICZ α BNH8. Thus, expression condition in shake flask of secreted OsXYL1 in the BMMY broth was induced with 0.5% methanol at 20 °C for 5 days. The 5-days-old broth was collected by centrifugation to remove the cell debris and kept on ice for purify protein in the day that collecting cell or kept on 15% glycerol at -80 °C. Initially, the secreted protein was precipitated from the supernatant with 70-75% (w/v) ammonium sulfate, followed by resuspension and dialysis in 20 mM Tris-HCl buffer, pH 8.0. This procedure resulted in contaminating pigments throughout the filtered dialyzed solution that interfered with protein binding during chromatographic purification, but it did not appear to affect the enzyme activity. Thus, the supernatant containing secreted OsXYL11 protein was adjusted to pH 7.5, then any precipitate salts were filtered out and the supernatant supplemented with 1 mM PMSF to avoid proteolytic degradation before loading to the IMAC column for purification. Initially, several chromatographic resins were tested for purifying the protein, including HiTrap Q FF, Phenyl Sepharose FF, nickel- or cobalt-bound IMAC resin and con-A Sepharose 4B. They were tested for high performance in protein binding and elution fractions were checked by activity assay with 4NPXyl and SDS-PAGE profiles.

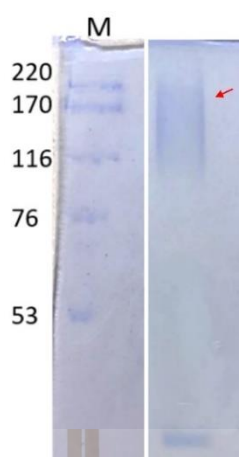


Figure 3.10 10% SDS-PAGE of pooled fractions of secreted OsXYL1 protein. The protein was purified by Ni-NTA IMAC with imidazole in equilibration buffer. Smeared protein is indicated with the red arrow. Lane M, high molecular weight marker.

As seen in Figure 3.10, which shows the 10% SDS-PAGE gel, the secreted OsXYL1 protein from *Pichia* was expressed in glycosylated form, which presented as a smear band at the top of the lane with a molecular mass over the 116 kDa. This is expected for glycosylated protein, since three glycosylation sites were predicted in the OsXYL1 protein sequence and yeast give heterogeneous glycosylation.

Thus, this OsXYL1 secreted glycoprotein was purified from *Pichia* culture media. A two-step chromatographic purification was performed to purify OsXYL1. Since this construct contains 8x- and 6x-histidine tags at the N-terminus site of OsXYL1 after the secretory peptide cleavage site, the Ni^{2+} -charged IMAC resin was selected to purify the secreted OsXYL1 which was obtained from large-scale culture medium after its pH was adjusted to 7.5. The IMAC resin was increased up to 30 mL volume to enhance the amount of bound protein. The bound protein was eluted from the IMAC column with 50-150 mM imidazole in IMAC buffer (pH 8.0). The β -xylosidase activity was tested by the 4NPXyl assay and SDS-PAGE analysis was done. The fractions with β -xylosidase activity were pooled and further purified by size-exclusion chromatography (SEC) over a S200 gel filtration column. The peak with β -xylosidase activity occurred in the fractions 20-29 (at an elution volume of 10-14 mL), corresponding to the major peak (Figure 3.11). The fractions that contained β -xylosidase activity were pooled and designated as purified OsXYL1.

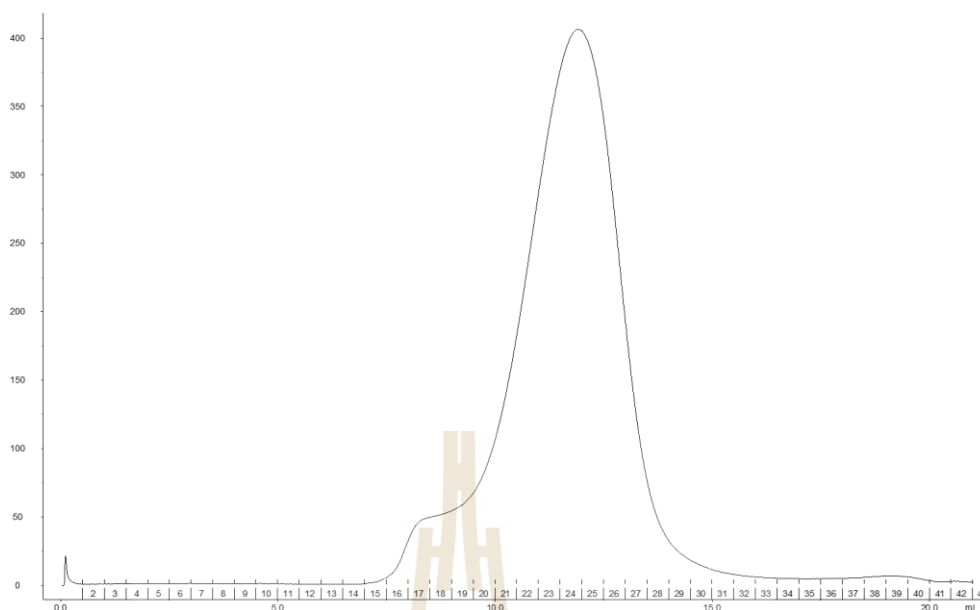


Figure 3.11 S200 Gel filtration protein elution profile of OsXYL1. The chromatography was run at the flow rate of 0.3 mL/min with 20 mM Tris-HCl buffer, pH 8.0, 150 mM NaCl. The sample volume was 0.5 mL injection of the pooled IMAC column fractions. The fractions were pooled with No. 20-29 and concentrated.

The purified OsXYL1 protein from *P. pastoris* medium is shown in Figure 3.12. The secreted OsXYL1 appeared as a high MW smear band that confirmed that the protein was glycosylated. When the protein was deglycosylated by treatment with Endoglycosidase H (Endo H), a major band appeared below the band of 97 kDa in the protein MW marker (Figure 3.12, Lane 5). The deglycosylated OsXYL1 resulted in an estimated molecular mass of 84 kDa. Another major band was seen at around 70 kDa, which might suggest that some of the protein had been degraded, and Endo H protein was apparent at a molecular mass of 29 kDa, so the band near the bottom of the gel in the deglycosylated protein sample likely represents Endo H.

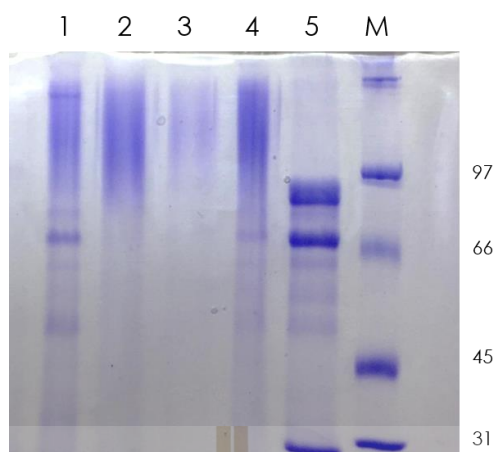


Figure 3.12 12% SDS-PAGE analysis of sample taken during the purification of secreted OsXYL1. Lanes 1-2, pool of IMAC imidazole fractions; lane 3, S200 pool before concentration; lane 4, purified OsXYL1; lane 5, purified OsXYL1 treated with Endo H; lane M, protein marker.

Pichia pastoris has been received attention as the heterologous host for proteins expression due to its remarkable advantages, such as inducible expression using controllable promoters and simplicity of the medium conditions (Macauley-Patrick, *et al.*, 2005; Dehnavi *et al.*, 2016). Using a codon optimization technique, β -xylosidase OsXYL1 was successfully expressed in this unicellular eukaryotic system. Enzyme yields, specific activity measured with 4NPXyl substrate, and the purification factors are given in Table 3.1. The purification resulted in a final yield 0.57% recovered activity compared to the crude medium. During the purification, the specificity increased from 0.00086 to 0.086 U/mg, with implies a degree of purification of 101-fold.

Table 3.1 Enzyme yields during purification of OsXYL1.

Purification Step	Volume (mL)	Total protein (mg)	Specific activity (U/mg)	Total activity (U)	Yield (%)	Purification (fold)
Crude protein	1600	28,953	0.00086	24.76	100	1
Ni-IMAC						
-E50	0.5	0.760	0.015	0.011	0.045	17
-E75	0.2	0.374	0.018	0.007	0.027	21
-E150	1	0.762	0.025	0.019	0.077	29
S200 gel filtration	0.28	1.640	0.086	0.14	0.571	101

Yields are expressed as percentage of enzyme activity in the crude protein, and purification factors are calculated on the specific activities.

3.5 Effects of pH and temperature on β -xylosidase OsXYL1

The effects of pH and temperature on the activity of purified OsXYL1 were determined. The pH profile exhibited a sharp bell-shaped curve that bit elongated toward the upper pH range (Figure 3.13), and the optimum pH for β -xylosidase activity occurred at pH 4.0. The activity versus pH profile increased rapidly from the pH 3.5 to 4.0, where it reached the maximum activity and slowly decreased with increasing pH to less than 10% at pH 8-11. OsXYL1 was projected to have 50% maximal activity at pH 3.4 and 5.7. The pH optima of rice OsXYL1 was 4.0 that this value is the same range pH 4-5 of those previously determined for β -xylosidase from barley (Lee *et al.*, 2003), stem of *Arabidopsis* (Minic *et al.*, 2004), alfalfa roots (Xiong *et al.*, 2007) and certain β -xylosidase from fungi and bacteria (Choengpanya *et al.*, 2015; Inoue *et al.*, 2016; Dehnavi *et al.*, 2016; Mhetras *et al.*, 2016).

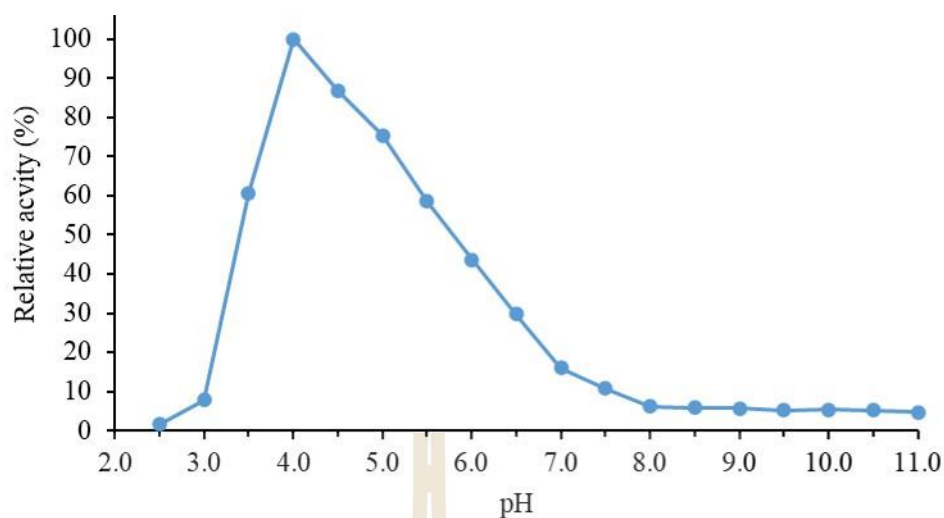


Figure 3.13 Activity versus pH profile of purified OsXYL1 over the range of 2.5-11.0 (in 0.5 increments). The β -xylosidase activity was assayed with 1 mM 4NPXyl substrate in McIlvaine buffers at 37 °C for 30 min.

As for the temperature effect on purified OsXYL1, the temperature profile was bell-shaped, and the highest activity of OsXYL1 was detected as 60 °C. The activity slowly increased from 30-60 °C, where is reached the maximum at 60-65 °C (Figure 3.14), and rapidly decreased at 75 to 80 °C. Again, this value is close to temperature optima reported for β -xylosidase stem of *Arabidopsis* (Minic *et al.*, 2004) and certain β -xylosidase from fungi and bacteria (Choengpanya *et al.*, 2015; Inoue *et al.*, 2016; Yan *et al.*, 2012, Dehnavi *et al.*, 2016; Mhetras *et al.*, 2016, Shi, *et al.*, 2013, Zhou, *et al.*, 2011, de Carvalho, D.R., *et al.*, 2018).

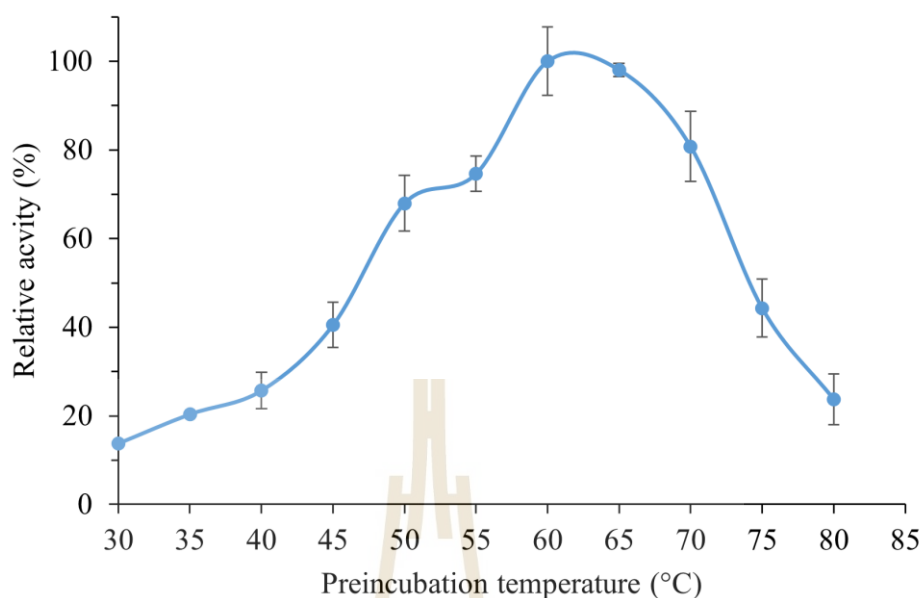


Figure 3.14 Activity versus temperature profile of purified OsXYL1 over temperatures ranging from 30 to 80 °C (in 5 °C increments). The β -xylosidase activity was assayed with 1 mM 4NPXyl substrate in 50 mM sodium acetate buffer, pH 4.0, for 30 min.

As shown in Figure 3.15, the residual activity of purified OsXYL1 demonstrated thermostability up to 50 °C, with more than 50% activity remaining after 4 h at temperatures ranging from 30-50 °C. At the optimum temperature (60 °C), the residual activity was similar with 30-50 °C when the enzyme was incubated for 30 min, but decreased to less than 50% by about 42 min. At 60 °C, less than 30% of the activity remained when incubated 1 h or longer. At 70 °C, all activity was lost within 1 h. The protein precipitated with higher temperatures and longer incubations. According to these results, β -xylosidase activity of rice OsXYL1 was determined at 40 °C in subsequent experiments.

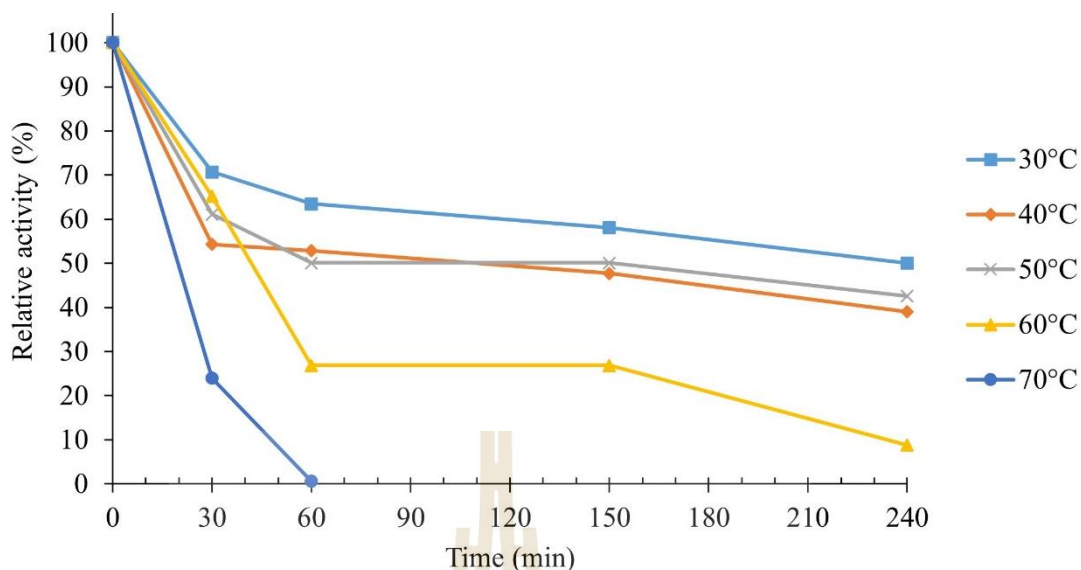


Figure 3.15 Thermostability of the purified OsXYL1. The residual activity was monitored after the enzyme was preincubated at 30 °C (filled squares), 40 °C (filled diamonds), 50 °C (x), 60 °C (filled triangles), and 70 °C (filled circles) for the designated time periods, then activity was assayed in the standard assay. The maximum activity was defined as 100%, which was the activity for enzyme with no preincubation.

Rice β -xylosidase OsXYL1 has a temperature and pH optimum different from typical in rice growth conditions as shown in β -glucan exohydrolase (Prawisut *et al.*, 2020) and β -glucosidase BGlu1 (Opassiri *et al.*, 2003), but similar to characterized plant GH3 β -xylosidase from *Arabidopsis* stem tissues, flower, and siliques (Goujon *et al.*, 2003; Minic *et al.*, 2004; 2006), barley seedling (Lee *et al.*, 2003), alfalfa roots (Xiong *et al.*, 2007), radish seeds (Kotake *et al.*, 2006), fruit development and ripening (Tateishi *et al.*, 2005; Bustamante *et al.*, 2006), and immature stalk of sugarcane (Chinen *et al.*, 1982).

3.6 Effect of carbohydrates on β -xylosidase OsXYL1

The effects of carbohydrates (monosaccharides and disaccharides) in reaction solutions on the β -xylosidase activity of purified OsXYL1 were tested as shown in Figure 3.16. The β -xylosidase activities against 4NPXyl substrate in the presence of xylose concentrations of 10 and 50 mM were decreased to 28.7% and 5.5%,

respectively, compared to the reaction without xylose additive, which indicates that xylose strongly inhibited to the purified OsXYL1. Other sugars (arabinose, glucose, mannose, galactose, fructose, lactose, maltose and sucrose) had small effects compared with xylose. In addition, the activity in the presence of 50 mM arabinose, glucose and mannose were decreased, which might suggest that they also affect β -xylosidase OsXYL1 as these monosaccharides are present as substituents in the arabinoxylan of the cell wall polysaccharides (Carpita *et al.*, 2001; Burton and Fincher, 2014).

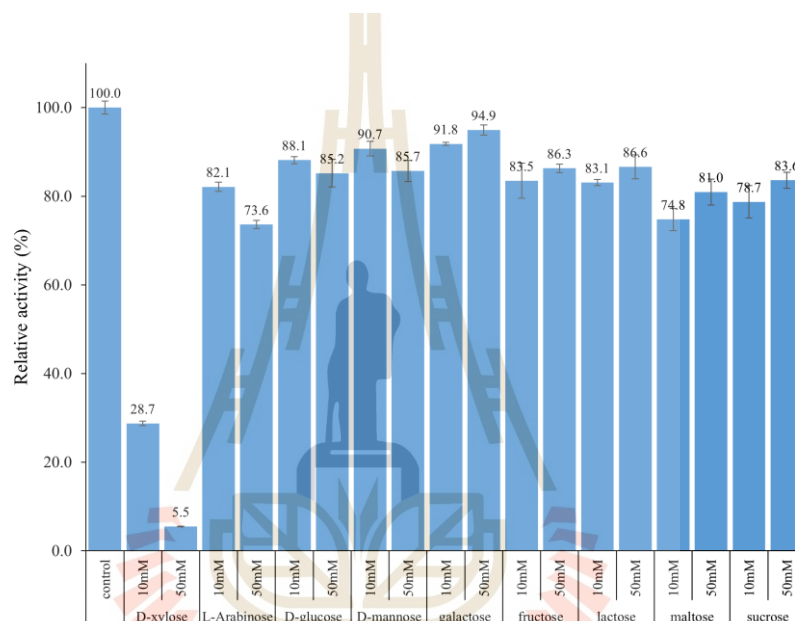


Figure 3.16 Effect of carbohydrates on OsXYL1 β -xylosidase. In the presence of 10 and 50 mM carbohydrates, activity toward 1 mM 4NPXyl was assayed in 50 mM sodium acetate buffer (pH 4.0), at 60 °C. The activity for enzyme in the absence of carbohydrates was defined as 100%.

3.7 Effect of metal ions and EDTA on β -xylosidase OsXYL1

The β -xylosidase activity of purified OsXYL1 was tested in the presence of metal ions and EDTA (Figure 3.17). The activity of purified OsXYL1 was insensitive to the presence of MgCl_2 , MgSO_4 , FeSO_4 , CoCl_2 , EDTA at both concentrations tested. In contrast, $\text{Co(NO}_3)_2$, NiSO_4 , and ZnSO_4 additives had little effect to decrease β -xylosidase activity at 5 mM concentration, but had increased effect to about 50% at the 10 mM concentration. Ten molecules of Zn ions were reported in the X-ray crystal structure

of fungal GH3 β -xylosidase Bxl1 (Mikkelsen *et al.*, 2015) which supports an effect of Zn^{2+} on the protein activity. In addition, OsXYL1 was highly sensitive to MnCl_2 , which completely depleted the activity at the 10 mM concentration. A strong inhibitory effect was also observed in Cu^{2+} ion of CuSO_4 that decreased activity at 5 and 10 mM by 25% and 60%, respectively. It has been previously reported that divalent Cu^{2+} and Hg^{2+} ions are potent inhibitors of a GH3 xylosidase (Tateishi *et al.*, 2005). OsXYL1 was sensitive to monovalent of Li^+ , Na^+ , and K^+ ions, which increased activity at 5 mM concentration but this effect was not seen at 10 mM concentration. EDTA had no influence on enzyme activity, suggesting that this enzyme is not a metalloprotein, and lack of metal requirements is a common feature of GH3 proteins. The results of biochemical properties of OsXYL1 were almost the same as those in previous β -xylosidase reports.

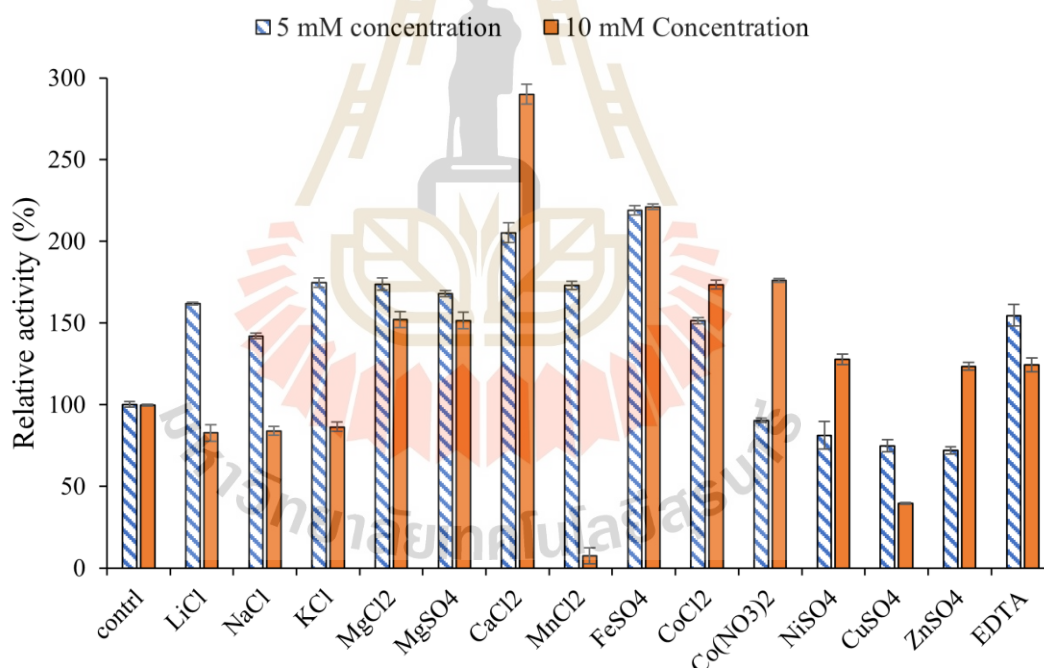


Figure 3.17 Effect of metal ions and EDTA on OsXYL1 β -xylosidase. In the presence of 5 mM (white and blue stripes) and 10 mM (solid orange color) metal ions or EDTA in reactions, activity was assayed toward 1 mM 4NPXyl in 50 mM sodium acetate buffer, pH 4.0, at 60 °C. The activity for enzyme in the absence of metal ions was defined as 100%.

3.8 Transglycosylation of β -xylosidase OsXYL1

Transglycosylation of OsXyl1 β -xylosidase in the presence of alcohols, including methanol, ethanol, 2-propanol, *n*-propanol, *n*-butanol, 3-methyl-butanol, and 1-octanol with 4NPXyl substrate was evaluated, since including alcohol increased the A_{405} values of the 4NP product in hydrolytic reactions. The transglycosylation activity of OsXyl1 with alcohols was analyzed by TLC, as shown in Figure 3.18. However, no product was initially observed in buffer with long chain alcohols, like 1-octanol, which was not miscible in the buffer.

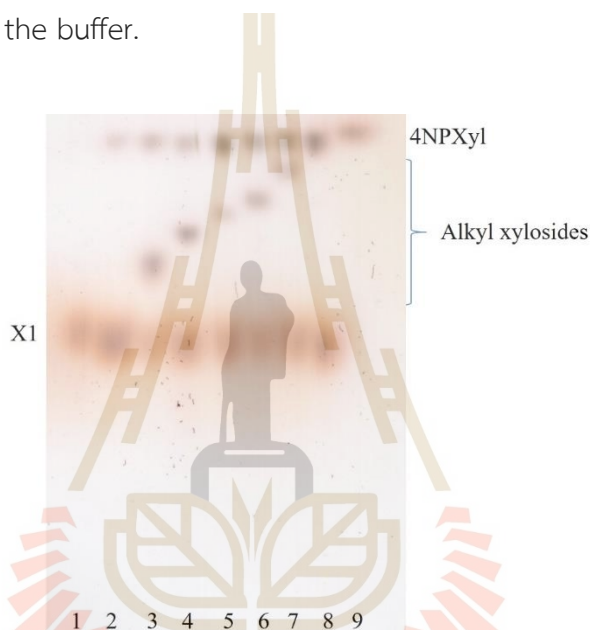


Figure 3.18 TLC pattern of transglycosylation products of OsXYL1 with alcohol acceptors. The reactions of 5 mM 4NPXyl and 15% alcohols in 50 mM sodium acetate buffer (pH 4.0) were incubated at 40 °C for 1 h. TLC was developed in ethyl acetate: acetic acid: water (2:1:1) and products were detected by staining with 10% sulfuric acid in alcohol. Lane 1, standard xylose; lane 2, control reaction without alcohol; lane 3, reaction with methanol; lane 4, reaction with ethanol; lane 5, reaction with iso-propanol; lane 6, reaction with *n*-propanol; lane 7, reaction with *n*-butanol; lane 8, reaction with 3-methy-1-buthanol; and lane 9, standard 4NPXyl.

As shown in Figure 3.18, the alkyl xyloside products of the transglycosylation activity were obtained in the same time as hydrolysis that produced xylose. The xylosyl residue in the complex of the glycosyl-enzyme intermediate was assumed to be

transferred to form the β -linkage with alcohols as acceptor groups, based on the mechanism of GH3 enzymes (Figure 1.10).

Since 1-octanol has low solubility in water (0.3 g/L) and showed no product in that condition, a co-solvent mixture with acetone was explored for transglycosylation activity toward 1-octanol (Thenchartana *et al.*, 2020). The reactions containing a co-solvent mixture of acetone and 1-octanol in sodium acetate buffer, pH 4.0, were tested with varied concentrations of acetone and octanol from 0-30% (v/v), as shown in Figure 3.19A. The optimized ratio of the co-solvent mixture in varied time 30 min to 6 h (Figure 3.19B), octyl xyloside product was obtained in the 20% (v/v) 1-octanol in 30% (v/v) acetone at 40 °C.

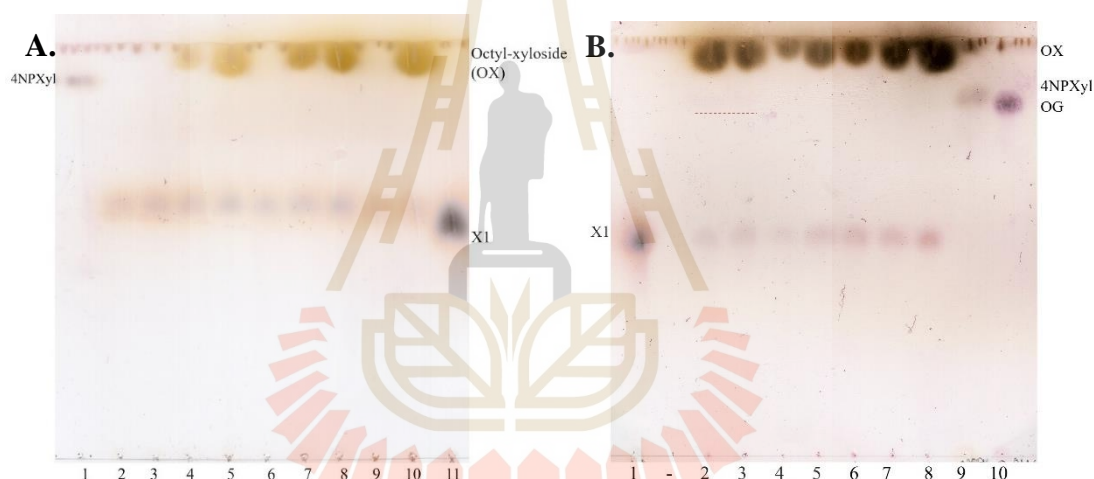


Figure 3.19 TLC patterns of transglycosylation products of OsXYL1 with 1-octanol in co-solvent mixtures. (A) Reactions with varied ratios of acetone and 1-octanol for 4 days. (B) Reactions at varied times in the 30% (v/v) acetone and 20% (v/v) octanol for 30 min - 6 h. The reactions incubated 0.5 nmol OsXYL1 with 5 mM 4NPXyl in co-solvent mixture at 40 °C. (A) TLC was developed in ethyl acetate: acetic acid: water (2:1:1). Lane 1, standard 4NPXyl; lane 2, control reaction; lane 3, 10% (v/v) acetone; lane 4, 10% (v/v) acetone and 10% (v/v) 1-octanol; lane 5, 10% (v/v) acetone and 20% (v/v) 1-octanol; lane 6, 20% (v/v) acetone; lane 7, 20% (v/v) acetone and 10% (v/v) 1-octanol; lane 8, 20% (v/v) acetone and 20% (v/v) 1-octanol; lane 9, 30% (v/v) acetone; lane 10, 30% (v/v) acetone and 20% (v/v) 1-octanol; lane 11, standard D-xylose. (B), TLC was developed in ethyl acetate: acetic acid: water (7:3:1). Lane 1, standard D-

xylose; lane 2, 30 min; lane 3, 1 h; lane 4, 2 h; lane 5, 3 h; lane 6, 4 h; lane 7, 5 h; lane 8, 6 h; lane 9, standard 4NPXyl; lane 10, standard octyl-glucoside (OG).

The octyl xyloside was major product from the transglycosylation activity of OsXYL1 in the cosolvent reaction, based on TLC, although the liberated xylose from the hydrolysis activity was observed as a by-product at all incubation times. Thus, the octyl xyloside product obtained from the transglycosylation reaction in co-solvent mixture were stable for 4 days or longer and not rapidly hydrolyzed by OsXYL1 enzyme as it accumulated in the reaction mixture. Similar results were seen for the shorter alkyl xylosides in the aqueous reactions. This suggests that OsXYL1 might be useful for enzymatic synthesis of alkyl xylosides for production by green chemistry (Park, *et al.*, 2017; Ochs, *et al.*, 2011; Nakamura, T., *et al.*, 2000; Smulek, W., *et al.*, 2017). This has been reported for other GH3 β -xylosidases with other acceptors, such as sugar alcohols, aliphatic and aromatic alcohols, and carbohydrates in enzymatic synthesis of β -D-xylosyl-oligomer products (Dilokpimol *et al.*, 2011; Korakake *et al.*, 2005; 2011). The importance of long-chain alkyl glycosides has been demonstrated for many industrial applications as non-ionic surfactants, the xylose derivative and xylose polymer (xylan) from the renewable biomass are candidates for xylosyl donors for production of new surfactants by the transglycosylation reaction.

However, it is not clear whether transglycosylation activity of OsXYL1 β -xylosidase can be used to imply its action in the cell wall remodeling of hemicellulose polysaccharide in plants by transglycosylation, since the conditions in the cell wall are different from those in the *in vitro* reactions. Further work could investigate this possibility.

3.9 Substrate specificity of β -xylosidase OsXYL1

Substrate specificity of purified OsXYL1 enzyme was assessed by testing hydrolytic activity toward various nitrophenyl glycosides. The activity compared at a standard substrate concentration of 5 mM for most glycosides and 1 mM for 4NPXyl, which was assayed at a reduced concentration of OsXYL1 enzyme. The results obtained show the β -xylosidase OsXYL1 enzymes had hydrolytic activity toward 4NP-

α -L-arabinofuranoside, 4NP- α -L-arabinopyranoside, 4NP-N-acetyl- β -D-glucosaminide, and 4NP- β -D-glucopyranoside. No hydrolytic activity was found with 4NP- α -D-mannopyranoside, 4NP- α -D-glucopyranoside, 4NP- α -L-fucopyranoside, 4NP- β -D-fucopyranoside, 2NP- β -D-glucopyranoside, 4NP- β -D-maltoside, 4NP- β -D-galactopyranoside, 4NP- α -D-galactopyranoside, 4NP β -D-glucoronide, or 2NP- β -D-galactopyranoside.

Table 3.2 Relative activity of β -xylosidase OsXYL1 with nitrophenyl glycosides.

Substrate ^a	Relative activity ^b (%)
4NP β -D-xylopyranoside ^c	100.0 \pm 2.1
4NP α -L-arabinofuranoside	5.98 \pm 10.2
4NP α -L-arabinopyranoside ^c	6.75 \pm 8.2
4NP N-acetyl- β -D-glucosaminide	2.3 \pm 0.5
4NP β -D-glucopyranoside	1.9 \pm 1.7

^a Reactions were incubated 3.57 nmol of OsXYL1 in standard reaction. Activity was determined in standard reaction and measured by the absorbance of 4NP released.

^b Values are the mean of triplicate independent experiments.

^c Reactions were incubated 0.89 nmol of OsXYL1 in standard reaction.

β -Xylosidase OsXYL1 was high specific for the β -xylosyl moiety of 4NPXyl, while it could hydrolyze the bonds to other sugar moieties in 4NPAraf and 4NPArap, 4NPGlcNac, and 4NPGlc with relative activity values varies not greater than 10% of that for 4NPXyl (Table 3.2). The enzymatic activity with the differently configured α -L-arabinosyl moieties in 4NPAraf and 4NPArap was previously observed in α -L-arabinofuranosidase from *Arabidopsis* and for bifunctional α -L-arabinofuranosidase/ β -xylosidase isolated from *Arabidopsis* stem (Goujon *et al.*, 2003; Minic *et al.*, 2004; 2006), barley seedling (Lee *et al.*, 2003), tomato fruit (Itali *et al.*, 2003), and alfalfa roots (Xiong *et al.*, 2007).

The activity toward β -1,4-xylosyl-oligosaccharides (XOSs) substrates with DP of 2-6, 1,4- β -D-xylobiose (X2), 1,4- β -D-xylotriose (X3), 1,4- β -D-xylotetraose (X4), 1,4- β -D-xylopentaose (X5), and 1,4- β -D-xylohexaose (X6) substrates was determined. The

hydrolytic products were separated by TLC and visualized by sulfuric acid staining, as shown in Figure 3.20.

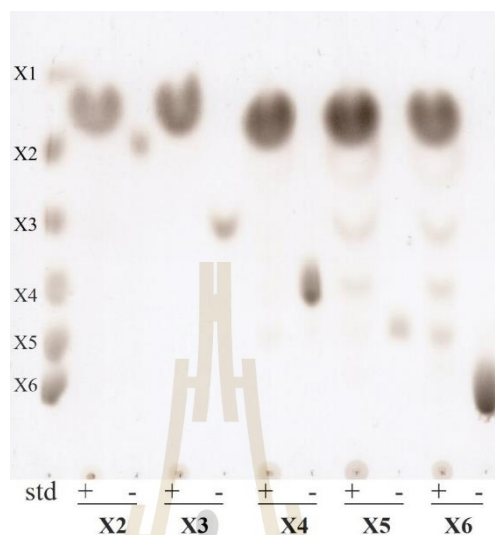


Figure 3.20 Hydrolysis activity of β -xylosidase OsXYL1 toward xylooligosaccharides. The reactions were incubated at 40 °C for 24 h. The TLC developing solvent was ethyl acetate: acetic acid: water (2:1:1). Lane (std), xylose (X1), and β -1,4-linked xylobiose to xylohexaose (X2-X6). Reaction with enzyme (+), and without enzyme (-).

The 1,4- β -D-xylobiose (X2) and 1,4- β -D-xylotriose (X3) were completely hydrolyzed to xylose, and 1,4- β -D-xylotetraose (X4) was mostly broken down to xylose after 24 h reaction with OsXYL1, while 1,4- β -D-xylopentaose (X5) and 1,4- β -D-xylohexaose (X6) remained shorter XOSs, with moderate yields X4, X3, X2 and X5, X4, X3, X2, respectively as residual intermediates. The major product of D-xylose in the hydrolysis reaction catalyzed by OsXYL1 β -xylosidase after the 24 h confirmed the exotype activity to remove terminal β -1,4-xylosyl residues. The completeness of the reaction was inversely proportional to the degree of polymerization, which suggests OsXYL1 is most efficient on and generally has highly specific hydrolysis of small unsubstituted XOS (Varghese, V. *et al.*, 1999; Karkehabadi, S., *et al.*, 2014; Polizeli *et al.*, 2005).

3.10 Kinetic parameters of OsXYL1 β -xylosidase

Kinetic parameters of the OsXYL1 β -xylosidase enzyme with nitrophenyl glycosides (4NPXyl, 4NPAr α f, and 4NPAr α p) and xylooligosaccharides (DP 2-6) substrates were determined. All kinetic assays of the β -xylosidase OsXYL1 were done at 40 °C, since the enzyme lost activity at its optimal temperature 60 °C within 1 h (Figure 3.15) and 40 °C is more similar to the temperature in a rice field.

Substrate saturation curves were fitted to Michaelis-Menten curves for 4XPXyl, while Hanes-Woolf plots were used for fitting 4NPAr α f and 4NPAr α p data to obtain kinetic parameters, as shown in Figure 3.21. The Michaelis-Menten constant (K_m), the catalytic rate constant (k_{cat}), and the catalytic efficiency or specificity constant (k_{cat}/K_m) of purified OsXYL1 toward 4NPXyl, 4NPAr α f, and 4NPAr α p substrates are listed in Table 3.3, and apparent k_{cat} values were calculated per subunit of 83.9 kDa.

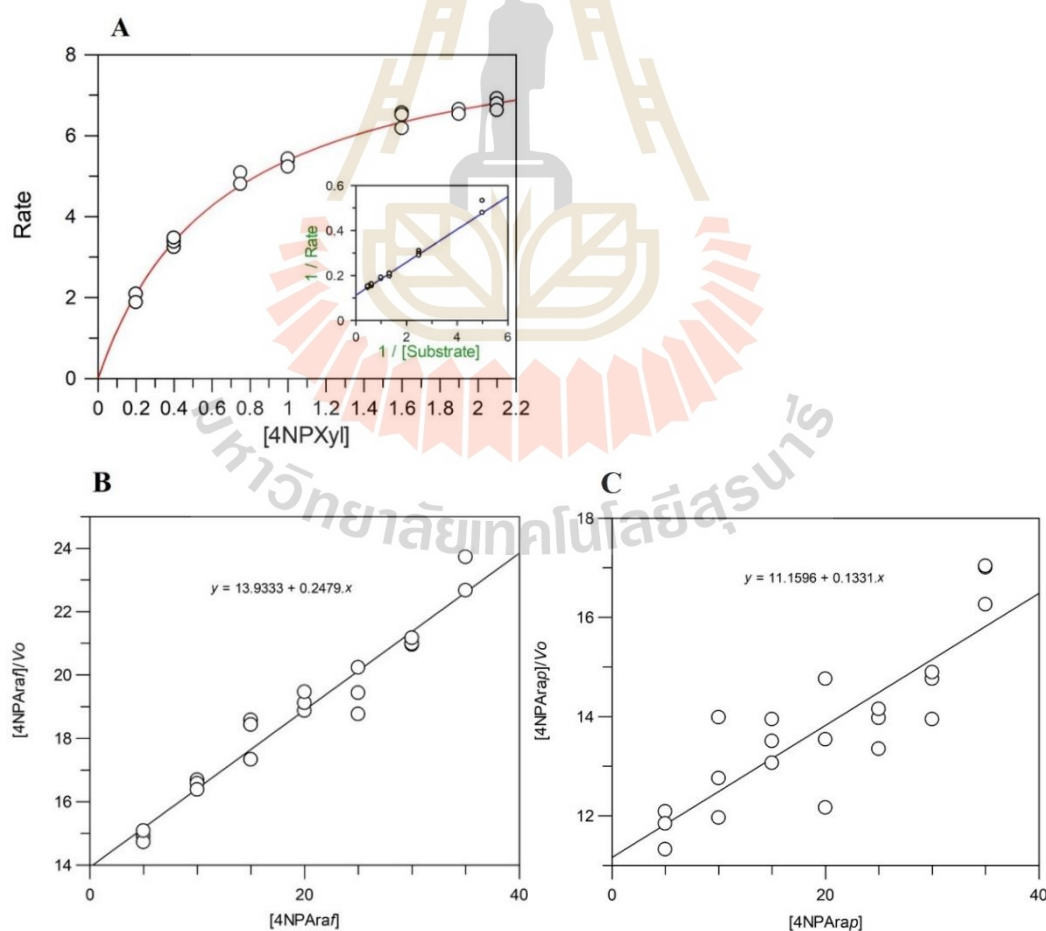


Figure 3.21 Michaelis-Menten (A) and Hanes-Woolf (B, C) plots of β -xylosidase OsXYL1 toward nitrophenyl glycoside substrates. Kinetic parameters of 4NPxyl (A), 4NPAr α f (B),

and 4NPArap (C) were determined from these curves. The concentrations of the hydrolytic products of nitrophenyl glycosides were calculated from a standard curve of NP. The curves were generated in GraFit 5 (Erithacus Software).

Table 3.3 Apparent kinetic parameters of β -xylosidase OsXYL1 toward nitrophenyl glycoside substrates.

Substrate	K_m (mM)	k_{cat} (s^{-1})	k_{cat}/K_m ($mM^{-1}s^{-1}$)
4NPXyl	0.65 ± 0.03	12.4 ± 0.2	19.01
4NPAr α f	56.2 ± 1.1	0.34 ± 0.013	0.0061
4NPAr α p	83.8 ± 3.1	0.19 ± 0.019	0.0022

The OsXYL1 β -xylosidase with preference for 4NPXyl with a K_m value of 0.65 ± 0.03 mM, which is similar to the other plant GH3 β -xylosidases (Lee *et al.*, 2003; Xiong *et al.*, 2007; Minic *et al.*, 2004; 2006). The specificity constant (k_{cat}/K_m), indicating catalytic efficiency at low substrate concentration and ability to compete as a substrate in mixed reactions, was >3000-fold higher for 4NPXyl than 4NPAr α f, and 4NPAr α p substrates (19.01, 0.0061, and 0.0022 $mM^{-1}s^{-1}$, respectively). The large difference in catalytic efficiency between hydrolysis of β -D-xylosyl and α -L-arabinosyl substrates, suggests that OsXYL1 β -xylosidase lacks the significant α -L-arabinosidase activity that is mostly found in bifunctional β -xylosidase/ α -L-arabinofuranosidase enzymes (Goujon *et al.*, 2003; Minic *et al.*, 2004; 2006; Lee *et al.*, 2003; Itali *et al.*, 2003; Sasaki *et al.*, 2004; Xiong *et al.*, 2007; Tateishi *et al.*, 2005; Tong, X., *et al.*, 2021).

Kinetic parameters of purified OsXYL1 toward β -1,4-xylosyl-oligosaccharides (X2-X6) substrates were determined, as release of D-xylose measured by a D-xylose assay kit. Substrate saturation curves were fitted to the Michaelis-Menten equation, as shown in Figure 3.22. The Michaelis-Menten constant (K_m), the catalytic rate constant (k_{cat}), and the catalytic efficiency (k_{cat}/K_m) of purified OsXYL1 toward XOS substrates (X2-X6) are listed in Table 3.4, where apparent k_{cat} values were calculated from the limiting velocity, V_{max} , by dividing protein concentration by the subunit mass of 83.9 kDa.

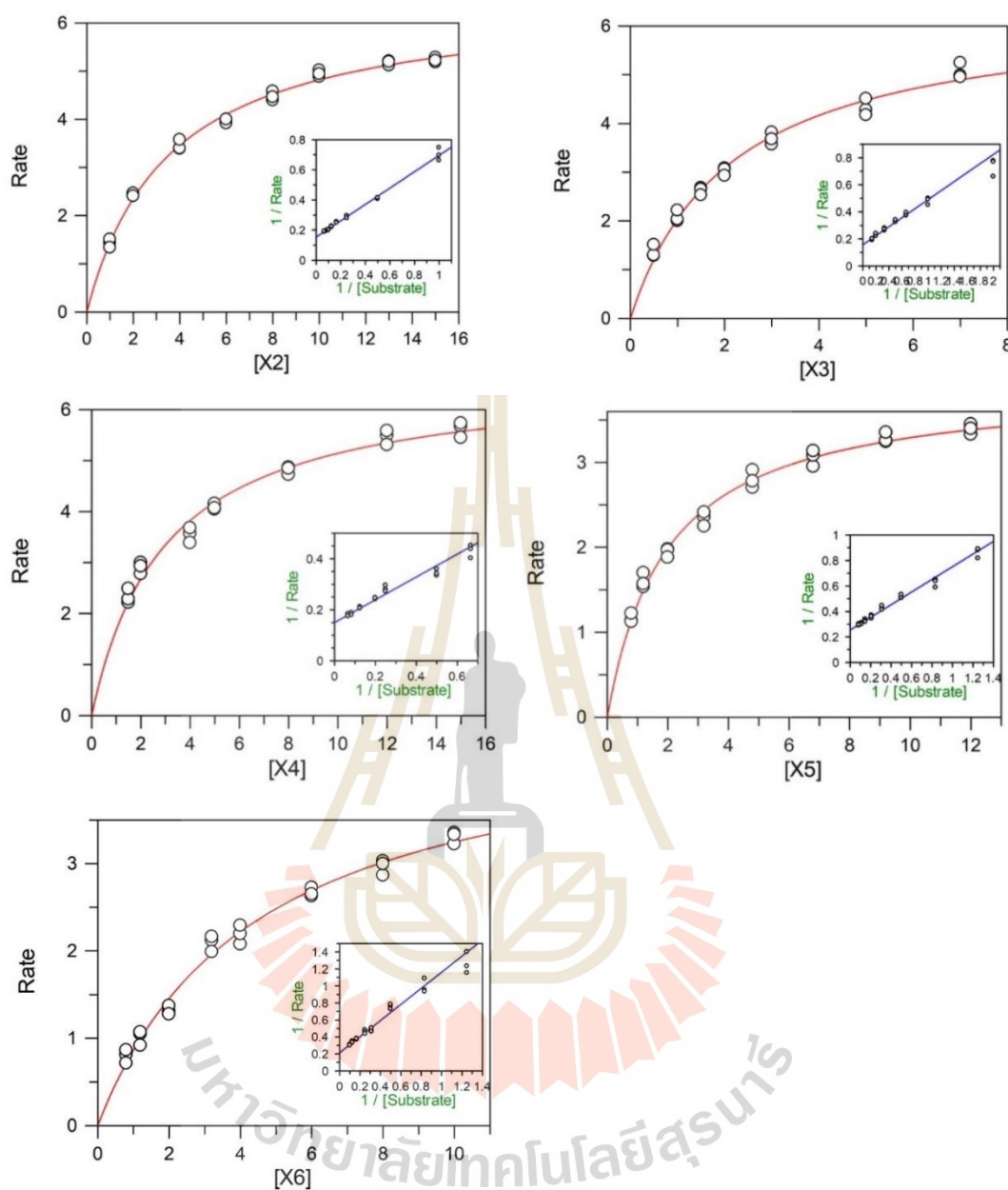


Figure 3.22 Michaelis-Menten plots of β -xylosidase OsXYL1 hydrolysis toward xylo-oligosaccharides substrates (DP 2-6). From these, kinetic parameters of xylobiose (X2), xylotriose (X3), xylotetraose (X4), xylopentaose (X5), and xylohexaose (X6) were determined. The amounts of hydrolytic products were calculated from standard curve of D-xylose. The figure was generated by GraFit 5 (Erithacus Software).

Table 3.4 Apparent kinetic parameters of β -xylosidase OsXYL1 toward xylo-oligosaccharides (DP 2-6).

Substrate	K_m (mM)	k_{cat} (s^{-1})	k_{cat}/K_m ($mM^{-1}s^{-1}$)
Xylobiose (X2)	3.54 ± 0.14	9.08 ± 0.09	2.56
Xylotriose (X3)	2.12 ± 0.14	8.88 ± 0.18	4.17
Xylotetraose (X4)	2.98 ± 0.17	9.29 ± 0.15	3.11
Xylopentaoase (X5)	1.96 ± 0.09	5.48 ± 0.06	2.80
Xylohexaoase (X6)	4.45 ± 0.32	6.53 ± 0.16	1.47

The kinetic parameters were calculated at initial velocity by assuming a single xylose was released per xylooligosaccharide substrates, whereas the kinetic parameters of xylobiose (X2) were obtained from divided by 2-folds of released xylose residues, since two xylose molecules are released in a single reaction. The catalytic efficiency (k_{cat}/K_m) of OsXYL1 was highest toward X3 and decreased with increasing DP above this, with lowest efficiency toward xylohexaoase (X6), which was supported by the TLC pattern (Figure 3.19). The high catalytic efficiencies (k_{cat}/K_m) of OsXYL1 against xylobiose and xylotriose suggest that its pocket-shaped active site with three monosaccharide-residue-binding subsites, each of which bind a xylobiosyl moiety of the XOS substrates (Hudson, R.C., *et al.*, 1991; Karkehabadi, S., *et al.*, 2014; 2018).

3.11 Xylose inhibition of β -xylosidase OsXYL1

The hydrolysis activity of OsXYL1 with 4NPXyl was inhibited by xylose, its product. The Lineweaver-Burk plot of xylose inhibition and derivative plot to determine the K_{ic} value are shown in Figure 3.24.

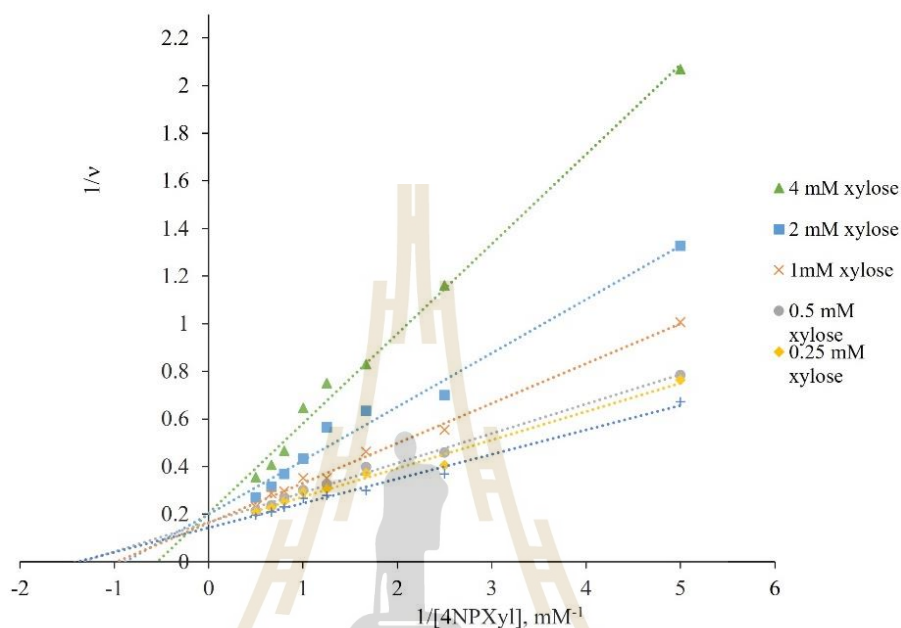


Figure 3.23 Lineweaver-Burk plot of β -xylosidase OsXYL1 toward 4NPXyl with different concentrations of xylose inhibitor.

Xylose has been determined to be mixed type or possibly a pure competitive inhibitor of OsXYL1 β -xylosidase, since the Lineweaver-Burk plots intercepted within error of the y-axis, but slightly to the left. Based on this competitive inhibition, the inhibition constant (K_i) of 1.41 ± 0.06 mM was calculated for xylose (Figure 3.24).

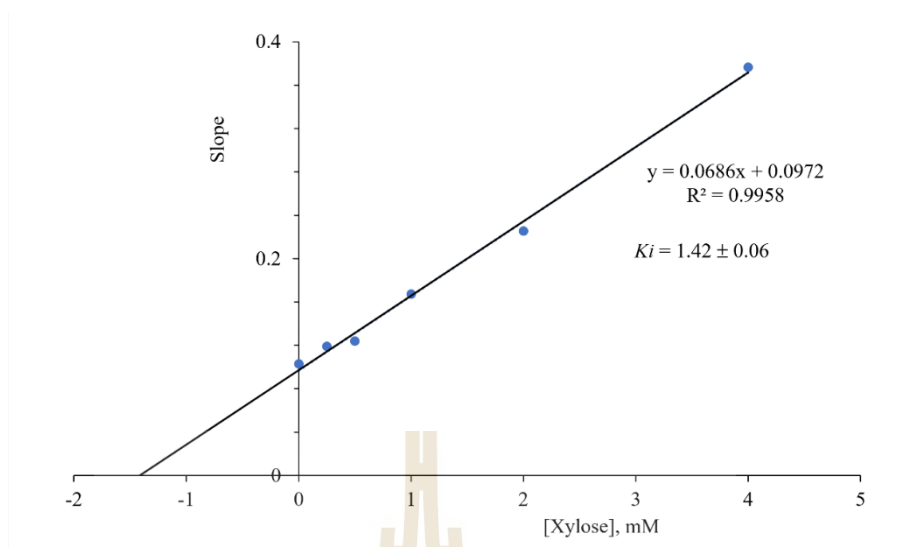


Figure 3.24 Derivative plot to determine the K_{ic} value. The slopes of the Lineweaver-Burk plots were plotted against the xylose concentrations and the data were subjected to linear regression ($R^2 = 0.996$).



CHAPTER IV

CONCLUSIONS

The rice β -xylosidase OsXYL1 gene (Genbank accession AK119887) has an open reading frame of 2,628 bp encoding a polypeptide 772 amino acids long, corresponding to a predicted molecular weight of 83,952 Da. Rice OsXYL1 is classified in the phylogenetic clade of β -xylosidase and α -L-arabinosidases among plant glycoside hydrolase family 3 members. A homology search of the amino acid sequence revealed that it is very similar to the previously studied barley β -xylosidase gene with 83% amino acid sequence identity. The homology model of β -xylosidase OsXYL1 was made based on the X-ray crystal structure of fungal *H. jecorina* Bxl1 (PDB code 5AE6), with which the amino acid sequence has 35% identity. The distribution in the secondary structures had the same conserved motifs around the catalytic residues as previously characterized family GH3 enzymes. These included the catalytic nucleophile aspartate residue Asp-299 in a conserved motif in the N-terminal domain, a conserved glutamate residue at the position of the catalytic acid/base, Glu-505, and the WGR and KH motifs at Trp-170 and Lys-216, respectively. The OsXYL1 sequence was cloned for expression and purification in *E. coli* and *P. pastoris* systems. Rice OsXYL1 β -xylosidase could not be successfully purified as soluble protein when expressed from the pET32a/OsXYL1 construct in *E. coli* strains. On the other hand, heterologous OsXYL1 β -xylosidase protein was successfully produced and purified when the pPICZ α BH8/OsXYL1 construct was expressed in the SMD1168H strain of *Pichia pastoris*, which secreted OsXYL1 into the medium when the culture was induced with methanol for 5 days at 20 °C.

The OsXYL1 β -xylosidase fusion protein with histidine tags, 3C Precision sites and three putative *N*-glycosylation sites was successfully expressed in the eukaryotic *Pichia pastoris* system. Two chromatographic purification steps isolated the secreted OsXYL1 with the fusion tags. Firstly, it was bound with a Ni²⁺-IMAC column and eluted with 50-

150 mM imidazole in IMAC buffer (pH 8.0) and the fractions containing β -xylosidase activity were combined and concentrated. The protein was further purified by SEC over an S200 gel filtration column. The peak fractions containing β -xylosidase activity were combined and designated as purified OsXYL1. The purification resulted in a final yield 0.57% recovered activity, while the specificity increased from 0.00086 to 0.086 U/mg, with a degree of purification of 101-fold. The purified glycosylated protein was used for optimization experiments. The pH and temperature optima of purified OsXYL1 β -xylosidase activity were pH 4.0 and 60 °C, respectively. It had moderate thermostability, since at temperatures ranging from 30-50 °C, it had more than 50% activity remaining after 4 h. At the optimum temperature of 60 °C, the activity decreased to less than 50% by about 42 min, and protein precipitated with higher temperatures and longer incubations. Based on these results, β -xylosidase activity of rice OsXYL1 was determined at 40 °C in subsequent experiments. OsXYL1 exhibited hydrolytic activities with artificial nitrophenyl glycosides and β -1,4-linked xylo-oligosaccharide (DP 2-6) substrates.

Rice OsXYL1 is a β -xylosidase that efficiently hydrolyzes bonds to nonreducing terminal β -Xylp, but hydrolyzed α -L-Araf and -Arap less, which indicates the bifunctional role found in other characterized plant GH3 members was only weakly present in rice OsXYL1. Kinetic parameters of OsXYL1 with its highly preferred for 4NPXyl substrate included an apparent Michaelis-Menten constant (K_m) value of 0.65 ± 0.031 mM, and a specificity constant catalytic efficiency (k_{cat}/K_m) value of $19.01 \text{ mM}^{-1}\text{s}^{-1}$. In comparison, hydrolysis of glycosidic bonds to α -L-arabinosyl moieties in 4NPAraf and 4NPArap obtained high apparent Michaelis-Menten constants (K_m) with values of 56.2 ± 1.1 mM and 83.8 ± 3.1 mM, respectively. In addition, the OsXYL1 also hydrolyzed β -1,4-Xylp in β -1,4-xylo-oligosaccharides (XOSs) substrates with DP of 2-6. The exotype action of OsXYL1 β -xylosidase had higher efficiency on the shorter xylobiose to xylotetraose, than the longer xylopentaose and xylohexaose with catalytic efficiency (k_{cat}/K_m) values of 2.56, 4.17, 3.11, 2.80, and $1.47 \text{ mM}^{-1}\text{s}^{-1}$, respectively, for DP 2-6. The approximately inverse relationship of efficiency to degree of polymerization

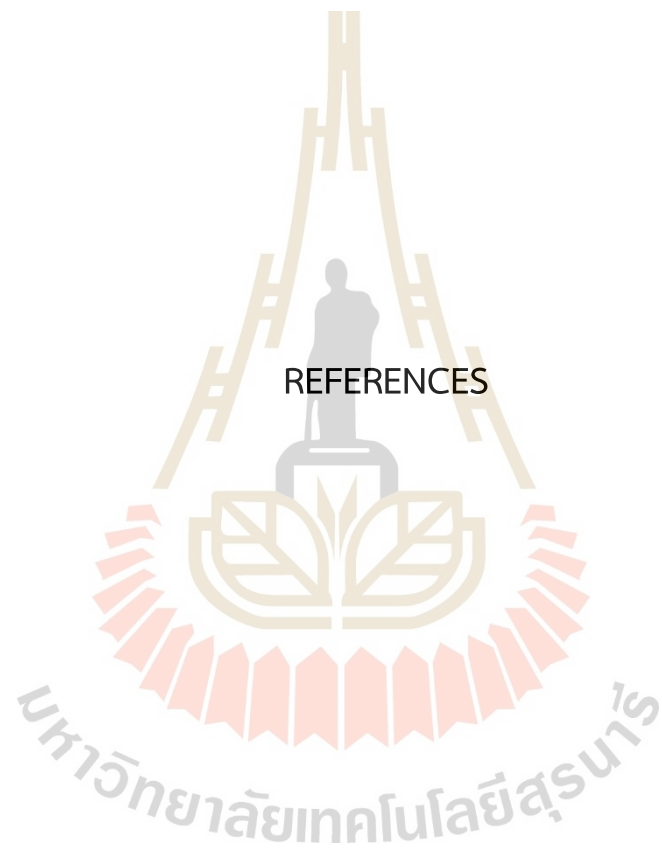
indicates that the catalytic active site is likely pocket-shaped with carbohydrate-binding negligible or unfavorable beyond the third xylopyranosyl residue.

The hydrolytic activities with 4NPXyl decreased when arabinose, glucose, mannose, galactose, fructose, lactose, maltose and sucrose were included in the reaction, but these sugars had small effects when comparing with xylose. The hydrolytic activity of OsXYL1 was inhibited by xylose in a mixed but primarily competitive manner with a competitive inhibition constant (K_i) of 1.41 ± 0.06 mM. Cu^{2+} and Mn^{2+} ions also strongly inhibited OsXYL1 β -xylosidase activity.

Transglycosylation activity of OsXYL1 with 4NPXyl substrate was found to produce alkyl xyloside products in reactions with methanol, ethanol, 2-propanol, *n*-propanol, *n*-butanol, and 3-methyl-butanol. Additionally, in reactions with 1-octanol in acetone co-solvent mixtures resulted in alkyl xyloside products strong accumulated in the reaction mixture. These results suggested that OsXYL1 may be useful for further enzymatic synthesis experiment.

In conclusion, rice OsXYL1 is a β -xylosidase that shows high efficiency to hydrolyze 4NPXyl and β -1,4-xylopyrano-oligosaccharides, with much lower specificity for hydrolysis of 4NPAraf and 4NPArap, which indicates rice β -xylosidase OsXYL1 may have less of a bifunctional role when compared with other characterized plant GH3 members. The β -xylosidase OsXYL1 might be functional in wall recycling in plant cell walls, but likely requires additional enzymes, such as α -L-arabinosidases, in addition to β -xylanases to hydrolyze the arabinoxylans found in rice. Moreover, OsXYL1 β -xylosidase has transglycosylation activity with alcohol acceptors that produce the alkyl xyloside products, which indicates it can be used for production of such xylosides.

REFERENCES



REFERENCES

- Amos, R.A., and Mohnen, D. (2019). Critical review of plant cell wall matrix polysaccharide glycosyltransferase activities verified by heterologous protein expression. *Front. Plant Sci.* 915, 1-27.
- Bar-Cohen, Y. (2012). Nature as a model for mimicking and inspiration of new technologies. *Int'l J. of Aeronautical & Space Sci.* 13(1), 1-13.
- Barnes, W.J. and Anderson, C.T. (2018). Release, recycle, rebuild: cell-wall Remodeling, autodegradation, and sugar salvage for new wall biosynthesis during plant development. *Mol. Plant.* 11, 31-46.
- Burmeister, W. P., Cottaz, S., Driguez, H., Palmieri, S., and Henrissat, B. (1997). The crystal structures of *Sinapis alba* myrosinase and of a covalent glycosyl-enzyme intermediate provide insights into the substrate recognition and active-site machinery of an S glycosidase. *Structure.* 5, 663-675.
- Burton, R.A., and Fincher, G.B. (2014). Evolution and development of cell walls in cereal grains. *Front. Plant Sci.* 5, 456.
- Bustamante, C.A., Rosli, H.G., Anon, M.C., Civello, P.M., and Martinez, G.A. (2006). β -Xylosidase in strawberry fruit: isolation of a full-length gene and analysis of its expression and enzymatic activity in cultivars with contrasting firmness. *Plant Sci. J.* 171, 497-504.
- Camacho-Fernandez, C., Segui-Simarro, J.M., Mir, R., Boutilier, K., and Corral-Martinez. (2021). Cell wall composition and structure define the developmental fate of embryogenic microspores in *Brassica napus*. *Front. Plant Sci.* 12, 737139.
- Cantarel, B. L., Coutinho, P. M. Rancurel, C., Bernard, T., Lombard, V., and Henrissat, B. (2009). The Carbohydrate-Active EnZymes database (CAZy): an expert resource for glycogenomics. *Nucleic Acids Res.* 37, D233-D238.
- Carpita, N. (1996). Structure and Biogenesis of the Cell Walls of Grasses. *Ann. Rev. Plant Physiol. Plant Mol. Biol.* 47, 445-476.

- Carpita, N.C., Defernez, M., Findlay, K., Wells, B., Shoue, D.A., Catchpole, G., Wilson, R.H., and McCann, M.C. (2001). Cell wall architecture of the elongating maize coleoptile. *Plant Physiol.* 127, 551-565.
- Caspers, M.P.M., Lok, F., Sinjorgo, K.M.C., van Zeijl, M.J., Nielsen, K.A., and Cameron-Mills, V. (2001). Synthesis, processing and export of cytoplasmic endo- β -1,4-xylanase from barley aleurone during germination. *Plant J.* 26(2), 191-204.
- Carpita, N., and McCann, M.C. (2015). Characterizing visible and invisible cell wall mutant phenotypes. *J. Exp. Bot.* 66(14), 4145-4163.
- Carpita, N., and McCann, M.C. (2020). Redesigning plant cell wall for biomass-based bioeconomy. *J. Biol. Chem.* 295(44), 15144-15157.
- Chinen, I., Oouchi, K., Tamaki, H., and Fukuda, N. (1982). Purification and properties of thermostable β -xylosidase from immature stalks of *Saccharum officinarum* L. (sugar cane). *J. Biochem.* 92(6), 1873-1881.
- Chir, J., Withers, S., Wan, C.-F., and Li, Y.-K. (2002). Identification of the two essential groups in the family 3 β -glucosidase from *Flavobacterium meningosepticum* by labeling and tandem mass spectrometric analysis. *Biochem. J.* 365, 857-863.
- Choengpanya, K., Arthornthurasuk, S., Wattana-amorn, P., Huang, W.-T., Plengmuankhae, W., Li, Y.-K., Kongsaree, P.T. (2015). Cloning, expression and characterization of β -xylosidase from *Aspergillus niger* ASKU28. *Protein Expr. Purif.* 115, 132-140.
- Cleemput, G., Hensing, M., van Oort, M., Deconynck, M., and Delcour, J.A. (1997). Purification and characterization of a β -xylosidase and an endo-xylanase from wheat flour. *Plant Physiol.* 113, 377-386.
- Collins, H.M., Burton, R.A., Topping, D.L., Liao, M.-L., Bacic, A., and Fincher, G.B. (2010). Variability in fine structures of noncellulosic cell wall polysaccharides from cereal grains: potential importance in human Health and nutrition. *Cereal Chem.* 87(4), 272-282.
- Cosgrove, D.J. (2016). Plant cell wall extensibility: connecting plant cell growth with cell wall structure, mechanics, and the action of wall-modifying enzymes. *J. Exp. Bot.* 67(2), 463-476.

- Davis, G., and Henrissat, B. (1995). Structures and mechanisms of glycosyl hydrolases. *Structure*. 3(9), 853-859.
- de Carvalho, D.R., Carli, S., Meleiro, L.P., Rosa, J.C. de Oliveira, A.H.C., Jorge, J.A., and Furriel, R.P.M. (2018). A halotolerant bifunctional β -xylosidase/ α -L-arabinofuranosidase from *Colletotrichum graminicola*: purification and biochemical characterization. *Int. J. Biol. Macromol.* 114, 741-750.
- Decou, R., Lhernould, S., Laurans, F., Sulpice, E., Leple, J.-C., Dejardin, A., Pilate, G., and Costa, G. (2009). Cloning and expression analysis of a wood-associated xylosidase gene (*PtBXL1*) in poplar tension wood. *Phytochem. Lett.* 70, 163-172.
- Dehnavi, E., Siadat, S.O.R., Roudsari, M.F., and Khajeh, K. (2016). Cloning and high-level expression of β -xylosidase from *Selenomonus ruminantium* in *Pichia pastoris* by optimizing of pH, methanol concentration and temperature conditions. *Protein Expr. Purif.* 124, 55-61.
- Deutschmann, R. and Dekker, R.F.H. (2012). From plant biomass to bio-based chemicals: Latest developments xylan research. *Biotechnol. Adv.* 30(6), 1627-1640.
- Dilokpimol, A., Nakai H., Gotfredsen, C.H., Appeldoorn, M.A., Baumann, M.J., Nakao, N., Schols, H.A., Hachem, M.A., and Svensson, B. (2011). Enzymatic synthesis of β -xylosyl-oligosaccharides by transxylosylation using two β -xylosidases of glycoside hydrolase family 3 from *Aspegillus nidulans* FGSC A4. *Carbohydr. Res.* 346, 421-429.
- Dodd, D., Kocherginskaya, S.A., Spies, A., Beery, K.E., Addas, C.A., Mackie, R.I., and Cann, I.K.O. (2009). Biochemical analysis of β -xylosidase and a bifunctional xylanase-ferulic acid esterase from a xylanolytic gene cluster in *Prevotella ruminicola* 23. *J. Bacteriol.* 191(10), 3328-3338.
- Drakakaki, G. (2015). Polysaccharide deposition during cytokinesis: challenges and future perspectives. *Plant Sci.* 236, 177-184.
- Oliveira, D.M., Mota, T.R., Salatta, F.V., Marchiosi, R., Gomez, L.D., McQueen-Mason, S.J., Ferrarese-Filho, O., and dos Santos, W.D. (2019). Designing xylan for improved sustainable biofuel production. *Plant Biotechnol. J.* 17(12), 2225-2227.

- Eneyskaya, E.V., Brumer III, H., Backinowsky, L.V., Ivanen, B.D., Kulminskaya, A.A., Shabalin, K.A., and Neustroev, K.N. (2003). Enzymatic synthesis of β -xylanase substrates: transglycosylation reactions of the β -xylosidase from *Aspergillus* sp. *Carbohydr. Res.* 338, 313-325.
- Eneyskaya, E.V., Ivanen, B.D., Bobrov, K., Isaeva-Ivanova, L.S., Shabalin, K.A., Savel'ev, A.N., Golubev, A.M., and Kulminskaya, A.A. (2007). Biochemical and kinetic analysis of the GH3 family β -xylosidase from *Aspergillus awamori* X-100. *Arch. Biochem. Biophys.* 457, 225-234.
- Figueroa, C.R., Rosli, H.G., Civello, P.M., Martinez, G.A., Herrera, R., and Moya-Leon, M.A. (2010). Changes in cell wall polysaccharides and cell wall degrading enzymes during ripening of *Fragaria chiloensis* and *Fragaria xananassa* fruits. *Sci. Hortic.* 124, 454-462.
- Fry, S.C. (2017). Plant cell wall polymers. *Biofuel and Bioenergy.* 59-87.
- Giovanna, M., Gramegna, G., Benedetti, M., and Mattei, B. (2020). Industrial use of cell wall degrading enzymes: the fine line between production strategy and economic feasibility. *Front. Bioeng. Biotechnol.* 8, 356.
- Goujon, T., Mimic, Z., Amrani, A.E., Lerouxel, O., Aletti, E., Lapierre, C., Joseleau, J.-P., and Jouanin, L. (2003). AtBXL1, a novel higher plant (*Arabidopsis thaliana*) putative beta-xylosidase gene, is involved in secondary cell wall metabolism and plant development. *Plant J.* 33, 677-690.
- Gruninger, R.J., Gong, X., Forster, R.J., and McAllister, T.A. (2014). Biochemical and kinetic characterization of the multifunctional β -glucosidase/ β -xylosidase/ α -arabinosidase, Bgxa1. *Appl. Microbiol. Biotechnol.* 98, 3003-3012.
- Han, Y., and Chen, H. (2010). A β -xylosidase from cell wall of maize: purification, properties and its use in hydrolysis of plant cell wall. *J. Mol. Catal. B Enzym.* 63, 135-140.
- Harvey, A.J., Hrmova, M., De Gori, R., Varghese, J.N., and Fincher, G.B. (2000). Comparative modeling of the three-dimensional structures of family 3 glycoside hydrolase. *Proteins.* 41, 257-269.

- Hatfield, R.D., Grabber, J., Ralph, J., and Brei, K. (1999). Using the acetyl bromide assay to determine lignin concentrations in herbaceous plants: some cautionary notes. *J. Agric. Food Chem.* 47(2), 628-632.
- Henrissat, B. (1991). A classification of glycosyl hydrolases based on amino acid sequence similarities. *Biochem. J.* 280, 309-316.
- Henrissat, B., and Bairoch, A. (1993). New families in the classification of glycosyl hydrolases based on amino acid sequence similarities. *Biochem J.* 293, 781-788.
- Henrissat, B., Callebaut, I., Fabrega, S., Lehn, P., Mornon, J.P., and Davies, G. (1995). Conserved catalytic machinery and the prediction of a common fold for several families of glycosyl hydrolases. *Proc. Natl. Acad. Sci. USA.* 92(15), 7090-7094.
- Henrissat, B., and Bairoch, A. (1996). Updating the sequence-based classification of glycosyl hydrolases. *Biochem J.* 316, 695-696.
- Henrissat, B., and Davies, G. J. (1997). Structural and sequence-based classification of glycosyl hydrolases. *Curr. Opin. Struct. Biol.* 7(5), 637-644.
- Heredia, A., Jimenez, A., and Guillen, R. (1995). Composition of plant cell walls. *Z Lebensm Unters Forsch.* 200, 24-31.
- Hernandez-Beltran, J.U., Lira, I.O.H.-D., Cruz-Santos, M.M.C., Saucedo-Luevanos, A., Hernandez-Teran, F., and Balagurusamy, N. (2019). Insight into pretreatment methods of lignocellulosic biomass to increase biogas yield: current state, challenges, and opportunities. *Appl. Sci.* 9, 3721.
- Houston, K., Tucker, M.R., Chowdhury, J., Shirley, N., and Little, A. (2016). The plant cell wall: A complex and dynamic structure as revealed by the response of gene under stress conditions. *Front. Plant Sci.* 7, 984.
- Hrmova, M., Harvey, A.J., Wang, J., Shirley, N.J., Jones, G.P., Stone, B.A., Hoj, P.B., and Fincher, G.B. (1996). Barley β -D-glucan exohydrolase with β -glucosidase activity. *J. Biol. Chem.* 271(9), 5277-5286.
- Hrmova, M., and Fincher, G.B. (1998). Barley β -D-glucan glucosylhydrolases. Substrate specificity and kinetic properties. *Carbohydr. Res.* 305, 209-211.
- Hrmova, M., and Fincher, G.B. (2001). Structure-function relationships of beta-D-glucan endo- and exohydrolases from higher plants. *Plant Mol. Biol.* 47(1-2), 73-91.

- Hrubá, P., Honys, D., Twell, D., Capková, V., and Tupy, J. (2005). Expression of β -galactosidase and β -xylosidase genes during microspore and pollen development. *Planta*. 220, 931-940.
- Hudson, R.C., Schofield, L.R., Coolbear, T., Daniel, R.M., and Morgan, H.W. (1991). Purification and properties of an aryl β -xylosidase from a cellulytic extreme thermophile expressed in *Escherichia coli*. *Biochem. J.* 273, 645-650.
- Inoue, H., Kitao, C., Yano, S., and Sawayama, S. (2016). Production of β -xylosidase from *Trichoderma asperellum* KIF125 and its application in efficient hydrolysis of pretreated rice straw with fungal cellulase. *World J. Microbiol Biotechnol.* 32,186.
- Itali, A., Yoshida, K., Tanabe, K., and Tamura, F. (1999). A β -D-xylosidase-like gene is expressed during fruit ripening in Japanese pear (*Pyrus pyrifolia* Nakai). *J. Exper. Bota.* 50, 877-878.
- Itali, A., Kotaki, T., Tanabe, K., Tamura, F., Kawaguchi D., and Fukuda, M. (2003). Rapid identification of 1-aminocyclopropane-1-carboxylate (ACC) synthase genotype in cultivars of Japanese pear (*Pyrus pyrifolia* Nakai) using CAPS marker. *Theor. Appl. Genet.* 51, 1266-1272.
- Itai, A., Ishihara, K., and Bewley, J.D. (2003). Characterization of expression and cloning, of β -D-xylosidase and α -L-arabinofuranosidase in developing and ripening tomato (*Lycopersicon esculentum* Mill.) fruit. *J. Exper. Bota.* 54(393), 2615-2622.
- Izydorczyk, M.S. and Dexter, J.E. (2008). Barley β -glucan and arabinoxylan: molecular structure, physicochemical properties, and used in food products-a review. *Int. Food Res. J.* 41, 850-868.
- Jordan, D.B. and Wagschal, K. (2010). Properties and applications of microbial β -D-xylosidases featuring the catalytically efficient enzyme from *Selenomonas ruminantium*. *Appl. Microbiol. Biotechnol.* 86, 1647-1658.
- Kanauchi, M., Chijimi, A., Ohnishi-Kameyama, M., and Bamforth, C.W. (2013). An investigation of two xylan-degrading enzymes and a novel xylanase inhibitor in malted barley. *J. Inst. Brew.* 119(1-2), 32-40.
- Karkehabadi, S., Helmich, K.E., Kaper, T., Hansson, H., Mikkelsen, N.-E., Gudmundsson, M., Piens, K., Fujidala, M., Banerjee, G., Scott-Craig, J.S., Walton, J.D., Phillips, G.N.,

- Jr., and Sandgren, M. (2014). Biochemical characterization and crystal structures of a fungal family 3 β -glucosidase, Cel3A from *Hypocrea jecorina*. *J. Biol. Chem.* 289(45), 31624-31637.
- Karkehabadi, S., Hansson, H., Mikkelsen, N. E., Kim, S., Kaper, T., Sandgren, M., and Gudmundsson, M. (2018). Structural studies of a glycoside hydrolase family 3 β -glucosidase from the model fungus *Neurospora crassa*. *Acta Crystallogr. F: Struct. Biol. Commun.* 74(12), 787–796.
- Kikuchi, S., Satoh, K., Nagata, T., Kawagashira, N., Doi, K., Kishimoto, N., Yazaki, J., Ishikawa, M., Yamada, H., Ooka, H., Hotta, I., Kojima, K., Namiki, T., Ohneda, E., Yahagi, W., Suzuki, K., Li, C.J., Ohtsuki, K., Shishiki, T., Otomo, Y., Murakami, K., Iida, Y., Sugano, S., Fujimura, T., Suzuki, Y., Tsunoda, Y., Kurosaki, T., Kodama, T., Masuda, H., Kobayashi, M., Xie, Q., Lu, M., Narikawa, R., Sugiyama, A., Mizuno, K., Yokomizo, S., Niikura, J., Ikeda, R., Ishibiki, J., Kawamata, M., Yoshimura, A., Miura, J., Kusumegi, T., Oka, M., Ryu, R., Ueda, M., Matsubara, K., Kawai, J., Carninci, P., Adachi, J., Aizawa, K., Arakawa, T., Fukuda, S., Hara, A., Hashizume, W., Hayatsu, N., Imotani, K., Ishii, Y., Itoh, M., Kagawa, I., Kondo, S., Konno, H., Miyazaki, A., Osato, N., Ota, Y., Saito, R., Sasaki, D., Sato, K., Shibata, K., Shinagawa, A., Shiraki, T., Yoshino, M., Hayashizaki, Y. and Yasunishi, A. (2003). Collection, mapping, and annotation of over 28,000 cDNA clones from japonica rice. *Science*. 301(5631), 376-379.
- Kim, J.-B., Olek, A.T., and Carpita, N.C. (2000). Cell wall and membrane-associated exo- β -D-glucanases from developing maize seedlings. *Plant physiol.* 123, 471-485.
- Kim, S.-J., and Brandizzi, F. (2016). The plant secretory pathway for the trafficking of cell wall polysaccharides and glycoproteins. *Glyobiology*. 26(9), 940-949.
- Kurakake, M., Fuji, T. Yata, M., Okazaki, T., and Komaki, T. (2005). Characteristic of transxylosylation by β -xylosidase from *Aspergillus awamori* K4. *Biochim. Biophys. Acta Gen. Subj.* 1726(3): 272-279.
- Koshlan, D.E. (1953). Stereochemistry and the mechanism of enzymatic reactions. *Biol. Rev.* 28, 416-436.

- Kotake, T., Nakagawa, N., Takeda, K., and Sakurai, N. (1997). Purification and characterization of wall-bound exo-1,3- β -D-glucanase from barley (*Hordeum vulgare* L) seedlings. *Plant Cell Physiol.* 38, 194-200.
- Kotake, T., Tsuchiya, K., Aohara, T., Konishi, T., Kaneko, S., Igarashi, K., Samejima, M., and Tsumuraya, Y. (2006). An α -L-arabinofuranosidase/ β -D-xylosidase from immature seeds of radish (*Raphanus sativus* L.). *J. Exper. Bota.* 57(10), 2353-2362.
- Kousar, S., Mustafa, G., and Jamil, A. (2013). Microbial xylosidase: production and biochemical characterization. *Pak. j. life soc. Sci.* 11(2), 85-95.
- Kurakake, M., Fujii, T., Yata, M., Okazaki, T., and Komaki, T. (2005). Characteristics of tranxylosylation by β -xylosidase from *Aspergillus awamori* K4. *Biochim. Biophys. Acta.* 1726, 272-279.
- Laemmli, U.K. (1970). Cleavage of structural proteins during the assembly of the head of bacteriophage T4. *Nature.* 227(5259), 680-685.
- Lampugnani, E.R., Khan, G.A., Somssich, M., and Persson, S. (2018). Building a plant cell wall at a glance. *J. Cell Sci.* 131(2), jcs207373.
- Lagaert, S., Pollet, A., Courtin, M., and Volckaert, G. (2014). β -Xylosidases and α -L-arabinofuranosidases: Accessory enzymes for arabinoxylan degradation. *Biotechnol. Adv.* 32, 316-332.
- Lee, R., Hrmova, M., Burton, R., Lahnstein, J., and Fincher, G. (2003). Bifunctional family 3 glycoside hydrolase from barley with α -L-arabinofuranosidase and β -D-xylosidase activity. *J. Biol. Chem.* 278(7), 5377-5387.
- Lombard, V., Ramulu, H.G., Drula, E., Coutinho, P.M., and Henrissat, B. (2014). The carbohydrate-active enzymes database (CAZy) in 2013. *Nucleic Acids Res.* 42, 490-495.
- Loque, D., Scheller, H.V., and Pauly, M. (2015). Engineering of plant cell walls for enhanced biofuel production. *Curr Opin Plant Biol.* 25, 151-161.
- Luang, S., Hrmova, M., and Ketudat-Cairns, J.R. (2010). High-level expression of barley β -D-glucan exohydrolase HvExoI from a codon-optimized cDNA in *Pichia pastoris*. *Protein Expr. Purif.* 73, 90-98.
- Macauley-Patrick, S., Fazenda, M.I., McNeil, B., Harvey, L.M. (2005). Heterologous protein production using the *Pichia pastoris* expression system. *Yeast J.* 22, 249-270.

- Malinovsky, F., Fangel, J.U., and Willats, W.G.T. (2014). The role of the cell wall in plant immunity. *Front. Plant Sci.* 5, 178.
- Marriott, P.E., Gomez, L.D., and McQueen-Masoo, S.J. (2016). Unlocking the potential of lignocellulosic biomass through plant science. *New Phytol.* 209, 1366-1381.
- Martinez, G.A., Chaves, A.R., and Civello, P.M. (2004). β -xylosidase activity and expression of a β -xylosidase gene during strawberry fruit ripening. *Plant Physiol. Biochem.* 42, 89-96.
- McCarter, J., and Withers, S.G. (1994). Mechanisms of enzymatic glycoside hydrolysis. *Curr. Opin. Struct. Bio.* 4, 885-892.
- Mhetras, N., Liddell, S., and Gokhale, D. (2016). Purification and characterization of an extracellular β -xylosidase from *Pseudozyma hubeiensis* NCIM3574 (PhXyl), an unexplored yeast. *AMB Express.* 6, 73.
- Minic, Z., Rihouey, C., Do, C. T., Lerouge, P., and Jouanin, L. (2004). Purification and characterization of enzymes exhibiting β -D-xylosidase activities in stem tissues of *Arabidopsis*. *Am. Soc. Plant Biolog.* 135, 867-878.
- Minic, Z., Do, C.-T., Rihouey, C., Morin, H., Lerouge, P., and Jouanin, L. (2006). Purification, functional characterization, cloning, and identification of mutants of seed-specific arabinan hydrolase in *Arabidopsis*. *J. Exp. Bota.* 57(10), 2339-2351.
- Minic, Z., and Jouanin, L. (2006). Plant glycoside hydrolases involved in cell wall polysaccharide degradation. *Plant Physiol. Biochem.* 44, 435-449.
- Minic, Z., Jamet, E., Negroni, L., der Garabedian, P.A., Zivy, M., and Jouanin, L. (2007). A sub-proteome of *Arabidopsis thaliana* mature stems trapped in Concanavalin A is enriched in cell wall glycoside hydrolases. *J. Exper. Bota.* doi:10.1093/jxb/erm-082.
- Minic, Z. (2008). Physiological roles of plant glycoside hydrolases. *Planta.* 227, 723-740.
- Mussatto, S.I., Fernandes, M., Milagres, A.M.F., and Roberto, I. (2008). Effect of hemicellulose and lignin on enzymatic hydrolysis of cellulose from brewer's spent grain. *Enz. Microb. Technol.* 43, 124-129.
- Nakamura, T., Toshima, K., and Matsumura, S. (2000). One-step synthesis of *n*-octyanol using acetone powder of *Aureobasidium pullulans* in supercritical fluids. *Biotechnol. Lett.* 1183-1189.

- Nieto-Dominguez, M., de Eugenio, L.I., Barriuso, J., Prieto, A., de Toro, B.F., Canales-Mayordomo, A., and Martinez, M.J. (2015). Novel pH-stable glycoside hydrolase family 3 β -xylosidase from *Talaromyces amestolkiae*: an enzyme displaying regioselective transxylosylation. *App. Envir. Microb.* 81(18), 6380-6392.
- Ochs, M., Muzard, M., Plantier-Royon, R., Estrine, B., Remond, C. (2011). Enzymatic synthesis of alkyl β -D-xylosides and oligosylosides from xylans and from hydrothermally pretreated wheat bran. *Green Chem.* 13, 2380-2388.
- Opassiri, R., Ketudat-Crains, J.R., Akiyama, T., Wara-Aswapati, O., Svati, J. and Esen, A. (2003). Characterization of a rice β -glucosidase gene highly expressed in flower and germinating shoot. *Plant Sci.* 165, 627-638.
- O'Neill, R.A., Albersheim, P., and Darvill, A.G. (1989). Purification and characterization of a xyloglucan oligosaccharide-specific xylosidase from pea seedlings. *J. Biol. Chem.* 264(34), 20430-20437.
- Prade, R.A. (1996). Xylanases: from biology to biotechnology. *Biotechnol. Genet. Eng. Rev.* 13, 101-132.
- Park, C., Choi, J., Kyung, M., Seo, S., Jo, S.-E., Lee, K., Kim, P., Linda, N.-H., and Jung, S. (2017). Application of *Bacillus pumilus* β -xylosidase reaction and simulated moving bed purification to efficient production of high-purity xylobiose from xylose. *J. Indus. Eng. Chem.* 47, 431-438.
- Peyer, C., Bonay, P., and Staudacher, E. (2004). Purification and characterization of a β -xylosidase from potatoes (*Solanum tuberosum*). *BBA.* 1672, 27-35.
- Polizeli, M.L.T.M., Rizzatti, A.C.S., Monti, R., et al. (2005). Xylanases from fungi: Properties and industrial applications. *Appl. Microbiol. Biotechnol.* 67, 577-591.
- Pozzo, T., Pasten, J.L., Karlsson, E.N., and Logan, D.T. (2010). Structural and functional analyses of β -glucosidase 3B from *Thermotoga neapolitana*: A thermostable three-domain representative of glycoside hydrolase 3. *J. Mol. Biol.* 397, 724-739.
- Pozzo, T., Romero-Garcia, J., Faijes, M., Planas, A., and Karlsson, E.N. (2016). Rational design of a thermostable glycoside hydrolase from family 3 introduces β -glycosynthase activity. *Glycobiology.* 1-11.

- Prawisut, A., Choknud, S., and Cairns, J.R. (2020). Expression of rice β -exoglucanase II (OsExoII) in *Escherichia coli*, purification, and characterization. *Protein Expr. Purif.* 175, 105708.
- Puzio, P., Blau, A., Walk, T.B., Gipmans, M., Haake, V., Weig, A., Plesch, G. and Ebner, M. (2009). Process for the production of a fine chemical. *Patent: WO 2008034648-A1*.
- Reen, F.J., Murray, P.G., and Tuohy, M.G. (2003). Molecular characterization and expression analysis of the first hemicellulase gene (*bxl1*) encoding β -xylosidase from the thermophilic fungus *Talaromyces emersonii*. *Biochem. Biophys. Res. Commun.* 305, 579-585.
- Rennie, E.A., and Scheller, H.V. (2014). Xylan biosynthesis. *Curr. Opin. Biotechnol.* 26, 100-107.
- Rajan, S.S., Yang, X., Collart, F., Yip, V.L., Withers, S.G., Varrot, A., Thompson, J., Davies, G.J., and Anderson, W.F. (2004). Novel catalytic mechanism of glycoside hydrolase based on the structure of an $\text{NAD}^+/\text{Mn}^{2+}$ -dependent phosphor-alpha-glucosidase from *Bacillus subtilis*. *Structure.* 12: 1619-1629.
- Rojas, A.L., Fischer, H., Eneiskaya, E.V., Kulinskaya, A.A., Shabalin, K.A., Neustroev, K.N., Craievich, A.F., Golubev, A.M., and Polikarpov, I. (2005). Structural insights into the β -xylosidase from *Trichoderma reesei* obtained by synchrotron small-angle x-ray scattering and circular dichroism spectroscopy. *Biochemistry.* 44, 15578-15584.
- Ruperti, B., Cattivelli, L., Pagni, S., and Ramina, A. (2002). Ethylene-responsive genes are differentially regulated during abscission, organ senescence and wounding in peach (*Prunus persica*). *J. Exper. Bota.* 53(368), 429-437.
- Sasaki, T., Matsumoto, T., Yamamoto, K., Sakata, K., Baba, T., Katayose, Y., Wu, J., Niimura, Y., Cheng, Z., Nagamura, Y., Antonio, B.A., Kanamori, H., Hosokawa, S., Masukawa, M., Arikawa, K., Chiden, Y., Hayashi, M., Okamoto, M., Ando, T., Aoki, H., Arita, K., Hamada, M., Harada, C., Hijishita, S., Honda, M., Ichikawa, Y., Idonuma, A., Iijima, M., Ikeda, M., Ikeno, M., Ito, S., Ito, T., Ito, Y., Ito, Y., Iwabuchi, A., Kamiya, K., Karasawa, W., Katagiri, S., Kikuta, A., Kobayashi, N., Kono, I., Machita, K., Maehara, T., Mizuno, H., Mizubayashi, T., Mukai, Y., Nagasaki, H., Nakashima, M.,

- Nakama, Y., Nakamichi, Y., Nakamura, M., Namiki, N., Negishi, M., Ohta, I., Ono, N., Saji, S., Sakai, K., Shibata, M., Shimokawa, T., Shomura, A., Song, J., Takazaki, Y., Terasawa, K., Tsuji, K., Waki, K., Yamagata, H., Yamane, H., Yoshiki, S., Yoshihara, R., Yukawa, K., Zhong, H., Iwama, H., Endo, T., Ito, H., Hahn, J.H., Kim, H.I., Eun, M.Y., Yano, M., Jiang, J. and Gojobori, T. (2002). The genome sequence and structure of rice chromosome 1. *Nature*. 420(6913), 312-316.
- Scheller, H.V., and Ulvskov, P. (2010). Hemicelluloses. *Annu. Rev. Plant Biol.* 61, 263-289.
- Shi, H., Li, X., Gu, H., Zhang, Y., Huang, Y., Wang, L., and Wang, F. (2013). Biochemical properties of a novel thermostable and highly xylose-tolerant β -xylosidase/ α -arabinosidase from *Thermotoga thermarum*. *Biotechnol. Biofuels*. 6, 27.
- Shibuya, N., Nakane, R., Yasui, A., Tanaka, K., and Iwasaki, T. (1985). Comparative studies on cell wall preparations from rice bran, germ, and endosperm. *Cereal Chem.* 62(4), 252-258.
- Smulek, W., Kaczorek, E., and Hricoviniova, Z. (2017). Alkyl xylosides: physico-chemical properties and influence on environmental bacteria cells. *J Surfact Deterg.* 20, 1269-1279.
- Somerville, C., Bauer, S., Brininstool, G., Facette, M., Hamann, T., Milne, J., Osborne, E., Paredes, A., Persson, S., Raab, T., Vorwerk, S., and Youngs, H. (2004). Toward a systems approach to understanding plant cell walls. *SCIENCE*. 306, 2206-2271.
- Suen, D.F., Wu, S.S.H., Chang, H.C., Dhugga, K.S., and Huang, A.H.C. (2003). Cell wall reactive proteins in the coat and wall of maize pollen. *J. Biol. Chem.* 278(44), 43672-43681.
- Sun, X., Yang, Q., Guo, W., Dai, L., and Chen, W. (2013). Modification of cell wall polysaccharaide during ripening of Chinese bayberry fruit. *Sci. Hortic.* 160, 155-162.
- Sunna, A., and Antranikian, G. (1997). Xylanolytic enzymes from fungi and bacteria. *Crit. Rev. Biotechnol.* 17, 39-67.
- Suzuki, K., Sumitani, J.-I., Nam, Y.-W., Nishimaki, T., Tani, S., Wakagi, T., Kawaguchi, T., and Fushinobu, S. (2013). Crystal structures of glycoside hydrolase family 3 β -glucosidase 1 from *Aspergillus aculeatus*. *Biochem J.* 452(2), 211-221.

- Takahashi, H., Kikuchi-Fujisaki, S., Yoshida, C., Yamada, H., Yamashita, T., Konno, N., and Takeda, T. (2018). Gtgen3A, A novel plant GH3-glucosidase, modulates gentio-oligosaccharide metabolism in *Gentiana*. *Biochem. J.* 475, 1309-1322.
- Tateishi, A., Mori, H., Watari, J., Nagashima, K., Yamaki, S., and Inoue, H. (2005). Isolation, characterization, and cloning of α -L-arabinofuranosidase expressed during fruit ripening of Japanese pear. *Plant Physiol.* 138, 1653-1664.
- Thongpoo, P., McKee, L., Araujo, A.C., Kongsaree, P.T., and Brumer, H. (2013). Identification of the acid/base catalyst of a glycoside hydrolase family 3 (GH3) β -glucosidase from *Aspergillus niger* ASKU28. *BBA.* 1830, 2739-2749.
- Thongpoo, P., Srisomsap, C., Chokchaichamnankit, D., Kitpreechavanich, K., Svasti, J., and Kongsaree, P.T. (2014). Purification and characterization of three β -glucosidases exhibiting high glucose tolerance from *Aspergillus niger* ASKU28. *Biosci.* 78(7), 1167-1176.
- Tong, X., Qi, Z., Zheng, D., Pei, J., Li, Q., and Zhao, L. (2021). High-level expression of a novel multifunctional GH3 family β -xylosidase/ α -arabinosidase/ β -glucosidase from *Dictyoglomus turgidum* in *Escherichia coli*. *Bioorg. Chem.* 111, 104906.
- Toonkool, P., Metheenukul, P., Sujiwattanasat, P., Paiboon, P., Tongtubtim, N., Cairns, M.K., Cairns, J.K., and Svasti, J. (2006). Expression and purification of dalcocinase, a beta-glucosidase from *Dalbergia cochinchinensis* Pierre, in yeast and bacterial hosts. *Protein Expr Purif.* 48(2), 195-204.
- Varghese, J., Hrmova, M., and Fincher, G.B. (1999). Three-dimensional structure of a barley β -D-glucan exohydrolase, a family 3 glycoside hydrolase. *Structure.* 7(2), 179-190.
- Voiniciuc, C., Pauly, M., and Usadel, B. (2018). Monitoring polysaccharide dynamics in the plant cell wall. *Plant Physiol.* 176, 2590-2600.
- Vogel, J. (2008). Unique aspects of the grass cell wall. *Curr Opin Plant Biol.* 11(3), 301-307.
- Vries, D.R., and Visser, J. (2001). *Aspergillus* Enzymes involved in degradation of plant cell wall polysaccharides. *Microbiol Mol Biol Rev.* 65(4), 497-522.
- Zechel, D.L., and Withers, S. (2001). Dissection of nucleophilic and acid-base catalysis in glycosidases. *Model systems.* 5(6), 643-649

- Xiong, J.-S., Balland-Vanney, M., Xie, Z.-P., Schultze, M., Kondorosi, A., Kondorosi, E., and Staehelin, C. (2007). Molecular cloning of a bifunctional β -xylosidase/ α -L-arabinosidase from alfalfa roots: heterologous expression in *Medicago truncatula* and substrate specificity of the purified enzyme. *J. Exper. Bota.* 58(11), 2799-2810.
- Yan, Q., Hua, C., Yang, S., Li, Y., and Jiang, Z. (2012). High level expression of extracellular secretion of a β -glucosidase gene (*PtBglu3*) from *Paecilomyces thermophila* in *Pichia pastoris*. *Protein Expr. Purif.* 84, 64-72.
- Yoshida, E., Hidaka, M., Fushinobu, S., Koyanagi, T., Minami, H., Tamaki, H., Kitaoka, M., Katayama, T., and Kumagai, H. (2010). Role of a PA14 domain in determining substrate specificity hydrolase family 3 β -glucosidase from *Kluyveromyces marxianus*. *Biochem. J.* 431, 39-49.
- Zanoelo, F.F., Polizeli, M.L.T.M., Terenzi, H.F., and Jorge, J.A. (2004). Purification and biochemical properties of a thermostable xylose-tolerant β -D-xylosidase from *Scytalidium thermophilum*. *J. Ind. Microbiol. Biotechnol.* 31(4), 170-176.
- Zhou, J., Bao, L., Chang, L., Liu, Z., You, C. and Lu, H. (2011). Beta-xylosidase activity of a GH3 glucosidase/xylosidase from yak rumen metagenome promotes the enzymatic degradation of hemicellulosic xylans. *Lett. Appl. Microbiol.* 54, 79-87.
- Zhu, J. Chen, S., Alvarrez, S., Asirvatham, V.S., Schachtman, D.P., Wu, Y., and Sharp, R.E. (2006). Cell wall proteome in the maize primary root elongation zone. I. extraction and identification of water-soluble and tightly ionically bound proteins. *Plant Physiol.* 140, 311-325.

CURRICULUM VITAE

NAME Ms. Kadsada Sala

DATE OF BIRTH May 27, 1983

PLACE OF BIRTH Loei, Thailand

EDUCATION

2001-2005 Maejo University, Chiang Mai, Thailand

Bachelor of Science (Chemistry)

2005-2010 Suranaree University of Technology, Nakhon Ratchasima, Thailand

Master of Science (Chemistry)

2015-present Suranaree University of Technology, Nakhon Ratchasima, Thailand

Ph.D. candidate (Biochemistry)

SCHOLARSHIP

Student fee exemption scholarship from One Research One Graduate student (OROG) Grant, Suranaree University of Technology (2015-2017)

มหาวิทยาลัยเทคโนโลยีสุรนารี